OUKA
The University of Osaka
Institutional Knowledge Archive

Title	Beta-and Gamma-Ray Spectroscopy of 106mAg
Author(s)	Inoue, Hikaru
Citation	大阪大学, 1971, 博士論文
Version Type	VoR
URL	https://hdl.handle.net/11094/1986
rights	
Note	

The University of Osaka Institutional Knowledge Archive : OUKA

https://ir.library.osaka-u.ac.jp/

The University of Osaka

Beta- and Gamma-Ray Spectroscopy of ^{106m}Ag

by

Hikaru Inoue

Contents

Abstract:

Gamma rays and internal conversion electrons following the decay of 8.3 d ^{106m}Ag were studied with Ge(Li) spectrometers and an orange type beta-ray spectrometer. Energies and intensities of some low energy gamma rays were measured precisely. An energy discrepancy found in previous works was solved by using these accurately determined gamma ray energies and a new 1909 keV level is proposed alternatively. Conversion coefficients for some weak transitions were determined from the intensity ratios of gamma rays and internal conversion elctrons. The spin and parity of the 2952 keV level was determined to be 5^+ from the observed conversion coefficients.

Two three phonon states were suggested on the basis of the observed gamma ray branching ratios to the low lying two phonon states. The multipolarities of these gamma rays were determined from the conversion coefficients.

New gamma rays of 69,71,80,83,178,434,522,950,1051,1077, 1168,1178,1349,1909 and 2077 keV were observed. Two tentative levels are proposed from some of these gamma rays.

The energy of the 512 keV gamma rays was determined accurately by referring to the annihilation gamma ray energy. A problem associated with this measurement is also described separately in Appendix.

1. Introduction

The decay of 8.3 d ^{106m}Ag has been investigated by several authors.[1-8] The low lying levels of the daughter nucleus ^{106}Pd exhibit clear vibrational mode of excitation. Experimental studies of these levels have also been attained through the decay of ^{106}Ag (24 min),[4,6] ^{106}Rh (30 sec)[1-4,6] and ^{106m}Rh (2.2 h).[9] But the most intensive informations including the high lying levels have been obtained from the decay of ^{106m}Ag. The decay scheme of ^{106m}Ag proposed by Moragues et al[8] is shown in Fig.1.

Fig.1

The 0^+,2^+ and 4^+ triplet levels which are predicted by the spherical vibrational model[10] have been found at twice the energy of first excited state. Spins of these levels have been well established by angular correlation measurements.[1,11] The angular correlation of the 616-512 keV cascade gamma rays show that the 616 keV transition from the second 2^+ state consist of more than 99 % E2 multipole.[1] The B(E2) ratio of this 616 keV gamma ray to that of the 1128 keV crossover gamma ray is 37. These facts show that these levels are almost pure vibrational ones.

In terms of the pure spherical vibrational model, Yoshizawa[12] pointed out the possible existences of higher phonon states for some even nuclei on the basis of the experimentally observed gamma ray branching ratios and the selection rule for the phonon number.

In this assignment he assumed the pure E2 multipolarity for the adopted gamma rays above 300 keV. Experimental evidence of the M1/E2 mixing ratio is scanty for these gamma rays. In this sense, the assignment is not conclusive but rather tentative. It is quite important to exemplify the higher phonon state in such a typical spherical nucleus as ^{106}Pd. If the higher phonon state as well as one and two phonon states are established, the character of higher excited state will be predicted on the same theoretical basis.

From the experimental viewpoint the character of the possible higher phonon state can be studied from the accurately determined gamma ray branching ratio and M1/E2 mixing ratio. High resolution Ge(Li) spectrometers are the useful instruments for this type of experiment. Measurements of conversion coefficients provide an estimate of M1/E2 mixing ratio.

For the case of ^{106}Pd, the 1558 keV level is depopulated by the 328,430 and 1046 keV gamma rays. The 328 and 430 keV gamma rays feed the 4^+ and 2^+ levels in the two phonon triplet ones. The relative intensities of these gamma rays were reported by some authers.[4-9] But the results show considerable fluctuation. No definite conclusion was obtained for the transition multipolarity.

The decay scheme proposed by Taylor et al[7] is identical in its essential point with that by Moragues et al[8]. Both decay schemes are constructed mainly by using the Ritz rule and intensity balance for proposed levels are satisfactory. Results of the coincidence measurement performed by Rao and Fink[6] for some prominent gamma rays do not contradict with these level scheme.

Therefore, these decay schemes are the most reliable ones at present. But a relatively large deviation from Ritz rule is found in Moragues's level scheme. The energy of the 680 keV gamma ray which depopulate the 2757 keV level in Fig.1 exceed the energy sum of the 451 and 229 keV gamma rays by about 1 keV. This deviation can not be limited within the quated accuracies. The deviation is insignificant for Taylor's data but the same deviation was observed in the earlier stage of present experiment in more refined way. This gamma ray must be excluded from the assigned position, though it feed the 2077 keV level with considerable intensity in Moragues's level scheme. The observed discrepancy in energy is small but critical one and requires reexamination of the transition assignments and the level scheme proposed by Moragues et al as well as Taylor et al on the basis of more rigorous application of Ritz rule.

Internal conversion electrons following the decay of ^{106m}Ag were measured by Smith[3] with a permanent magnet spectrograph and by Scheuer et al[13] with a double focussing beta-ray spectrometer. These measurement were made for main transitions below 1527 keV. Measurement of weak and high energy conversion electrons with an orange type beta ray spectrometer in our laboratory are able to provide further experimental data for spins and parities assignment of the levels in ^{106}Pd.

In the present experiment gamma rays and internal conversion electrons following the decay of ^{106m}Ag were measured with Ge(Li) spectrometers and an eight gap orange type beta-ray spectrometer. Energies and intensities of some low energy gamma rays were

measured precisely by referring to the selected set of standard gamma rays.

The energy of the 512 keV gamma ray was measured by reffering to the energy of the annihilation gamma ray.[14] From this measurement the 512 keV gamma ray energy is accurately determined without the X ray scale. In the course of this measurement a remarkable result was obtained; the energy of annihilation gamma ray shows considerable fluctuation depending on the material in which positrons annihilate. It means a existence of a serious problem for the measurements of nuclear gamma ray energies. The problem is described in some length in Appendix A.

2. Source preparation

The 8.3 d ^{106m}Ag radioisotope was produced by the $^{103}Rh(\alpha,n)$ ^{106m}Ag reaction. In order to reduce the 40 d ^{105}Ag contamination, the bombarding alpha particle energy was kept at about 14 MeV. A inner target system was used for this porpose. Bombarding beam currents×time are typically 8 × 12 and 8 × 40 μa hours for a gamma-ray source and for a internal conversion electron source, respectively.

The ^{106m}Ag sample used for measurements was chemically separated from the target material by following procedure. The bombarded Rh powder was fused with $KHSO_4$ and digested with water. The solution was then filtered and the undissolved residue was again treated as before, until all Rh powder was fused completely with $KHSO_4$. The total volume of the final solution used to be 30 to 40 ml. A few ml of 1 N HNO_3, 1 to 2 ml 5% $Hg_2(NO_3)_2$ solution and then an excess amount of HCl were added to the solution. The Ag activity was coprecipitated with mercurrous chloride as collector.

The gamma ray source were prepared by packing the precipitate into a standard type lucite holder capsule used in our laboratory.

Further elimination of Hg carrier and remaining Rh was necessary to prepare carrier-free source for internal conversion electron measurements. The precipitate was dissolved in aqua regia. In order to remove chloride ion, a few ml of conc. HNO_3 was added and the solution was evapolated just to dryness. The residue was dissolved into water and the coprecipitation procedure was repeated as before. Mercurrous chloride was then sublimated

by gentle heating while the Ag activity was not sublimated. A carrier-free solution was obtained by dissolving the remaining Ag activity in water.

The solution was dryed up on a myler film to give an internal conversion electron source. The spot size of the sources used to be 5 to 10 mm in diameter.

3. Apparatus

3.1. Ge(Li) spectrometers

Gamma rays following the decay of ^{106m}Ag were measured with Ge(Li) spectrometers. Four different type ORTEC Ge(Li) detectors and two different type electronics system were available in separate stage of the present experiment. Two 20 cc detectors (vertical type and horizontal type) and a 30 cc detector were used in combination with a Hewelet Packard 1024 channel pulse height analyser and a 40 cc detector with a Packard 4096 channel analyser. All these detectors are true coaxial type. The ORTEC amplification modules were used in both spectrometers. The typical FWHM values at 512 keV are 2.1 keV, 2.6 keV, 1.7 keV and 2.4 keV for 20 cc vertical type, 20 cc horizontal type, 30cc and 40 cc detector, respectively. A block diagram of 20 cc spectrometer system is represented in Fig.2. This system was used most frequently for energy measurements.

Fig. 2

3.2. Calibration of the Ge(Li) spectrometers

The detection efficiency and the linearity of each spectrometer was calibrated by using a number of standard sources. The gamma ray energies and intensities of the standard sources used for the calibration are listed in Table 1 and 2, respectively.[15]

Table 1

Table 2

A typical example showing the overall linearity characteristics are shown in Fig.3-a and Fig.3-b.

Fig. 3-a

Fig. 3-b

Fig. 3-a show the deviation from linearity in the energy region between 300 and 1350 keV while the Fig. 3-b between 1050 and 2650 keV. The dots and the open circles show the values obtained in separate runs. The error bars in both Figures indicate two different type uncertainties. The length between two horizontal bars show the quated uncertainties of energy standard gamma rays listed in Table 1. The length above and below the horizontal bars indicate the uncertainties in peak

channel determination. These two plots have a similar pattern though the energy region between 1050 to 1350 keV is commonly included in both runs. It indicate that the main source of nonliniarity is in the biased amplifier plus multichannel analyser system. A similar pattern was also observed in different amplifier gain parameter setting for this spectrometer.

It should be also noticed in Fig. 3-a and 3-b that the energy uncertainties of standard gamma rays are larger than those of peak channels even in the energy region near 700 keV. The accurate determination of these gamma ray energies is an urgent problem for precise calibration.

In the 20 cc system which is used frequently for energy measurement a reliable method was applied to correct the linearity in the biased amplifier plus multichannel analyser system. The method is as followings.

A gamma ray pair which has an adequate energy separation was displayed on multichannel scale at various locations and the difference in the peak channels was measured at respective location. This channel difference between two peak shows systematic change for its location. The gain parameter of main amplifier was kept constant during this measurement, therefore, the height difference of input pulses for full energy peaks remains constant. The plot of these peak channel difference with respect to the peak location on multichannel scale can be interpreted to an channel number correction curve of the multichannel plus biased amplifier system though the linearity of each system

can not be known separately. The correction curves obtained by this method are represented in Fig. 4.

Fig. 4

These curves provide a necessary correction in channel number to read the main amplifier out put pulse, i.e., input pulse of biased amplifier linearily on multichannel scale. The results of correction are illustrated in Fig. 5.

Fig. 5

The dots show the overall deviation from the linearity and the open circle the correction results in which the deviation due to the main amplifier plus detector preamplifier remains still.

The relative detection efficiency of each spectrometer were determined by using gamma-ray sources whose relative intensities are known with good accuracy. The gamma ray sources which decay in 100 % cascade transitions are the most reliable ones for this purpose.

The sources used for detection efficiency calibration are listed in Table 2. Of these standard sources ^{60}Co, ^{108m}Ag and ^{178}Ta emit the gamma rays in 100 % cascade transitions. Corrections for internal conversion electron branchings are less than 1 % for ^{60}Co and ^{108m}Ag while it amounts to 20 % for ^{178}Ta 214 keV transition. The values for ^{22}Na, ^{75}Se and ^{88}Y are

taken from the literature in footnote. The relative intensities of ^{133}Ba gamma rays were determined in the separate experiment[16] by referring to the ^{178}Ta and ^{75}Se.

The photo peak detection efficiency curve of vertical type 20 cc detector are represented in Fig. 6.

Fig. 6

The relative value of this curve was determined by using ^{22}Na, ^{60}Co, ^{75}Se, ^{88}Y, ^{108m}Ag and ^{178}Ta. The 2.2 h ^{178}Ta was produced by bombarding alpha particles on Lu powder. The precision of this curves is 2 to 3 % for the relative values between 200 to 750 keV where the ^{178}Ta and ^{108m}Ag sources were available. Some consideration on this resulted precision should be described a little more. The count sum in FWTM was taken as convenient definition of peak total count. There are three uncertainty sources in this analysis method; statistical fluctuation, ambiguity in background estimation and cut off 0f peak tail. The first is negligibly small if the peak maximum count is above 10^4. The second is typically 1 % or lower except a few peaks in low energy region. The third type uncertainty is estimated to be about 0.1X peak maximum count, for example, to be about 2 % of peak total count if ten data points are included in FWTM. The uncertainties were added in quadrature. The resulted uncertainty in a total count for single peak is in most cases in the precision written above. This method is certified by some repeated

measurements. An example of result is shown in Table 3.

Table 3

The absolute values was obtained from 4 μc standard sources of ^{22}Na, ^{60}Co, ^{65}Zn, ^{75}Se and ^{137}Cs calibrated at Japan Radioisotope Co. The accuracies of these source strength are 5 %.

The detection efficiency of 40 cc detector was determined in the same way. But ^{178}Ta was not used for this calibration. ^{133}Ba was used instead. It is also represented in Fig. 7.

Fig. 7

The curve designated as sum was obtained by using the prominent peak in summing peak spectrum of ^{106m}Ag source. It is difficult to estimate the contribution of sum count in appearent total count in a consistent way. It serves only as a semi quantitative guide for the analysis of summing peak spectrum.

3.3. Beta-ray spectrometer

Internal conversion slectrons were measured with an eight gap orange type beta ray spectrometer. Fig. 8 show the

---

Fig. 8

---

horizontal section of the spectrometer. The spectrometer is similar to that of Copenhagen.[17] The source to detector distance is 30 cm. The best resolution obtained with a single gap is 0.8 %, while it degrade to 1.0 % with 8 gaps. The transmission for all gap varies up to 8 %.

Electrons were detected with an antheracene crystal and a 6342A photomultiplier.

Electron energy values were calibrated by using the ^{137}Cs K-line as 3381.0 gauss·cm. The K and L line spectrum of this standard source are shown in Fig. 9.

Fig. 9

It is possible to measure electrons up to 4 MeV. The coil current was measured by using a potentiometer. A simple automatic current scanning and count recording can also be used as an auxiliary equipment. A more complete describtion of the design and performance are given in Appendix C.

4. Measurements

4.1. Gamma ray measurements

Three different types of measurements for ^{106m}Ag gamma rays were performed separately in present experiment: energy measurements, intensity measurements and summing peak measurement. Details of each measurement are described in this section. The absolute measurement of 512 keV gamma ray energy is described in Apperidix A. . An Example of gamma ray Spectrum of full energy region is shown in Fig. 10-a, -b, -c and -d.

Fig. 10

As the source to detector distance was 7 cm a number of sum peak are observed in this spectrum.

Energies were measured by using the 20 cc spectrometer and the 40 cc Ge(Li) spectrometer. To construct a reliable level scheme, gamma ray energies were measured as precicely as possible and the measurements were repeated a few time. The 680 keV gamma ray which was assigned as the transition from 2757 keV level to 2077 keV level show a small discrepancy with the energy sum of 451 and 228 keV gamma rays in Moraques's level scheme[8], while no discrepancy was found in Taylor's values[7]. As the same discrepancy was found in earlier stage of present experiment, these energy measurement were undertaken to check the other energy relation as widely as possible. A method of

mixed source measurement was applied for the determination of prominent peak energies. The energy standard gamma rays were measured simulaneously. An example of spectra for these measurement is illustrated in Fig. 11.

Fig. 11

All the sources were located on the axis of coaxial type detector so as to make the gamma rays incident to the detector front surface to avoid possible field increment effect. In the case where some standard gamma ray peaks overlap with the ^{106m}Ag gamma ray peaks, two sources were measured in separate runs. Some other standard gamma ray peaks were included commonly in both run to check the gain and base line drift during measurement. For such cases, however, accurate comparison of two gamma ray energies is possible, as in the case of comparison measurement of 512 keV and 511 keV gamma ray. By this mixed source measurement the energy determination is possible only for the prominent peaks in the spectrum. Energies of weak gamma rays were determined by referring to the energies of these prominent peaks. A total of 16 runs were recorded for these energy measurements. Analyses of these spectra are described in following chapter.

The relative intensities of low energy gamma rays were measured mainly with the 20 cc spectrometer, whose relative detection efficiency in this energy region is calibrated by referring to ^{75}Se, ^{108m}Ag and ^{178}Ta gamma rays. The same type

of source capsules made in our laboratory was used for ^{106m}Ag, ^{108m}Ag and ^{178}Ta to cancel the absorption effect for low energy gamma ray as well as to attain a good reproducibility of source position. The relative intensity of 328 and 430 keV gamma rays which depopulate 1558 keV level was measured repeatedly, in various geometrys. The main information on gamma ray intensities above 1 MeV were obtained by using 40 cc spectrometers.

In order to check the cascade relation in level scheme summing peak spectrum was taken by using 40 cc spectrometer. This method provides a kind of Ge-Ge coincidence spectrum conveniently. A weak ^{106m}Ag source was set close to the detector. An example of this spectrum is shown in Fig. 12.

Fig. 12

4.2. Internal conversion measurements

Internal conversion electrons up to 1850 keV were measured with the eight gap spectrometer. Spectra are shown in Fig.13-a and Fig. 13-b. The purpose of the measurement are at first to determine the weak line intensities which were not reported by Morgues et al. A conversion coefficient of the 645 keV transion is of interest related to the spin and the parity of 2952 keV level. Secondly the determination of the conversion coefficients of 328 keV and 430 keV transitions which depopulate the 1557 keV level can give the estimation of the transition multipolarities in combination with the gamma ray data. The third purpose is to determine the intensity ratio of the K and L conversion electrons in 328 keV transition. The ratio gives a multipolarity of the transition independent on the gamma ray data.

Fig. 13-a

Fig. 13-b

The capability of the orange type beta ray spectrometer to collect a peak count in high statistics is useful for these purposes. The sources used for the measurements were prepared as described in chapter 2. The output pulse of the detector were discriminated with a single channel annalyser. The discrimination levels were chosen to give an optimum S/N ratio. The pulse spectrum of the detected electrons with the

antheracene crystal were monitored with a 400 channel pulse height analyser during the measurements. Fluctuation in the high voltage for phtomultiplier was also monitered continuousely by a pen recorder. A minor fluctuation of the background counts due to "on and off" of the cyclotron beam were also checked before the measurements. A considerable counts loss was observed for low energy electrons below 200 keV. A correction curves were prepared for a few values of discrimination levels by using the observed pulse height spectrum. The counting times are, for example, 10 min and 40 min for K and L line of the 328 keV transitions, respectively.

5. Analyses and Results

5.1. Determination of gamma ray energies and intensities

Experimental results of the energies and intensities are given in Table 4 together with the results of Moragues et al.[8] and Taylor et al.[7]

Table 4

Procedure to determine these values are described in this section.

The gamma ray energies were determined by referring to the standard gamma rays listed in Table 1. The table is taken from reference 15. All the energy values in the table are based on the universal constants of 1965.[14] There are two energy bases for the standard gamma ray energies presented in the table. The first is the positron annihilation gamma ray and the second is the wavelength of W-Kα_1 X ray. The consistency of these two energy bases is certified within 17 ± 28 ppm.[18] The designations A, B, C, and D identify these energy bases and the used instruments.(see footnote of the table) A more detailed dicussion on these two energy bases and the quated values are described elsewhere.

In order to fully utilize the capability of Ge(Li) spectrometer in determining the peak channel, some computer programs were developed. The usefullness as well as the inadequacies of these programs were checked by some model experiments and model analyses. In general the precision in peak channel determination

are as good as 0.03 channel or 10 eV for low energy gamma rays if the peak is isolated and has sufficient counting statistics. The detail of these programs are described in Appendix A.

All the prominent peaks in energy measurement runs were analysed with the aid of a program STANDARD ANALYSIS in which a simple Gaussian function is used to fit the peak profile. The program calculate peak channels, linear interpolation energies and the uncertainties in these calculations. The deviation from linearity in the spectrometer system causes a severe problem to determine the gamma ray energies by inter-polation. An application of polynomial least square fit is possible to reproduce the energy standard points in a convenient way with an adequate precision. In the present experiment, however, this method was not applied, because the contribution from each energy standard are smeared out in the resulted polynomial. A graphical correction method was applied instead. Though this method is somewhat a tedious one, it has a merit that the relations between the reference energies and the determined energies can be made clearer by this method than by the polynomial least square method.

In the energy region between 220 to 660 keV where a number of accurate energy standard gamma rays are available the resulted accuracies of the prominent gamma ray energies are, in general, 20 to 30 eV. The energy values given in Table 4 for this energy region are the results of weighted mean of three or four separare runs which were measured with different spectrometers and also in different amplifier gain parameter settings. The weights

used here are the uncertainties in interpolation and do not include the uncertainties in standard gamma ray energies. As an alternative way an unweighted mean and a sample standard deviation was also calculated for each line and if the standard deviation was larger than the uncertainty given in the weighted mean calculation the former are taken instead of the latter. Comparison between thses two procedure are represented in Fig. 14.

Fig. 14

A small dot with a bar represents the measured value in each run and the uncertainty in interpolation which was obtained as the quadrature sum of the uncertainty in channel and the one in linearity correction. A large dot and a open circle indicate the results of weighted mean and the unweighted mean, respectively. In most cases the standard deviation is smaller than the weighted uncertainty. The energy uncertainties given in the table consist of two different type uncertainties. The first is the one described above and the second is the one in reference energy. A quadrature sum was not taken for this case.

In the energy region above 700 keV where the accurate standard gamma rays are scanty the uncertainty due to linearity correction becomes inevitably large.

Only the prominent peak energies were determined by the mixed sources method described above. The energies of weak gamma rays as well as those of doublet gamma rays were determined by

referring to these strong gamma ray energies. The spectra for intensity measurements were used for this purpose.

According to the transition assignments made by Moragues et al, Ritz Rule was applied for main cascade and crossover transitions. The results are represented in Table 5.

Table 5

Almost all the energy relations are satisfied within the quated accuracies. However, a clear discrepancy was found for the 680 keV gamma ray. The discrepancy is pointed out by adding the estimated accuracies to the resulted energy differences in column 5. The energies of 222 keV and 451 keV gamma rays are the most accurate ones, the sum of which clearly contradict with that of 680 keV. In column 5 one more large deviation is pointed out for the energy sum of 717 keV and 847 keV gamma rays and the energy of 1565 keV gamma ray. A solution of these discrepancies is discussed in chapter 6.

Relative intensities of gamma rays were determined by using detection efficiency curves shown in Figs. 6 and 7. The relative intensities of 328 and 429 keV transitions are of interest as described in chapter 1. For this purpose the detection efficiency curve obtained from the ^{178}Ta source is useful. Two cascade gamma rays of 326 and 427 keV in ^{178}Ta can give precise relative values of the 328 and 429 keV gamma rays in ^{106m}Ag. The accuracy of detection efficiency at these energies ratio is about 2 %.

The peak total counts of 429 keV gamma ray was also determined in same precision. But the uncertainty in peak total counts of 328 keV gamma ray could not be reduced below 5 % because of unfortunate Compton background due to strong 512 keV gamma ray. The same definition of peak total count that was taken for detection efficiency determination was also adopted throughout the intensity snalysis. The relative intensities of low energy gamma rays below 511 keV in Table 4 are those which were determined by this 20 cc detector. In the energy range between 511 and 1500 keV averaged values obtained with 20 cc detector and 40 cc detector were taken to give the resulted values in the table. Above 1500 keV results with the 40 cc detector are given in the table.

Above 900 keV a number of weak were observed, as is shown in Fig. 10. However, these line have possibility of being sum peaks of two prominent gamma rays. The contribution of sum peak count was estimated quantitatively for most of these peaks by using the branching ration of prominent gamma rays and the absolute detection efficiency of the corresponding geometry. For some weak peaks, more than 70 % of integrated peak count were accounted for sums of two cascade gamma rays. These peaks were assigned as sum peaks and were excluded from the list of new gamma rays except a few crossover transitions of considerable counting statistics. As a consequence more than half of these peaks were excluded. These sum peak assignments are given in Figs. 10 and 12.

New gamma rays at 69, 70, 80, 83, 178, 434, 522, 949, 1077, 1168, 1178, 1349, 1909, and 2077 keV were found in present experiment. Weak evidences for 987 and 1419 keV gamma rays are observed. The upper limit of 0.03 was given for 1932 keV gamma ray after subtraction of sum peak counts. The 2245 keV gamma ray reported by Taylor was completely accounted for as sum peak of five cascade transitions. The total count of a peak at 2077 keV which form a doublet line with 2084 keV peak can not be accounted for as sum peak count. A possible value is given to this gamma-ray intensity with different upper and lower limits.

Summing peak spectra, an example of which is given in Fig. 12, were analysed only in a semi quantitative way except some important cases. Results of observation are summarised in Table 6 for direct cascade sum peaks.

Table 6

Peak counts are designated by p, c and w which mean prominent, considerable and weak, respectively. The results are also represented in Fig. 15.

Fig. 15

5.2. Internal Conversion Coefficients

Internal convension coefficients were obtained from electron and gamma ray intensities. Electron intensities measured with the orange type beta ray spectrometer are given in Table 7 together with the results of Scheuer et al.[13]

Table 7

In present experiment the electron intensities below 230 keV have an ambiguity due to counting loss. In the energy region between 790 and 850 keV the measurement with the orange type beta-ray spectrometer is not able to give better values than the previous one because of overlapping of some K and L lines. In these energy regions the results by Scheuer et al.[13] were adopted to give the conversion coefficients. All the gamma-ray intensies to calculate the conversion coefficients in column 4 of Table 10 were taken from column 2 of Table 4. The values of conversion coefficients are normalized to that of theoretical one 4.85×10^{-3} for 512 keV E2 transition to give an absolute measure. The theoretical values in column 5-7 are taken from the table of Hager and Selzer.[19] The results are also represented in Fig. 16.

Fig. 16

The conversion coefficients show that the 229, 451, 645, 748 and 1572 keV transitions have an E1 multipolarity. All the

other transitions show M1 and/or E2 character. The 195 and 222 keV transitions are predominant M1 in their characters. The 328, 391, 406 and 429 keV ones proved to be predominant E2 within the quated accuracies. The E2/M1 mixing ratio were estimated for some low energy transitions from these conversion coefficients. The results are shown in Table 8.

Table 8

For the 328 keV transition the ratio of K and L+M conversion electron intensities was also determined with the orange type spectrometer. The value is 5.9±0.4. The theoretical values of this ratio are 7.1 and 6.1, respectively. The fraction of E2 multipolarity estimated from these values is also shown in Table 8.

6. Level scheme and spin and parity assignments

All the levels proposed by Moragues et al.[8] as well as Taylor et al.[7] are well certified by applying Ritz rule to some sets of stopover and crosover gamma rays and by observing sum peaks whose energies correspond to level separations. Only one exception to which no support was found in sum peak spectrum is the 2282 keV level. But the results of application of Ritz rule as well as "in and out" intensity balance which is shown later in this section is quite satisfactory one for this level. Therefore no discussion is made about the existence of the levels in Fig. 1. The discussion in this chapter is at first concentrated to the solution of observed energy discrepancies for 680 and 848 keV gamma rays. Secondly, the spin and parity assignments for some levels are discussed, a tentative proposals of new levels being also included there.

As seen in Table 5 the observed energy difference between the sum energy of 229 and 451 keV gamma rays and the 680 keV gamma ray energy provide a sufficient evidence to exclude the 680 keV gamma ray from the position assigned by Moragues et al. One more large deviation in Ritz rule was observed for 848 keV gamma ray which forms a cascade set with the 680 keV gamma ray. In order to make these situations more clear the level energies were calculated on the basis of some selected gamma rays whose energies were determined with the best accuracies in present experiment. Gamma rays above 1500 keV were not used for this purpose not only because of their large uncertainties but also

because of ambiguity in standard gamma rays.

A particular feature of the levels in ^{106}Pd is shown in Fig. 17.

Fig. 17

The figure explain the procedure to determine the level energies by using the gamma ray energies in Table 4. A brief explanation is given in the caption. The resulted level energies have sufficient accuracies to examine the validity of assignments of all other gamma rays, though some arbitrariness remain still in the selection of gamma rays. These values are used throughout the discussion and the possible adjustment to obtain an alternative one for compromise with other gamma rays which are not included in Fig. 17 are not made also in later chapter. Such a treatment is necessary to localize the remaining discrepancies in its clear forms. By this treatment the energy discrepancies described above become more appearant.

The 847.82 keV gamma ray can not fit to the level energy separation of 849.19 keV between the 2077 and 1229 keV levels. The deviation of 0.37 keV can not be limited within the accuracy of measurements. The energy of 2077 keV level is determined from that of 2351 keV level by subtracting the 222 keV gamma ray energy and the energies of 2351 as well as 2366 and 2306 keV levels are dertermined from the mean value of three cascade gamma rays and one crossover gamma ray, as seen in Fig. 17.

The results are also supported by the energy of 703 plus 825 and 804 plus 825 cascade gamma ray pairs. In other words, the energy of 2351 keV level is very consistent with six gamma ray energies between 703 and 825 keV. The energy fo these gamma rays were determined by referring mainly to that of ^{54}Mn 834.795 ± 0.040 keV gamma ray to which that of 848 keV was also referred. Therefore, the discrepancy of 0.37 keV can not be accounted for as a inadequacy of energy standard gamma ray.

Two energy discrepancies mentioned above are not independent. The 680 and 848 keV gamma rays are in cascade in Moragues's level scheme, therefore, a part of these discrepancies in energy cancell each other if a new level is proposed at slightly lower position of 2077 keV level. But such a alternation causes a new severe discrepancy in "in and out" intensity balance for 2077 keV level. In Moragues's level scheme the 2077 keV level is fed mainly by 229 and 680 keV gamma rays and depopulated mainly by the 848 keV gamma ray. The relative intensities of 229,680 and 848 keV gamma rays are 25, 24 and 50, respectively.

The unique solution to be allowed for this situation is to decompose the 848 keV gamma ray into double components of almost equal intensities. A slight broadening was observed for the 848 keV peak. The FWHM of 848 keV peak is 11.1 channel, while that of 825 keV is 10.3. This broadening can be accounted for neither by accidental cause nor by energy dependence of FWHM. The fraction of intensity in each component can be estimated from the intensities of other gamma rays. Other possible feeding

to be considered is the 875, 949 and 1565 KeV ones. But the deviations of the gamma ray energy from the given energy separations are 0.17, 0.17 and -0.12 keV for 875, 949 and 1565 keV gamma rays, respectively. Therefore, no evidence was found for possible gamma ray to feed or depopulate a new level if it locate at slightly lower position of 2077 keV level. One of the alternative location of the new level is a 1909 keV level which is fed by one component of 848 keV gamma ray and depopulated by the 680 keV gamma ray. A new gamma ray of the energy 1909.2 ± 0.6 keV fit well to this level. Therefore, this level is proposed by present experiment. The discussion above is summarized as following: the decomposition of 848 keV gamma ray for two components of almost equal intensities is supported by solving the observed energy discrepancies in a quantitatively satisfactory way, secondly by maintaining the intensity balance for 2077 keV level, thirdly by observing the slight increase of FWHM of the 848 keV peak and finally by postulating a new 1909 keV level associated with a new 1909 keV gamma ray.

Another weak evidences concerning the 680 keV peak should be noticed. A slight increase of FWHM was also observed for the 680 keV peak, i.e. the 680 keV peak has also a possibility of being decomposed. But the evidence alone is too weak to obtain a conclusive result. In addition, the situation is rather complex as described below.

Two weak sum peaks were observed at 2535 and 2520 keV, as seen in Fig. 12. The former is accounted for as sum peak of

the 451 and 2084 keV gamma rays. The quantitative agreement including triple sum is satisfactory for this sum peak. The latter seems to have double components, one of which is the sum peak of the 1394 and 1128 keV gamma rays. The other component can be accounted for only, at least energetically, as the sum peak of 680 and 1839 keV gamma rays. About 1/3～1/5 of the 680 keV gamma ray intensity is necessary to give the observed sum peak intensity. It means a new level of 3031 keV level depopulated by this 680 keV gamma ray. The level has also a possibility of being depopulated by the 748 and 1122 keV gamma rays which terminate at the 2283 and 1909 keV level, respectively. But the result of inspection of the 748 and 1122 keV peaks is inconclusive. The 680 keV gamma ray might be decomposed into three component if it has a weak component which depopulate the 2757 keV level. The evidences described above are to weak to obtain a definite conclusion and this problem can be solved only by a more intensive study with a instrument of higher resolution. Therefore, the discussion to this point remains only to point out the possibility of the 3031 keV level associated with the slight broadening of the 680 keV peak. The 680 keV gamma ray is assumed to be single component in later discussion.

New gamma rays of 69, 71, 80, 178, 434, 522, 950, 1051, 1077, 1168, 1178, 1350, 1909 and 2077 keV were observed in present experiment. Of these gamma rays the 83, 434, 950, 1077, 1178 and 2077 keV ones are accomodated succesfully in Moragues's level scheme. The 1051 keV gamma ray has been observed in the decay

of ^{106}Ag as well as ^{106}Rh.[4,6] It depopulate the 1562 keV level in ^{106}Pd. The 522 keV gamma ray feed this level. The 433 keV gamma ray can also be assigned to depopulate from this level but it has not been observed in the ^{106}Ag decay. Therefore, it is not assigned here. A tentative new level of 2759 keV is proposed. The level is fed and depopulated by the 178 and 1349 keV gamma rays. But there is no other gamma ray to support this level. One more tentative level is at 2016 or 2001 keV and accommodate the 69 and 83 keV gamma ray. But the intensity balance is unsatisfactory for this level. Other new gamma rays cannot be successfuly acommodated and remain unsolved. The results are summarized in Fig. 25. The intensity balance is satisfactory except a few tentative levels. The intensities of 847.6 and 848.2 keV gamma rays are determined to give the optimum balance by assuming the 680 keV gamma ray to be single component.

The K internal conversion coefficients show that the 1572 and 646 keV transition have E1 multipolarity. As the spin of ^{106m}Ag is 6[20] and the 222 keV transition has M1 multipolarity, the cascade transitions of 646, 222, 1572 keV determine the spins of 2084, 2306 and 2952 keV levels uniquely to be 3^-, 4^- and 5^+, respectively. The spin and parity of new 1909 keV level is assigned as 3^+, because it is fed by the 848 keV E2 transition from the 2757 keV 5^+ level and depopulated to the 1229 keV 4^+ level as well as to the 0^+ ground state by weak branching of the 1909 keV gamma ray. The weak branching of the 2077 keV gamma ray to the ground state shows that the 2077 keV level is fed by

the 229 keV E1 transition from the 2351 keV 4^- level and has the spin and parity of 3^+. The spin and parity of the 1562 keV level is assigned as 2^+ in the ^{106}Rh decay.[4,6]

7. Discussion

The experimental results are compared with the prediction of the spherical vibrational model of liquid drop.[10,12] The model identifys excited states of spherical nuclei with the phonon quantum number N. The vibrational states are expected to be located in equal energy separations with increasing N. Electromagnetic transitions are expected to take place only between the neighbouring states for which N is unity. The first 2^+ level and the second $0^+,2^+$ and 4^+ levels of ^{106}Pd are identified as the N=1 and N=2 state,respectively. The basic characteristics of these levels are listed in Table 9 together with the describtion of the spherical vibrational model. The conventional notations 0,2,0',2' and 4 are used to identify the levels. All the B(E2) values and their ratios have been obtained from Coulomb excitation measurements.[21,22] As listed in the table,the basic nature of these levels are well approximated by the model. Therefore,the nature of higher excited levels can also discussed on the basis of this model. The experimental data available for this purpose is the branching ratios of the gamma rays to feed these levels.

According to the model,there are five possible excited states for N=3,the spins and parities of which are $0^+,2^+,3^+,4^+$ and 6^+. The theoretical B(E2) values from this states to the N=2 states are represented in Fig.19.

Fig.19

All the B(E2) values in the figure are represented with the unit of $B(E2;2\rightarrow0)$.

The levels which are depopulated through considerable gamma-ray branching to these N=2 levels are the 1558 and 1932 keV ones. These are assigned to be N=3 states. The gamma-ray branching ratios and the B(E2) ratios from these 1558 and 1932 keV levels are tabulated in Table 10.

Table 10

For the gamma rays for which the fraction of E2 component are unknown, 100% E2 multipolarities are assumed to give the B(E2) ratio. The spin of the 1558 keV level has been determined by an angular correlation measurement to be 3.[23] The theoretical B(E2) ratio from the (I,N)=(3,3) state to the N=2 states agree fairly well with the corresponding experimental ratio from the 1558 keV level. The evidence indicate that the spherical vibrational model can also represent the basic nature of this level with the phonon quantum number N=3. This basic nature could be treated on the same theoretical basis, though the absolute values of B(E2) are difficult to determine experimentally. For the 1932 keV level, the experimental data for M1/E2 ratio in the 703 and 824 keV transitions are inconclusive. But this level is depopulated dominantly by these gamma rays. The 1419 keV transition is very weak. The 375 keV transition is also weak and prove to be dominant M1 in its character. The spin and parity of the 1932 keV level is assigned as 3^+ or 4^+ from the conversion coefficients. Therefore, the level is identified as (I,N)=(4,3) state. The 375 keV M1 transition has its origin in the configulation mixing of the particle state in the N=3 state. The experimental B(E2) ratio are also in

fair agreement with the corresponding theoretical one.

No evidence was found for (I,N)=(2,3) state in the present experiment. The 1562 keV 2^+ level is not assigned as this state. The level is fed with considerable beta decay branching in the ^{106}Rh decay.[4,6] But no gamma ray has been found to feed the N=2 levels from the 1562 keV level. The 6^+ and 0^+ levels are not fed in the ^{106m}Ag decay. Therefore, only the 3^+ and 4^+ states are able to be identified as the possible N=3 states in the ^{106m}Ag decay. The 1909 keV level as well as the 2077 keV one are not assigned as vibrational state from the observed gamma ray branching ratios. The crossover transition to the ground state is established for these levels. It is difficult to assign N=4 states for the level above 2200 keV from the observed gamma ray branching ratios. The 2084 keV 3^- level has been excited in coulomb[21] excitation experiment and identified as the first octupole vibrational state.

Acknowledgement:

The author wishes to express his sincere thank to Dr. Y. Yoshizawa for his valuable discussion. He would like to express his appreciation to Prof. T. Wakatsuki for his encouragement in experiment. He is also grateful to Dr. S. Fukushima for his aid in chemical separation,and to Mr. T. Shibata,Mr. Y. Aoki and Mr. J. Kawa for their helps in experiment.

References

1) R.L.Robinson,F.K.McGowan and W.G.Smith, Phys.Rev. 119 (1960) 1692

2) W.G.Smith, Phys.Rev. 122 (196]) 1600

3) W.G.Smith, Phys.Rev. 131 (1962) 35]

4) Klaus-Dieter Strutz, Zeit.f.Phys. 201 (1967) 20

5) J.K.Temperley and A.A.Temperley, Nucl.Phys. A101 (1967) 641

6) P.Venugopala Rao and R.W.Fink, Nucl.Phys. A103 (1967) 385

7) H.W.Taylor,N.Neff,and J.D.King, Nucl.Phys. A106 (1968) 49

8) J.A.Moragues,P.Reyes-Suter and T.Suter, Nucl.Phys. A106 (1968) 289

9) E.Y.de aisenberg and J.F.Saurez, Nucl.Phys. 83 (1966) 289

10) A.Bohr, Dan.Mat.Fys.Medd. 27 (1953) no.16
A.Bohr,B.R.Mottelson, Dan.Mat.Fys.Medd. 27 (1953) no.16

11) E.D.Klema,and F.K.McGowan,Phys.Rev. 92 (1953) 1469

12) Y.Yoshizawa, Phys.Lett. 2 (1962) 261

13) W.Scheuer,T.Suter,P.Reyes-Suter and E.Aasa, Nucl. Phys. 54 (1964) 221

14) E.R.Cohen and J.W.M.DuMond, Rev.Mod.Phys. 37 (1965) 537

15) Y.Yoshizawa, Gamma Ray Energy Standard (March 1971)

16) H.Inoue,T.Morii and Y.Yoshizawa, to be published

17) O.Kofoed-Hansen,J.Lindhard and O.B.Nielsen, Det. Kgl.Dansk.Vid.Selsk. 25 (1950) no.16

18) R.C.Greenwood,R.G.Helmer and R.J.Gehrke, Nucl.Inst. Meth. 77 (1970) 141

19) R.S.Hager and E.C.Seltzer, CALT-63-60 (1967) Internal Conversion Tables

20) W.B.Ewbank, W.A.Nierenberg, H.A.Shugart and H.B.Silsbee Phys.Rev. 110 (1958) 595

21) R.L.Robinson, F.K.McGowan, P.H.Stelson, W.T.Milner and R.O.Sayer, Nucl.Phys. A124 (1969) 553

22) D.Eccleshall, B.M.Hind, M.L.J.Yates and M.MacDnald, Nucl.Phys. 37 (1962) 377

23) Y.Gono, private comunication

Figure Captions

Fig.1 Decay scheme of ^{106m}Ag proposed by Moragues et al.[8)]

Fig.2 Block diagram of a 20 cc Ge(Li) spectrometer.

Fig.3 Linearity characteristics of a 40 cc Ge(Li) spectrometer. Open circles and closed circles indicate the values obtained in the separate runs. Error bars indicate the sum of the uncertainties in standard gamma ray energy and that in peak channel. The former are indicated with the length between two horizontal bars.

Fig.4 Linearity correction curves used for the 20 cc Ge(Li) spectrometer system.

Fig.5 An example of corrected linearity by using the correction curve in Fig.4

Fig.6 Detection efficiency of the 20 cc Ge(Li) detector (vertical type).

Fig.7 Detection efficiency of the 40 cc Ge(Li) detector. The curve designated as SUM show the detection efficiency at about 3mm from the front surface of detector capsule.

Fig.8 Horizontal section of an orange type beta ray spectrometer.

Fig.9 Internal conversion line of ^{137}Cs used as calibration standard for the spectrometer.

Fig.10 Gamma-ray spectrum of ^{106m}Ag in full energy range. The source was set at 7 cm from the detector. A number of sum peaks are observed in the spectrum.

Fig.11 An example of the spectrum for energy measurement with the mixed spectrum method.

Fig.12 An example of summing peak spectrum measured with the 40 cc spectrometer.

Fig.13 Internal conversion electron spectrum obtained by the orange type beta ray spectrometer.

Fig.14 Comparison of the energy values obtained in the separate runs with the Ge(Li) spectrometers. Small dots with a bar represent the result in each measurement. Large dots with a bar show the results of the unweighted mean with standard deviation. Open circles indicate the result of the weighted mean and their bars that of uncertainties. Of these two type uncertainties, the larger ones are adopted to give the quated uncertainties in Table 4.

Fig.15 Results of the summing peak spectrum measurements. The observed summing peak energies and their assignments are represented by dashed lines. Only the summing peaks for direct cascade gamma rays are accomodated in the figure.

Fig.16 Results of the internal conversion coefficients. The values are normalized to that of the 512 keV E2 transition.

Fig.17 Schematic illustration of the procedure to determine the level energies. Only the gamma rays used to determine the level energies are represented in the figure. The energies of these gamma rays were determined with the best accuracies in present experiment. The determined level energies are written at the left side of each level, while the procedures to obtain the resulted values are written at the right side of corresponding levels. For example, the level energy of the 1229 keV level are obtained by subtracting the 328 keV gamma ray energy from the 1558 keV level energy which is obtained by adding the 512,616 and 430 keV gamma ray energies. This exemplified procedure can give a better accuracy to the 1558 keV level energy than the procedure in which the 717 keV gamma ray is adopted to give the same one. The 2757 and 2952 keV level energies are determined from the compromise one of three cascade gamma ray pairs and a crossover gamma ray.

Fig.18 Decay scheme proposed in present experiment. The energies of two 848 keV gamma rays are determined from the corresponding level separation.

Fig.19 Theoretical B(E2) ratios between one, two and three phonon states.

Table 1

Gamma-ray energy standards used in present experiment

Parent nucleus	Energy	class	Reference
^{75}Se	66.05 ± 0.01	A	a
^{182}Ta	84.678 ± 0.003	A	b
^{75}Se	96.731 ± 0.007	D	c
^{182}Ta	100.102 ± 0.002	A	b
^{75}Se	121.113 ± 0.010	D	c
^{75}Se	135.998 ± 0.010	D	c
^{182}Ta	179.392 ± 0.004	A	b
^{75}Se	198.600 ± 0.020	D	c
^{182}Ta	222.104 ± 0.005	A	b
^{182}Ta	229.317 ± 0.008	A	b
^{75}Se	264.651 ± 0.015	D	c
^{75}Se	279.522 ± 0.012	D	c
^{192}Ir	295.952 ± 0.006	B	d
^{192}Ir	308.451 ± 0.006	B	d
^{192}Ir	316.501 ± 0.006	B	d
^{133}Ba	356.004 ± 0.017	D	c
^{133}Ba	383.850 ± 0.020	D	c
^{198}Au	411.795 ± 0.007	B	e
^{192}Ir	468.066 ± 0.010	B	d
mc^2	511.006 ± 0.002		f
^{207}Bi	569.674 ± 0.020	D	g
^{228}Th	583.139 ± 0.023	c	h
^{192}Ir	588.575 ± 0.017	B	e
^{192}Ir	604.463 ± 0.011	B	d
^{192}Ir	612.453 ± 0.011	B	d
^{110m}Ag	657.72 ± 0.03	D	i
^{137}Cs	661.635 ± 0.019	C	j
^{110m}Ag	686.83 ± 0.03	D	i

Table 1 (continued)

Parent nucleus	Energy	class	Reference
^{110m}Ag	706.66 ± 0.04	D	i
1 ^{110m}Ag	744.20 ± 0.04	D	i
^{110m}Ag	763.88 ± 0.04	D	i
^{54}Mn	834.795 ± 0.040	D	g
^{110m}Ag	884.66 ± 0.04	D	i
^{88}Y	897.996 ± 0.034	D	g
^{110m}Ag	937.47 ± 0.04	D	i
^{207}Bi	1063.614 ± 0.040	D	g
^{65}Zn	1115.51 ± 0.07	D	k
^{60}Co	1173.226 ± 0.040	C	e
^{22}Na	1274.52 ± 0.07	D	k
^{60}Co	1332.483 ± 0.046	C	e
^{110m}Ag	1384.22 ± 0.04	D	i
^{40}K	1460.9 ± 0.3	D	e
^{110m}Ag	1475.74 ± 0.04	D	i
^{110m}Ag	1504.91 ± 0.08	D	i
^{228}Th	1592.46 ± 0.10	C	h
^{88}Y	1836.075 ± 0.050	D	g
^{228}Th	2103.46 ± 0.10	C	h
^{228}Th	2614.47 ± 0.10	C	h

References of Table 1

a) W.F.Edwards and C.J.Gallagher.Jr., Nuclear Physics 26 (1961) 649; W.F.Edwards, J.W.M.DuMond and F.Boehn, Nuclear Physics 26 (1961) 670

b) U.Gruber, R.Koch, B.P.Maier and O.W.B.Schult, Z.Naturforschg. 20a (1965) 929

c) R.C.Greenwood, R.G.Helmer and R.J.Gehrke, Nucl. Inst. Meth. 77 (1970) 141

d) J.J.Reidy, Private communication

e) G.Murray, R.L.Graham and J.S.Geiger, Nuclear Physics 63 (1965) 353

f) E.R.Cohen and J.W.M.DuMond, Rev. Mod. Phys. 37 (1965) 537

g) R.G.Helmer, R.J.Gehrke and R.C.Greenwood, Nucl. Inst. Meth. to be published

h) R.L.Graham, G.Murray and J.S.Geiger, Can. J. Phys. 43 (1965) 171

i) J.H.Hamilton and S.M.Bramavar, Conference on Radioactivity in Nuclear Spectroscopy (1969); S.M.Bramavar, J.H.Hamilton, A.V.Ramayya, E.F.Zgajar, and C.E.Bemis.Jr., Nuclear Physics A125 (1969) 217

j) R.L.Graham, Private communication

k) W.W.Black and R.L.Heath, Nuclear Physics A90 (1967) 650

l) Y.Yoshizawa, T.Morii, T.Katoh and H.Gotoh, J. Nucl. Scie. Tech. 5 (1968) 432

Table 2

Gamma-ray relative intensity standards used for detection efficiency calibration in present experiment

Parent Nucleus	Gamma ray Energy (keV)	Relative Intensity	Reference
^{22}Na	511	180	a)
	1275	100	
^{60}Co	1173	100	
	1332	100	
^{75}Se	66	1.63 ± 0.06	b)
	97	5.57 ± 0.18	
	121	28.0 ± 0.6	
	136	95.5 ± 1.8	
	199	2.4 ± 0.1	
	265	100	
	280	42.2 ± 0.6	
	304	2.29 ± 0.14	
	401	19.5 ± 0.6	
^{88}Y	898	93	a)
	1836	99	
^{108m}Ag	434	99.1	c)
	614	99.7	
	722	99.8	
^{133}Ba	276	11.5 ± 0.3	d)
	303	29.5 ± 0.6	
	356	100	
	384	14.8 ± 0.4	
^{178}Ta	89	67.4	e)
	93	17.8	
	214	81.5	
	326	94.1	
	427	97.1	

References of Table 2

a) C. M. Lederer, J. M. Hollander and I. Perlman, Table of Isotopes sixth Edition(Table 5 of Appendix 1.)

b) W. F. Edward, J. W. M. DuMond and F. Boehm, Nucl. Phys. 26 (1961) 670

c) M. A. Wahlgren and W.W. Meinke , Phys. Rev. 118(1960) 181

d) H. Inoue, T. Morii and Y.Yoshizawa, to be published

e) F.F. Felber, Jr., F. S. Stephens, Jr., and Frank Asaro, J., Inorg. Nucl. Chem. 7(1958)153

C. J. Gallagher, Jr. and H. L. Nielsen, Phys. Rev. 126(1962)1525

Table 3

Reproducibility of peak counts ratio in separate measure-ment. the analysis method is described in text. A ^{178}Ta source was measured with 20cc detector.

Gamma ray energy (keV)	Relative value of peak counts			
	run 1	run 2	run 3	run 4
426.8	1.00	1.00	1.00	1.00
325.7	1.442	1.442	1.432	1.451
213.6	2.201	2.178	2.210	2.198
93.2	0.606	-----	0.626	-----

Table 4

Energies and Relative Intensities of the Gamma Rays emitted by ^{106m}Ag

present work		Moragues et al.		Taylor et al.	
energy (keV)	intensity	energy (keV)	intensity	energy (keV)	intensity
69.0 ± 0.4	5.9 ± 1.6				
70.3 ± 0.3	10.4 ± 1.6				
80.1 ± 0.2	3.9 ± 0.8				
83.2 ± 0.6	0.9 ± 0.5				
178.2 ± 0.5	0.6 ± 0.2				
195.05 ± 0.16	3.5 ± 0.5	194.93 ± 0.15	6 ± 3	194.8 ± 0.1	5
221.701 ± 0.015	75 ± 3	221.51 ± 0.10	83 ± 8	221.4	73
228.633 ± 0.021	24.0 ± 1.1	228.53 ± 0.12	29 ± 5	228.3	24
328.463 ± 0.023	13.0 ± 0.6	328.27 ± 0.25	18 ± 3	328.8	13
374.46 ± 0.13	3.0 ± 0.4	375.1 ± 0.7	3 ± 1	374.6	2.5
391.035 ± 0.026	42 ± 2	390.90 ± 0.20	43 ± 3	391.2	45
406.182 ± 0.020	153 ± 4	406.00 ± 0.15	152 ± 10	406.3	144
418.55 ± 0.23	3.8 ± 0.7	418.6 ± 0.7	7 ± 3	419.1	4
429.646 ± 0.022	150 ± 4	429.46 ± 0.15	161 ± 14	429.8	143
433.9 ± 0.5	1.0 ± 0.4				
450.976 ± 0.022	322 ± 8	450.80 ± 0.20	310 ± 16	451.1	330
474.061 ± 0.030	10.6 ± 0.6	474.2 ± 0.3	12 ± 3	474.1	12
511.852 ± 0.010	1000 ± 30	511.77 ± 0.20	1000 ± 30	511.8	1000
522.3 ± 0.3	1.0 ± 0.2				
585.97 ± 0.10	5.0 ± 1.1	586.0 ± 0.8	9 ± 3	585.8 ± 0.2	4
601.17 ± 0.07	18.4 ± 1.0	600.88 ± 0.25	23 ± 7	601.0	16
616.169 ± 0.031	246 ± 7	616.05 ± 0.25	236 ± 20	616.0	232
646.026 ± 0.046	16.6 ± 1.1	645.5 ± 1.0	18 ± 3	645.4	22
680.19 ± 0.10	24.9 ± 0.9	680.3 ± 0.6	25 ± 8	679.9	24
703.11 ± 0.08	51 ± 2	703.3 ± 0.5	52 ± 4	702.8	50
717.34 ± 0.09	330 ± 9	717.1 ± 0.4	320 ± 12	717.1	312
748.36 ± 0.11	235 ± 7	748.2 ± 0.3	227 ± 10	748.1	257
793.17 ± 0.10	67 ± 3	792.8 ± 0.3	65 ± 13	793.0	64
804.28 ± 0.10	141 ± 6	803.9 ± 0.3	124 ± 10	804.1	142

808.36	± 0.11	46	± 5	807.5	± 0.5	42	± 8	808.1		67
824.69	± 0.07	175	± 5	824.5	± 0.3	160	± 14	824.4		173
847.82	± 0.06	50	± 2	847.5	± 0.4	45	± 10	847.6		43
874.81	± 0.18	3.8	± 0.5	875	± 2	7	± 3	874.9	± 0.2	4
949.52	± 0.25	2.2	± 0.4							
956.21	± 0.23	5.4	± 0.9	956	± 2	8	± 3	956.3	± 0.2	4
986.8	± 0.4	0.04								
1019.72	± 0.15	11.9	± 1.8	1019.7	± 0.8	9	± 5	1019.5	± 0.2	10
1045.83	± 0.08	337	± 11	1045.7	± 0.4	285	± 25	1045.6	± 0.1	337
1050.6	± 0.5	3.0	± 1.5							
1053.77	± 0.21	11.0	± 1.6	1053	± 3	11	± 3	1052.6	± 0.2	12
1077.2	± 0.5	0.6	± 0.2							
1121.59	± 0.18	6.5	± 0.7	1121	± 2	9	± 3	1122.3	± 0.2	10
1128.02	± 0.07	134	± 6	1127.8	± 0.5	106	± 6	1127.9		130
1136.85	± 0.19	2.6	± 0.3					1135.8	± 2.0	5
1168.25	± 0.25	1.1	± 0.3							
1178.07	± 0.21	1.3	± 0.3							
1199.39	± 0.10	128	± 6	1199.1	± 0.6	106	± 8	1199.2		116
1222.88	± 0.12	80	± 4	1222.8	± 0.6	61	± 6	1222.7		62
1349.5	± 0.6	1.4	± 0.5							
1394.35	± 0.14	17	± 2	1394.2	± 1.0	17	± 6	1394.2	± 0.2	12
1419.4	± 0.8	0.4	± 0.2							
1527.65	± 0.19	186	± 15	1527.0	± 1.0	155	± 5	1527.4		161
1565.40	± 0.30	5.5	± 0.5	1565	± 2	8	± 4	1565.6	± 0.3	8
1572.35	± 0.15	75	± 6	1572.1	± 1.0	70	± 5	1572.1		67
1690.2	± 0.4	0.41	± 0.07	1691	± 2	0.5	± 0.2			
1722.76	± 0.18	16	± 2	1722.1	± 1.2	15	± 1	1722.3	± 0.2	12
1771.06	± 0.31	0.46	± 0.08	1770	± 2	0.6	± 0.2	1770.6	± 1.0	0.4
1794.01	± 0.27	0.43	± 0.17	1793	± 2	0.6	± 0.2	1793.3	± 1.0	0.4
1839.05	± 0.10	23	± 3	1837.9	± 1.2	20	± 2	1838.5		18
1909.1	± 0.6	0.15	± 0.05							
1932.5	± 0.4	0.03								
2077.3	± 0.8	0.02	+ 0.02 − 0.01							
2084.0	± 0.4	0.19	± 0.15	2082	± 2	0.20	± 0.06	2084.2	± 1.0	0.1
								2244.9	± 1.0	0.2

Table 5

Application of Ritz Rule based on the transition assignments of Moragues et al.
All the energy values are written in keV

Level		Gamma Ray Energy		Sum		Gamma Ray Energy	Difference
base	inter-mediate	E_i	E_j	$E_i + E_j$		E_{ij}	$E_i+E_j-E_{ij}$
0	512	511.849	+ 616.169	= 1128.018	± 0.033	1128.022 ± 0.065	-0.00_4
	512		+ 1565.40	= 2077.25	± 0.30	2077.3 ± 0.8	-0.05
	512		+ 1572.35	= 2084.20	± 0.15	2084.0 ± 0.4	0.2
512	1128	616.169	+ 429.646	= 1045.815	± 0.039	1045.83 ± 0.08	-0.01_5
			+ 1222.88	= 1839.05	± 0.13	1839.05 ± 0.10	0.0
512	1229	717.34	+ 328.463	= 1045.80	± 0.10	1045.83 ± 0.08	-0.03
			+ 847.82	= 1565.16	± 0.12	1565.40 ± 0.30	-0.24
			+ 1121.59	= 1838.93	± 0.20	1839.05 ± 0.10	-0.12
512	1558	1045.83	+ 748.358	= 1794.19	± 0.15	1794.01 ± 0.27	0.18
			+ 793.17	= 1839.00	± 0.13	1839.05 ± 0.10	-0.05
512	2084	1572.35	+ 221.701	= 1794.05	± 0.15	1794.01 ± 0.27	0.04
1128	1557	429.646	+ 374.458	= 804.10	± 0.13	804.28 ± 0.10	-0.18
			+ 793.17	= 1222.82	± 0.11	1222.88 ± 0.12	-0.06
1128	1932	804.28	+ 418.55	= 1222.83	± 0.29	1222.88 ± 0.12	-0.05
1229	1557	328.463	+ 374.46	= 702.92	± 0.13	703.11 ± 0.08	-0.19
			+ 793.17	= 1121.63	± 0.10	1121.59 ± 0.18	-0.04
			+ 808.36	= 1136.82	± 0.11	1136.85 ± 0.19	-0.03
			+ 1199.39	= 1527.85	± 0.12	1527.65 ± 0.19	+0.20
			+ 1394.35	= 1722.82	± 0.15	1722.76 ± 0.18	0.06

Table 5 (continued)

1229	1932	703.11	+	418.55	=	1121.66	± 0.24	1121.59	± 0.18	0.07
			+	824.69	=	1527.80	± 0.11	1527.65	± 0.19	0.15
			+	1019.72	=	1722.83	± 0.17	1722.76	± 0.18	0.07
1229	2077	847.82	+	680.19	=	1528.01	± 0.12	1527.65	± 0.19	0.36±0.23
			+	874.81	=	1722.63	± 0.19	1722.76	± 0.18	-0.13
1229	2282	1053.77	+	474.06	=	1527.83	± 0.22	1527.65	± 0.19	0.18
1229	2757	1527.65	+	195.05	=	1722.70	± 0.25	1722.76	± 0.18	-0.06
1558	2306	748.36	+	450.976	=	1199.34	± 0.12	1199.39	± 0.11	-0.05
			+	646.026	=	1394.39	± 0.13	1394.35	± 0.15	+0.04
1558	2531	793.17	+	406.182	=	1199.35	± 0.10	1199.39	± 0.11	-0.04
			+	601.17	=	1394.34	± 0.12	1394.35	± 0.15	-0.01
1558	2366	808.36	+	391.035	=	1199.40	± 0.12	1199.39	± 0.11	0.01
			+	585.97	=	1394.33	± 0.16	1394.35	± 0.15	-0.02
1558	2757	1199.39	+	195.05	=	1394.40	± 0.20	1394.35	± 0.15	0.09
1932	2757	824.69	+	195.05	=	1019.74	± 0.20	1019.72	± 0.15	0.02
2077	2306	228.633	+	450.976	=	679.609	± 0.031	680.19	± 0.10	-0.58±0.12
			+	646.026	=	874.659	± 0.051	874.81	± 0.18	-0.05
2306	2757	646.026	-	450.976	=	195.050	± 0.052	195.05	± 0.16	0.00
2350	2757	601.168	-	406.182	=	194.986	± 0.08			-0.06
2366	2757	585.97	-	391.035	=	194.94	± 0.10			-0.11

Table 6

Observed sum peaks of direct cascade gamma rays for which no crossover gamma ray was found

Sum peak energy (keV)	Peak count		
	Expected (relative)	Observed[a]	
673 = 451 + 222		340	p
1229 = 717 + 512		390	p
1238 = 808 + 430		18	c
1558 = 1046 + 512	260	310	p
= 430 +1128	47		
1629 = 406 +1123	59	170	p
= 825 + 804	80		
= 1199 + 430	33		
1824 = 1020 + 804	4.4	15	c
= 601 +1223	4.5		
= 1394 + 430	5.8		
1854 = 1137 + 717	1.5	17	c
= 808 +1046	15		
1932 = 804 +1128		22	p
2245 = 406 +1839	11	110	p
= 1199 +1046	27		
= 1528 + 717	69		
2306 = 222 +2084	0.4	0.3	c
= 1794 + 512	0.18		
2351 = 1223 +1128	8	18	p
= 1839 + 512	10		
2440 = 874 +1565	0.2	11	p
= 601 +1839	5.2		
= 1394 +1046	4.9		
= 1723 + 717	0.9		
2519 = 680 +1839		1.1[b]	w

a) The designation p, c and w represent prominent, considerable and weak, respectively.

b) A weak sum peak was observed at 2520 keV. Half of this peakcount can be accounted for as that of indirect cascade sum of the 1394 and 1128 keV gamma rays. Other half is tentatively assigned as that of this direct cascade sum.

Table 7

Internal Conversion Electron Intensities and Conversion Coefficients

Transition Energy (keV)	K Electron Intensity		Conversion Coefficient $\times 10^3$			
	Present Work	Scheuer et al.	Experiment	Theory E1	Theory M1	Theory E2
195		44± 6	60 ±12	19.5	53	107
222		630±50	40.7 ± 3.8	13.5	37.5	68
229		67± 8	13.5 ± 1.8	12.7	35.0	62
328	53 ± 4	32±16	19.8 ± 1.8	4.85	13.8	18.9
375	5.5± 0.8		8.9 ± 1.8	3.50	9.9	12.5
391	94 ± 6	98±25	10.9 ± 0.9	3.05	8.8	10.8
406	300 ±15	300±20	9.5 ± 0.6	2.82	8.0	9.66
429	264 ±15	260±20	8.5 ± 0.6	2.50	7.0	8.1
451	146 ± 8	160±15	2.20± 0.15	2.15	6.2	7.0
474	12 ± 4[b]	17± 5	5.5 ± 1.9	1.92	5.5	6.0
512	1000 ±40	1000±40	(4.85)	1.58	4.55	4.85
586	4.8± 1.5		4.6 ± 1.4	1.16	3.40	3.40
601	9.5± 1.0	15± 4	2.5 ± 0.3	1.10	3.15	3.15
616	155 ± 3	155±15	3.06± 0.14	1.03	3.05	3.00
645	1.9± 0.6		0.56± 0.18	0.92	2.75	2.65
680	8.9± 1.2		1.7 ± 0.3	0.82	2.40	2.25
703	17 ± 3	30±10	1.6 ± 0.3	0.76	2.20	2.10
717	134 ± 7	130±10	1.97± 0.13	0.73	2.10	2.00
748	29 ± 5	37± 4	0.60± 0.11	0.68	1.92	1.80
793		24± 3	1.7 ± 0.3	0.60	1.69	1.55
804		40± 4	1.38± 0.16	0.58	1.65	1.48
808		12± 3	1.3± 0.3	0.57	1.64	1.45
824		54± 5	1.50± 0.15	0.55	1.55	1.40
847		14± 4	1.4 ± 0.4	0.52	1.45	1.32
1020	2.8± 0.6		1.1 ± 0.3	0.36	0.96	0.83
1046	61 ± 3	48± 4	0.88± 0.06	0.35	0.90	0.80
1128	20 ± 3	13± 3	0.72± 0.12	0.30	0.77	0.68
1199	17 ± 3	13± 4	0.64± 0.12	0.27	0.68	0.60
1223	10 ± 2	8± 3	0.61± 0.13	0.26	0.65	0.57
1395	1.7± 0.3		0.49± 0.06	0.205	0.49	0.44

Table 7 (continued)

1527	15 ± 2	0.39 ± 0.06	0.175	0.40	0.36
1572	3.1± 0.7	0.20 ± 0.05	0.166	0.38	0.34
1723	0.9± 0.3	0.27 ± 0.10	0.143	0.31	0.28
1836	1.4± 0.3	0.30 ± 0.07	0.13	0.27	0.24

Table 8

Fraction of E2 Component in some low Energy Gamma Rays

Transition Energy(keV)	Fraction of E2 Component(%)
195	$0.13 \begin{smallmatrix} + 0.22 \\ - 0.13 \end{smallmatrix}$
222	$0.10 \begin{smallmatrix} + 0.12 \\ - 0.10 \end{smallmatrix}$
328	$1.0 \begin{smallmatrix} + 0.0 \\ - 0.2 \end{smallmatrix}$ $1.0 \begin{smallmatrix} + 0.0 \\ - 0.3 \end{smallmatrix}$ a)
375	$0.0 \begin{smallmatrix} + 0.3 \\ - 0.0 \end{smallmatrix}$
391	$1.0 \begin{smallmatrix} + 0.0 \\ - 0.4 \end{smallmatrix}$
406	$0.9 \begin{smallmatrix} + 0.1 \\ - 0.4 \end{smallmatrix}$
429	$1.0 \begin{smallmatrix} + 0.0 \\ - 0.2 \end{smallmatrix}$

a) The value is calculated from K/L + M ratio

Table 9

Basic Properties of the N=1 and N=2 states in ^{106}Pd

Level energy and transition property	Experimental result	Theoretical prediction	Reference
E_2	511.9 keV		
E_4/E_2	2.40	2	
E_2'/E_2	2.20	2	
E_0'/E_2	2.22	2	
$B(E2:2\rightarrow0)$	$(14.2\pm0.8)\ 10^{-50}cm^4$		a
$B(E2:2\rightarrow0)/B_{sp}$	48		a
$B(E2:2'\rightarrow2)/B(E2:2\rightarrow0)$	0.96 ± 0.13	2	a
$B(E2:4\rightarrow2)/B(E2:2\rightarrow0)$	1.53 ± 0.17	2	a
	2.11 ± 0.36		b
$B(E2:0'\rightarrow2)/B(E2:2\rightarrow0)$	0.63 ± 0.11	2	a
$I(M1:2'\rightarrow2)/I(E2:2\rightarrow2)$	1/200	0	c

a) R.L. Robinson, F.K. McGowan, P.H. Stelson, W.T. Milner and R.O.Sayer, Nucl. Phys. A 124(1969) 553

b) D.Eccleshall, B.M. Hinds,M.J.L. Yate and N. Macdonald, Nucl. Phts. 37(1962) 377

c) R.L. Robinson, F.K. McGowan andW.G. Smith, Phys. Rev. 119(1960)1962

Table 10

Comparision of B(E2) ratio

Level Energy (keV)	Gamma Ray Energy	Gamma Ray Intensity	Fraction of E2 Component	B(E2) ratio Exp.	B(E2) ratio Theo.
1558	328	0.0866±0.0046	$1.0^{+0.0}_{-0.2}$	0.33±0.07	0.4
	430	1.0	$1.0^{+0.0}_{-0.2}$	1.0	1.0
	1046	2.24±0.10		0.026	0
1932	375	0.021±0.003	$0.0^{+0.3}_{-0.0}$	$0.0^{+0.16}_{-0.0}$	0
	703	0.362±0.017		0.71	0.91
	804	1.0		1.0	1.00
	1419	weak			0

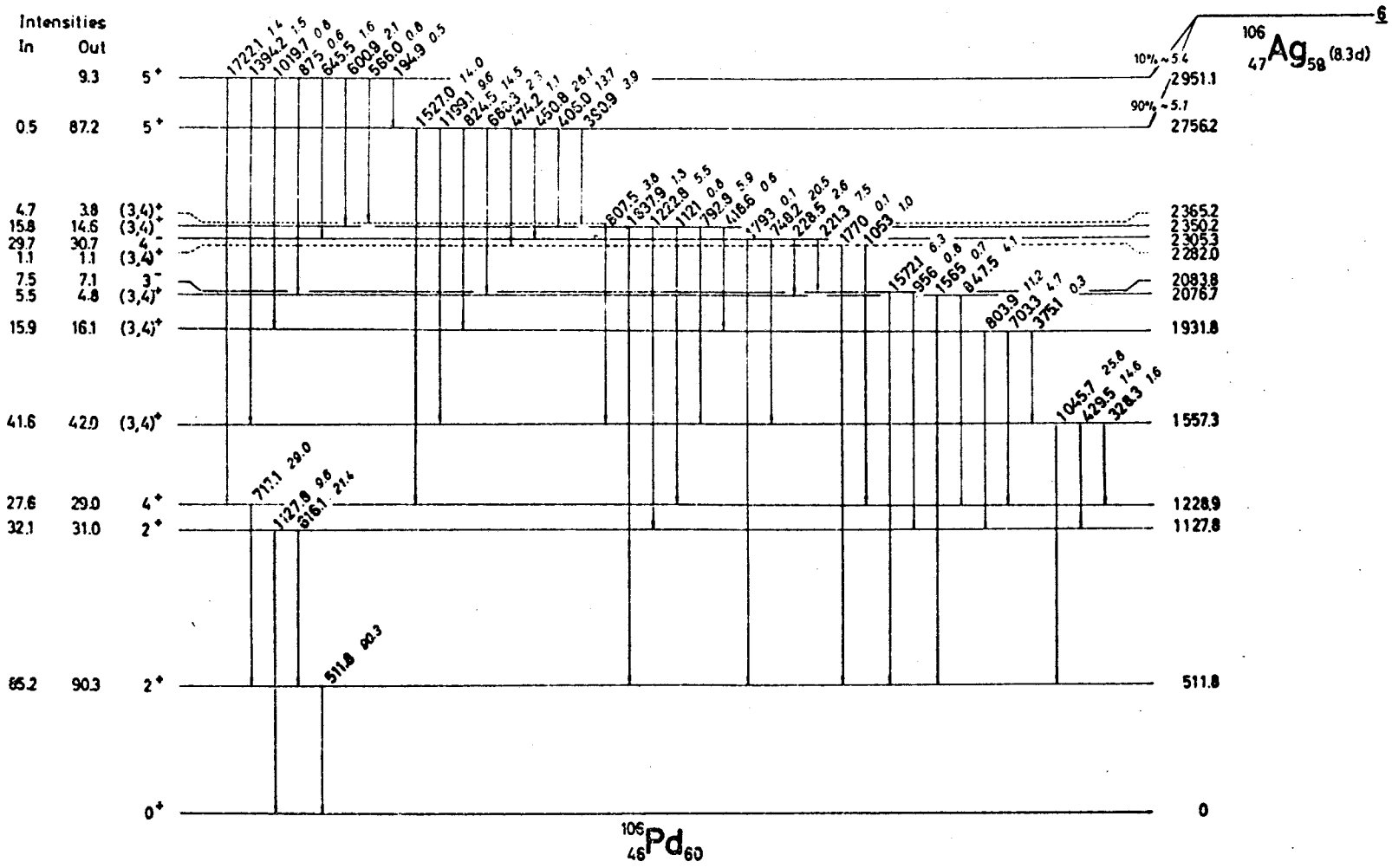

Fig. 1

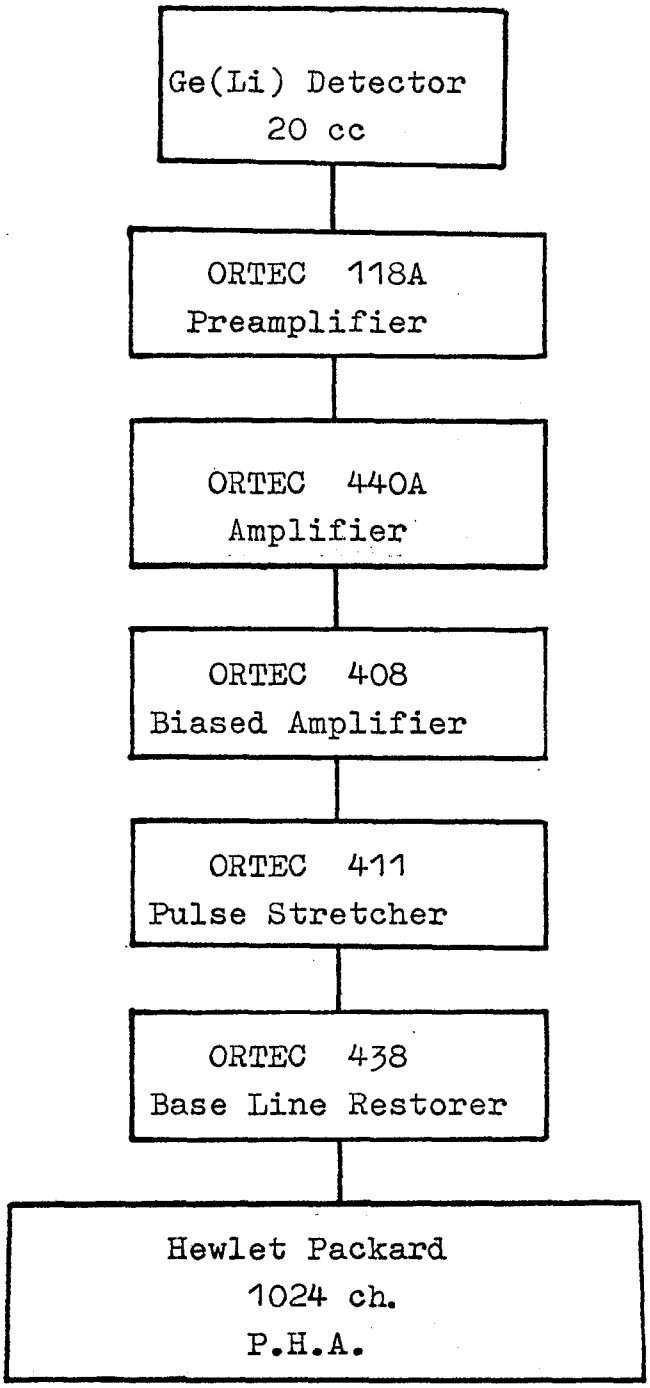
Ge(Li) Detector
20 cc
ORTEC 118A
Preamplifier
ORTEC 440A
Amplifier
ORTEC 408
Biased Amplifier
ORTEC 411
Pulse Stretcher
ORTEC 438
Base Line Restorer
Hewlet Packard
1024 ch.
P.H.A.

Fig. 2

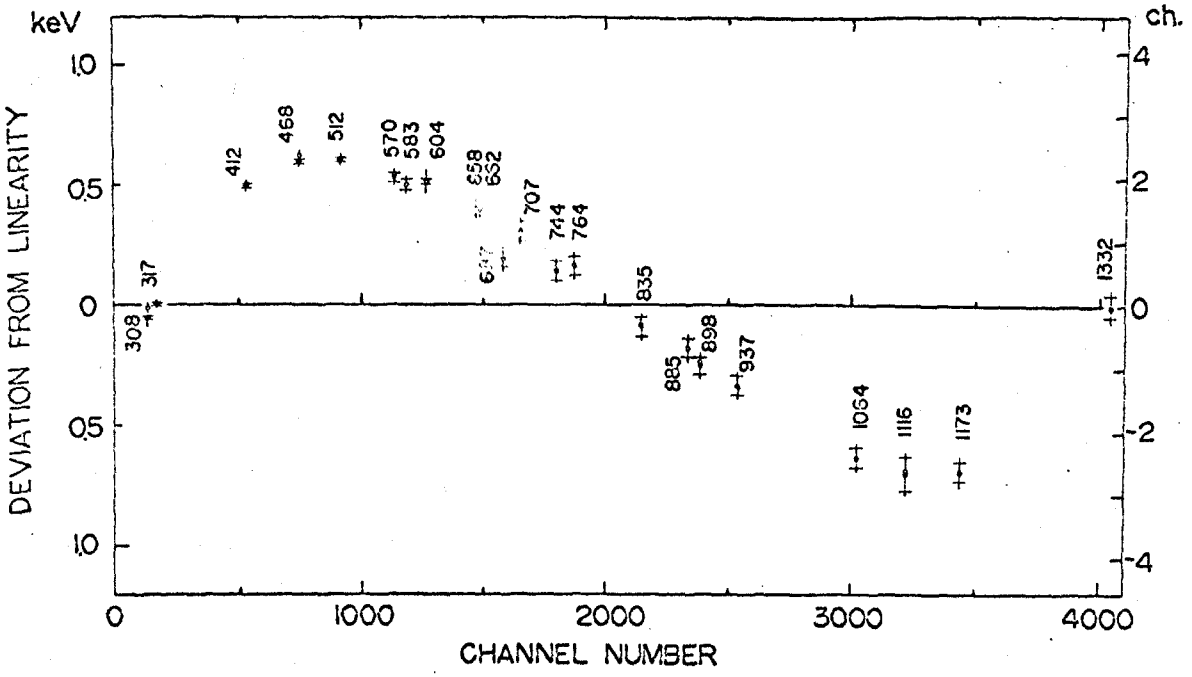
keV
ch.
DEVIATION FROM LINEARITY
CHANNEL NUMBER
1.0
0.5
0
0.5
1.0
4
2
0
-2
-4
0
1000
2000
3000
4000
317
412
468
512
570
583
604
658
632
707
714
764
835
885
898
937
1064
1116
1173
1332
308

Fig.3-a

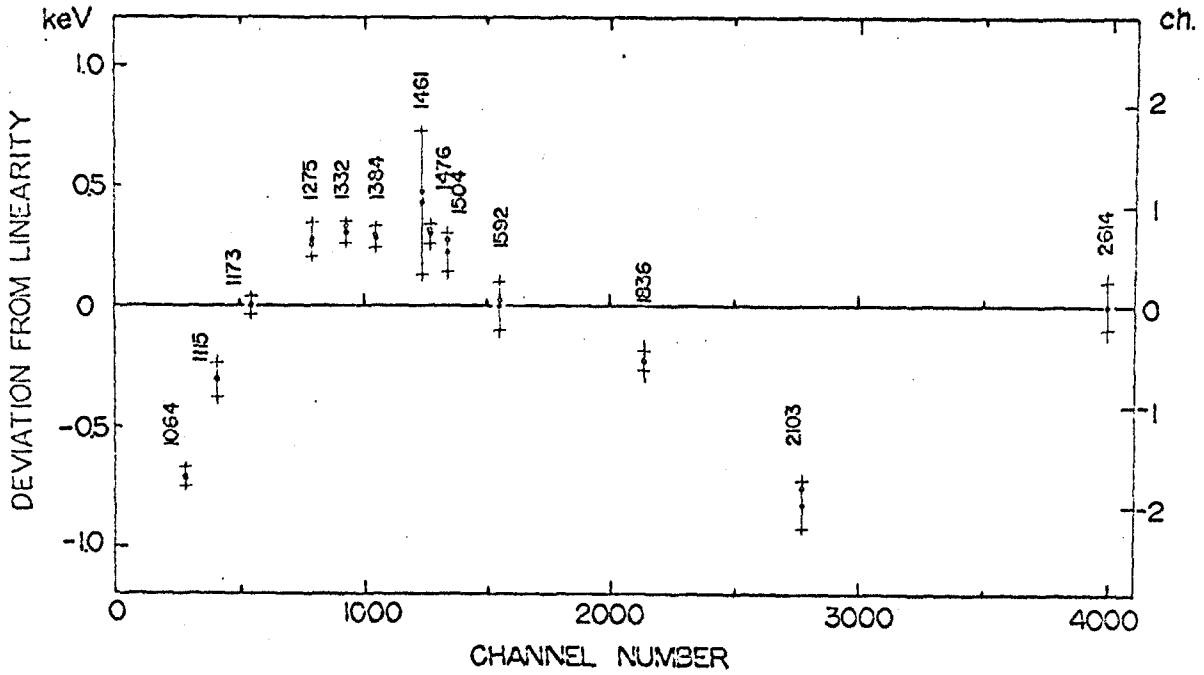
keV
ch.
DEVIATION FROM LINEARITY
CHANNEL NUMBER
1.0
0.5
0
-0.5
-1.0
2
1
0
-1
-2
0
1000
2000
3000
4000
1461
1275
1332
1384
1476
1504
1592
1173
1115
1064
1836
2103
2614

Fig.3-b

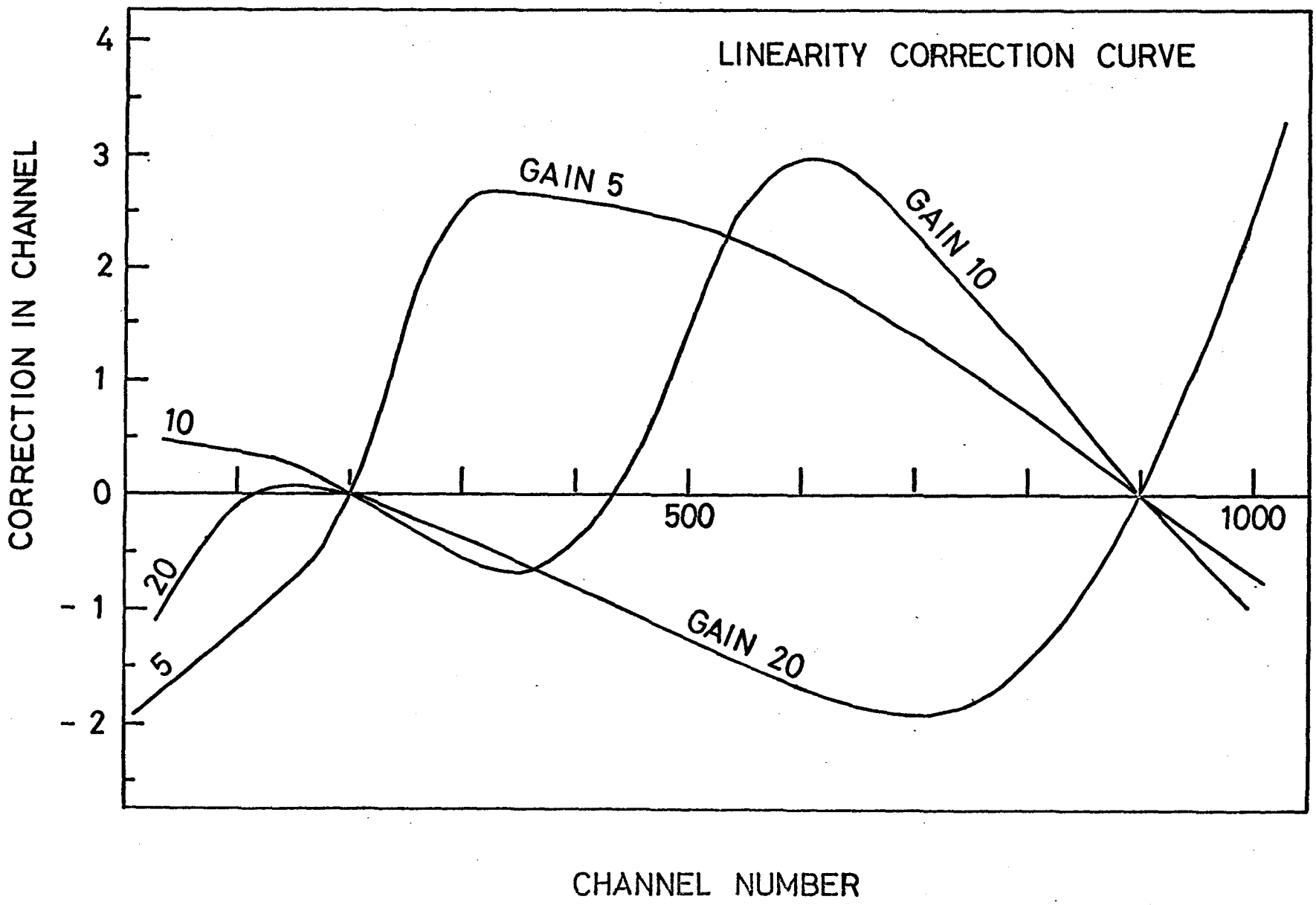
LINEARITY CORRECTION CURVE
CORRECTION IN CHANNEL
4
3
2
1
0
- 1
- 2
GAIN 5
GAIN 10
GAIN 20
10
20
5
500
1000
CHANNEL NUMBER

Fig.4

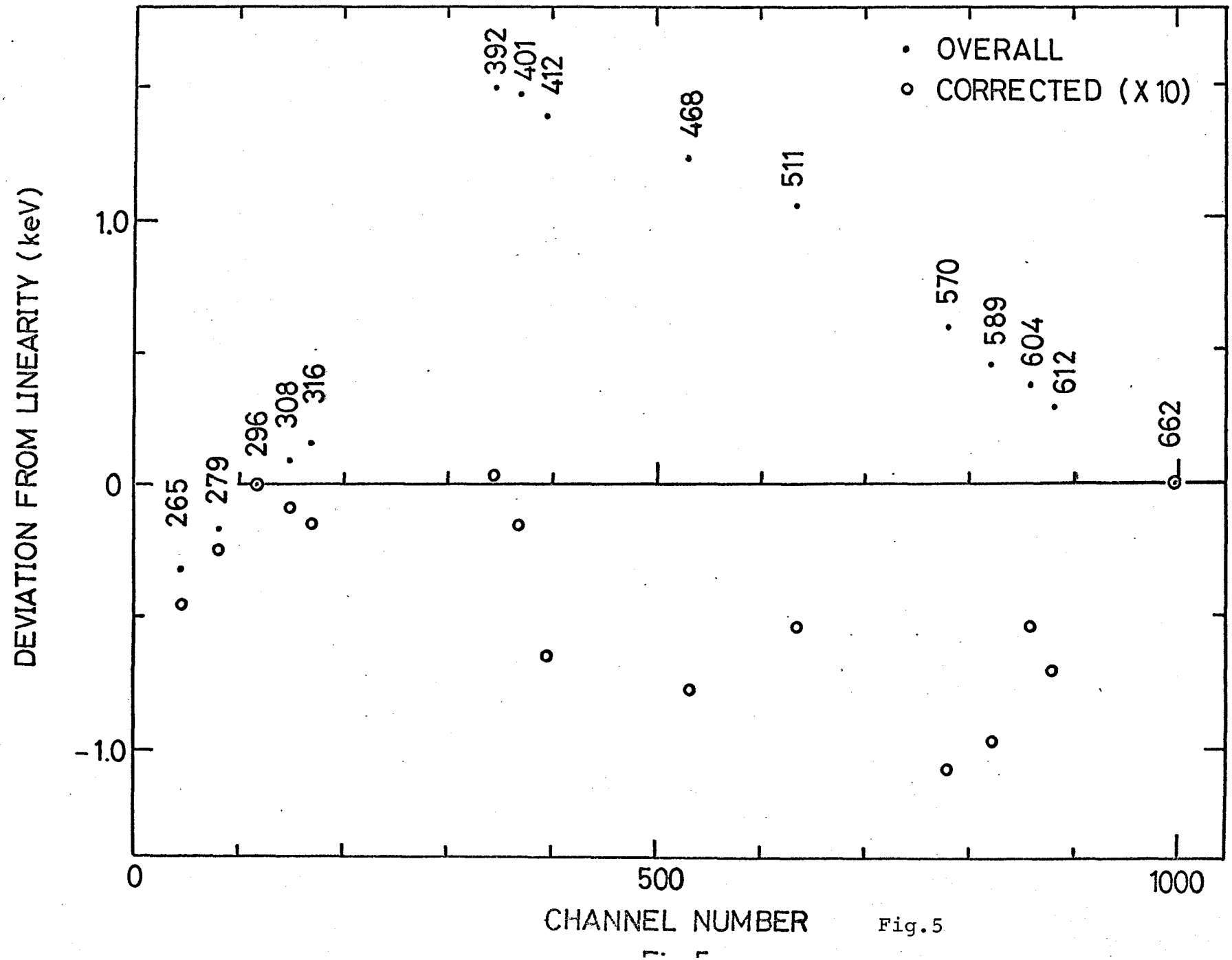
OVERALL
CORRECTED (X 10)
DEVIATION FROM LINEARITY (keV)
1.0
0
-1.0
0
500
1000
CHANNEL NUMBER
265
279
296
308
316
392
401
412
468
511
570
589
604
612
662

Fig.5

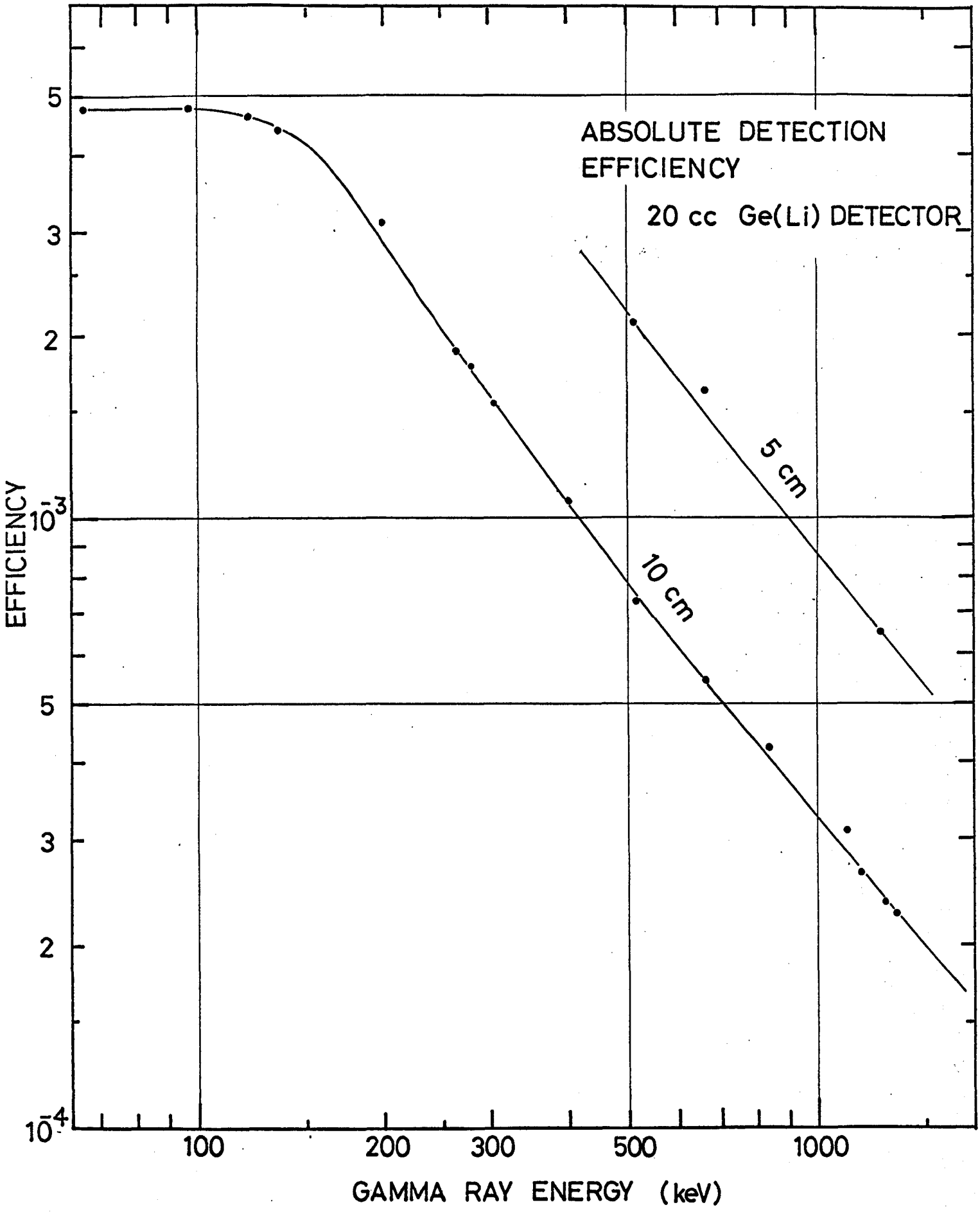
ABSOLUTE DETECTION
EFFICIENCY
20 cc Ge(Li) DETECTOR
5 cm
10 cm
EFFICIENCY
5
3
2
10^{-3}
5
3
2
10^{-4}
100
200
300
500
1000
GAMMA RAY ENERGY (keV)

Fig.6

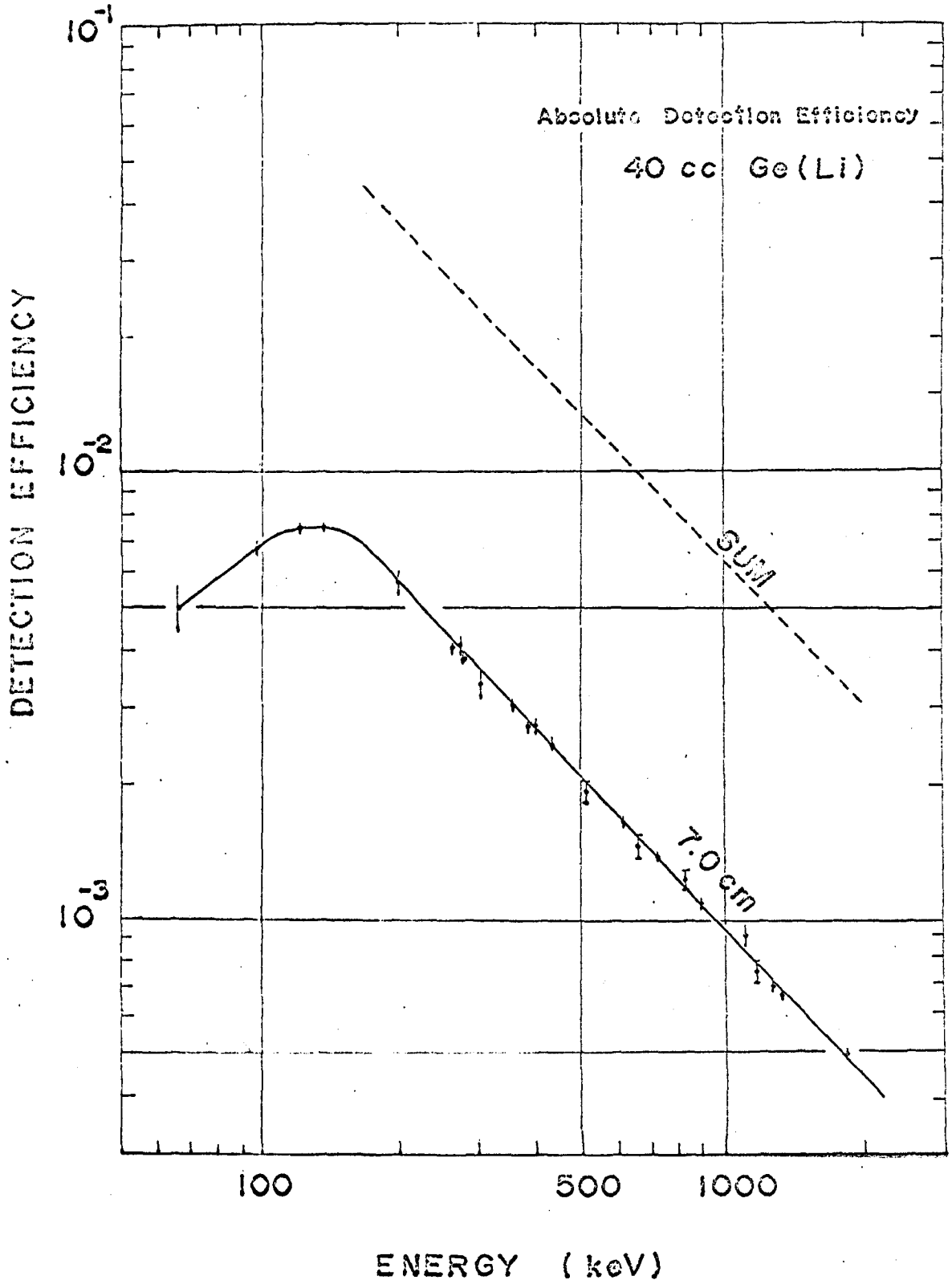
Absolute Detection Efficiency
40 cc Ge(Li)
SUM
7.0 cm
DETECTION EFFICIENCY
10^{-1}
10^{-2}
10^{-3}
100
500
1000
ENERGY (keV)

Fig.7

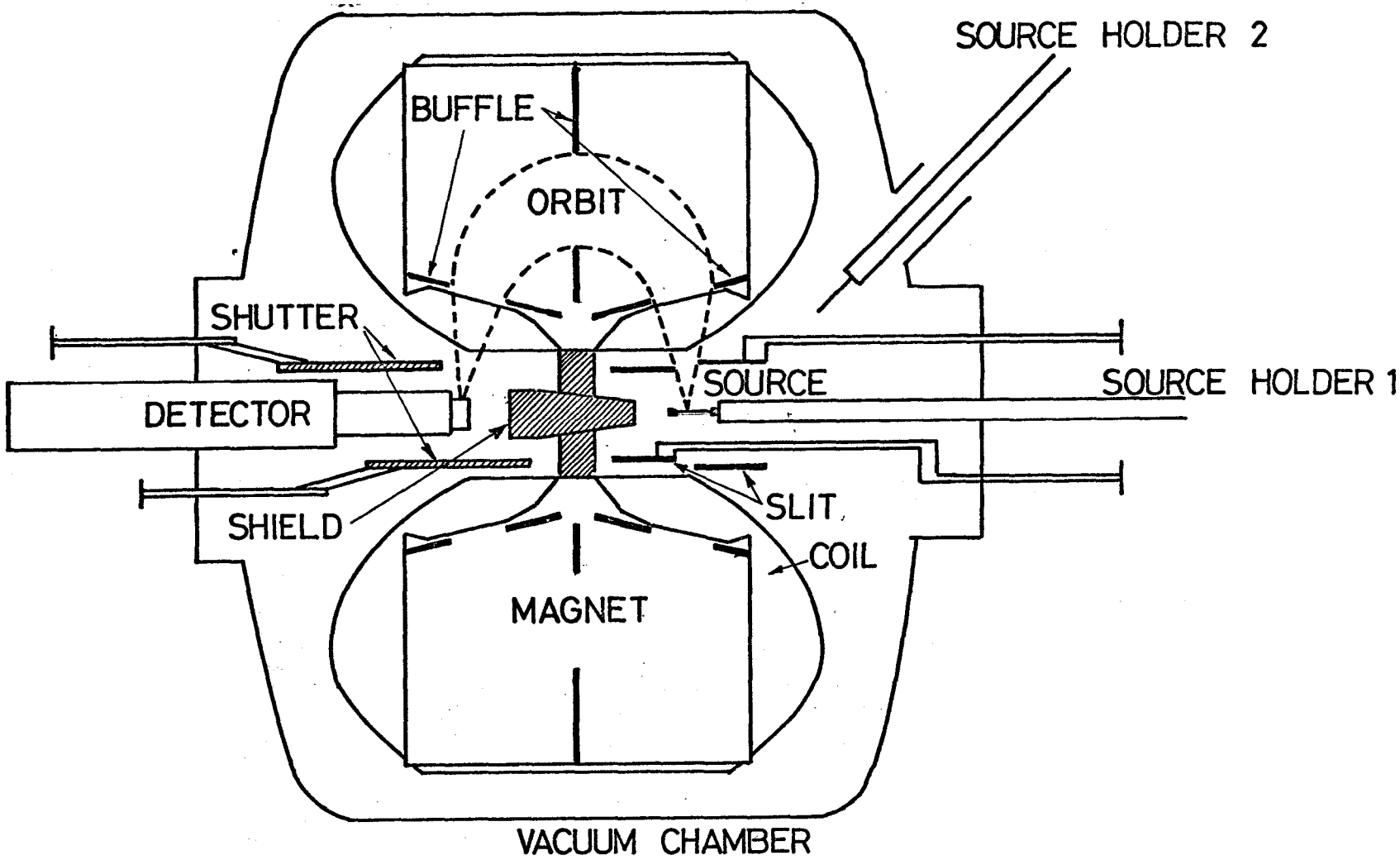
SOURCE HOLDER 2
BUFFLE
ORBIT
SHUTTER
DETECTOR
SOURCE
SOURCE HOLDER 1
SHIELD
SLIT
COIL
MAGNET
VACUUM CHAMBER

Fig.8

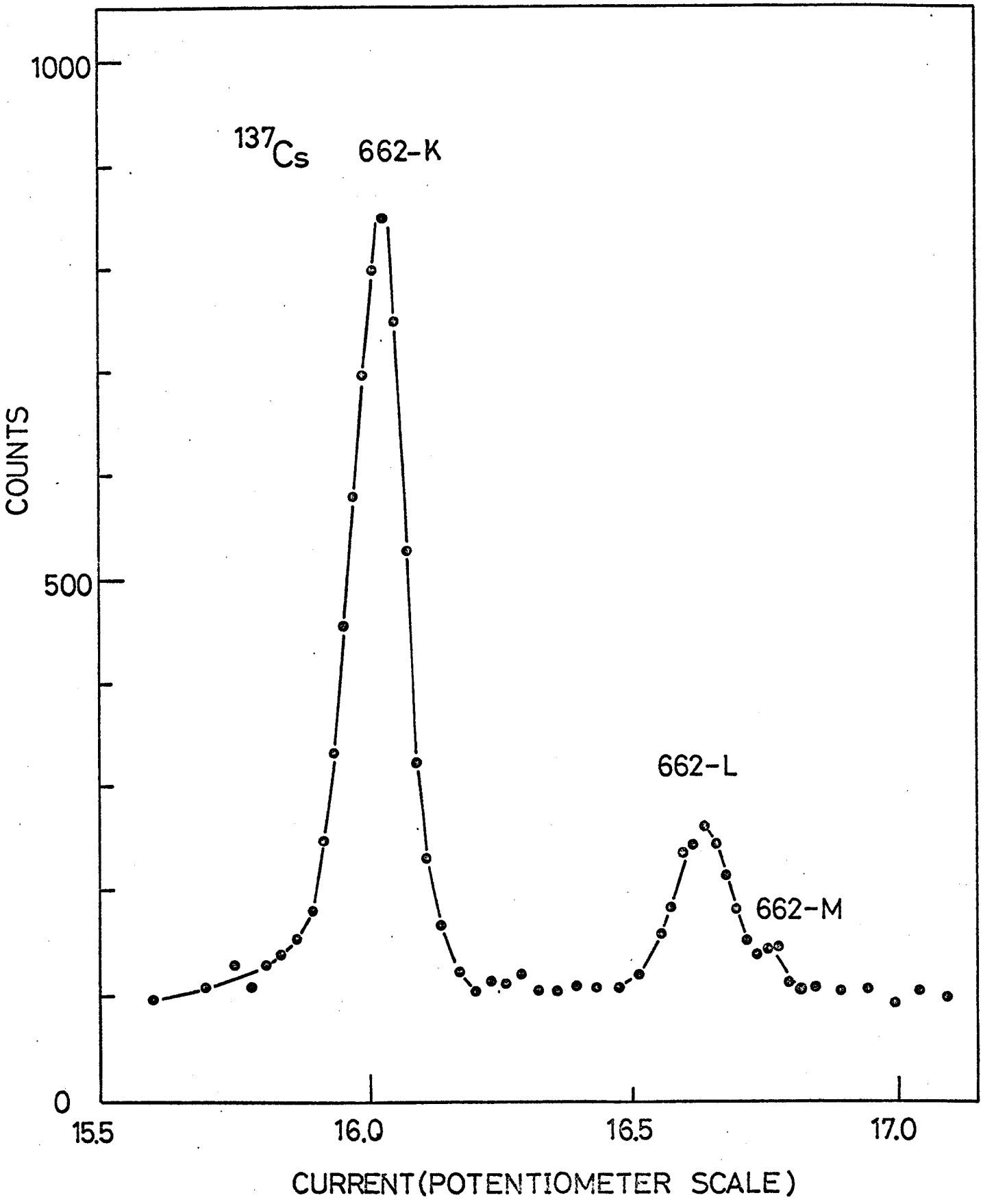
1000
500
0
COUNTS
^{137}Cs 662-K
662-L
662-M
15.5
16.0
16.5
17.0
CURRENT(POTENTIOMETER SCALE)

Fig. 9

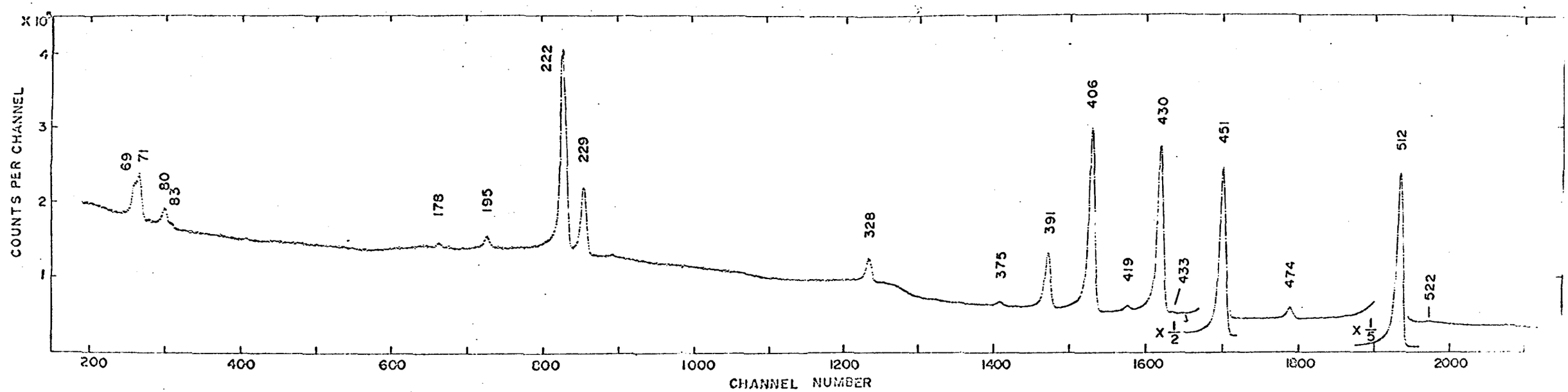

Fig.10-a

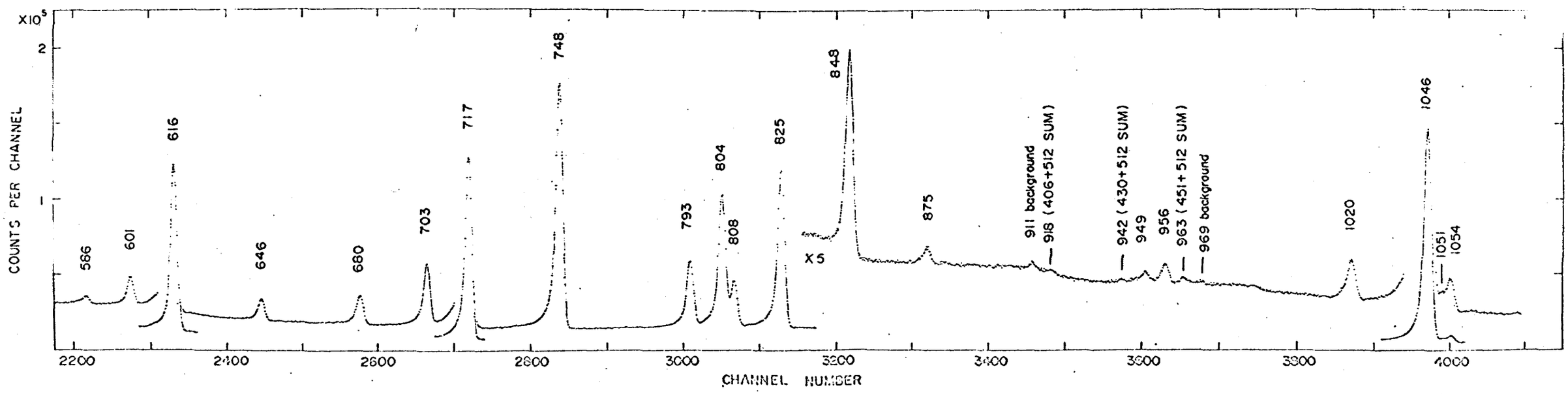

Fig.10-b

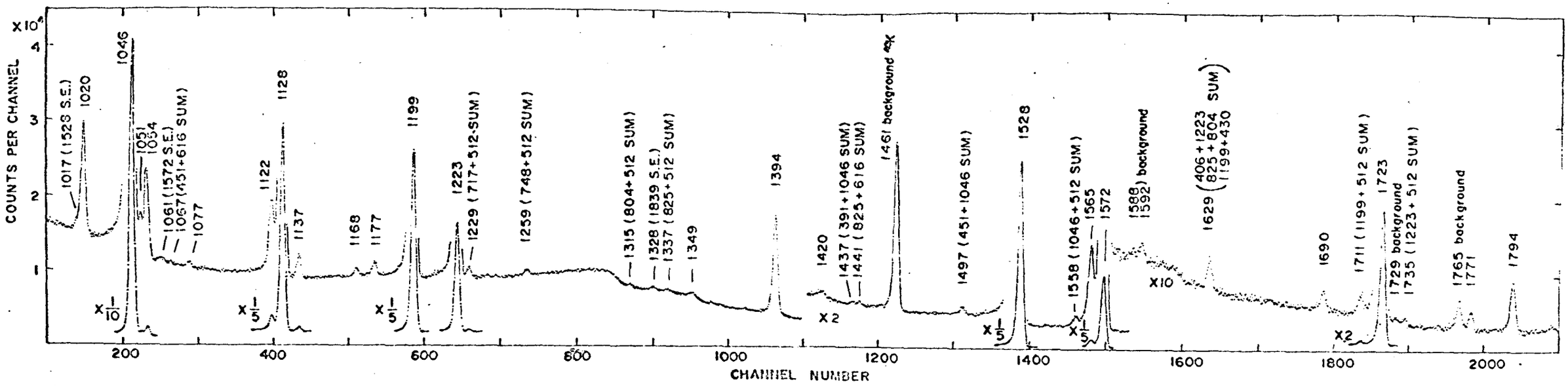

Fig.10-c

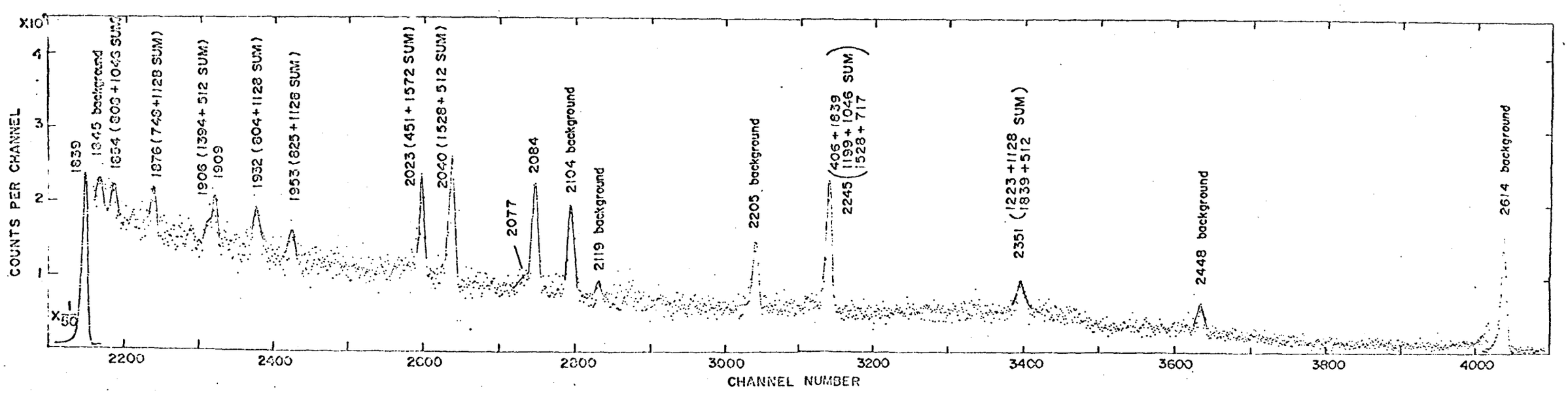

Fig.10-d

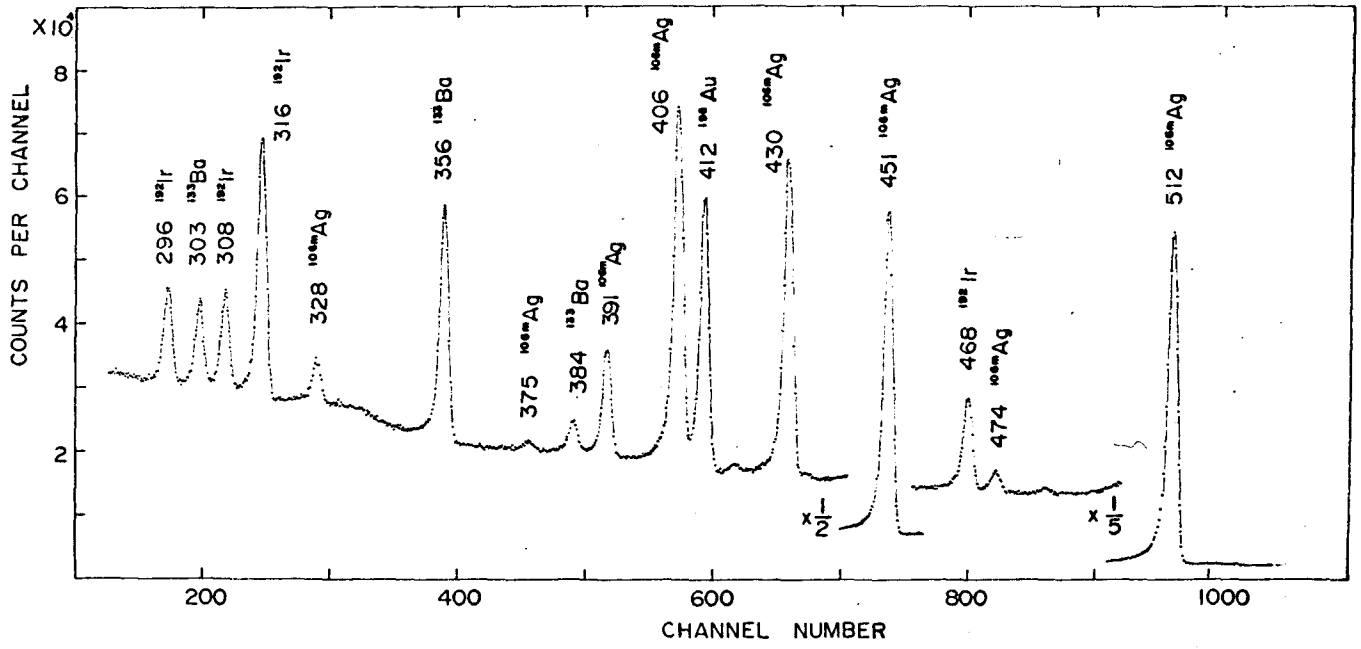
X10³
8
6
4
2
COUNTS PER CHANNEL
296 ¹⁹²Ir
303 ¹³³Ba
308 ¹⁹²Ir
316 ¹⁹²Ir
328 ¹⁰⁶ᵐAg
356 ¹³³Ba
375 ¹⁰⁶ᵐAg
384 ¹³³Ba
391 ¹⁰⁶ᵐAg
406 ¹⁰⁶ᵐAg
412 ¹⁹⁸Au
430 ¹⁰⁶ᵐAg
451 ¹⁰⁶ᵐAg
468 ¹⁹²Ir
474 ¹⁰⁶ᵐAg
512 ¹⁰⁶ᵐAg
x 1/2
x 1/5
200
400
600
800
1000
CHANNEL NUMBER

Fig.11

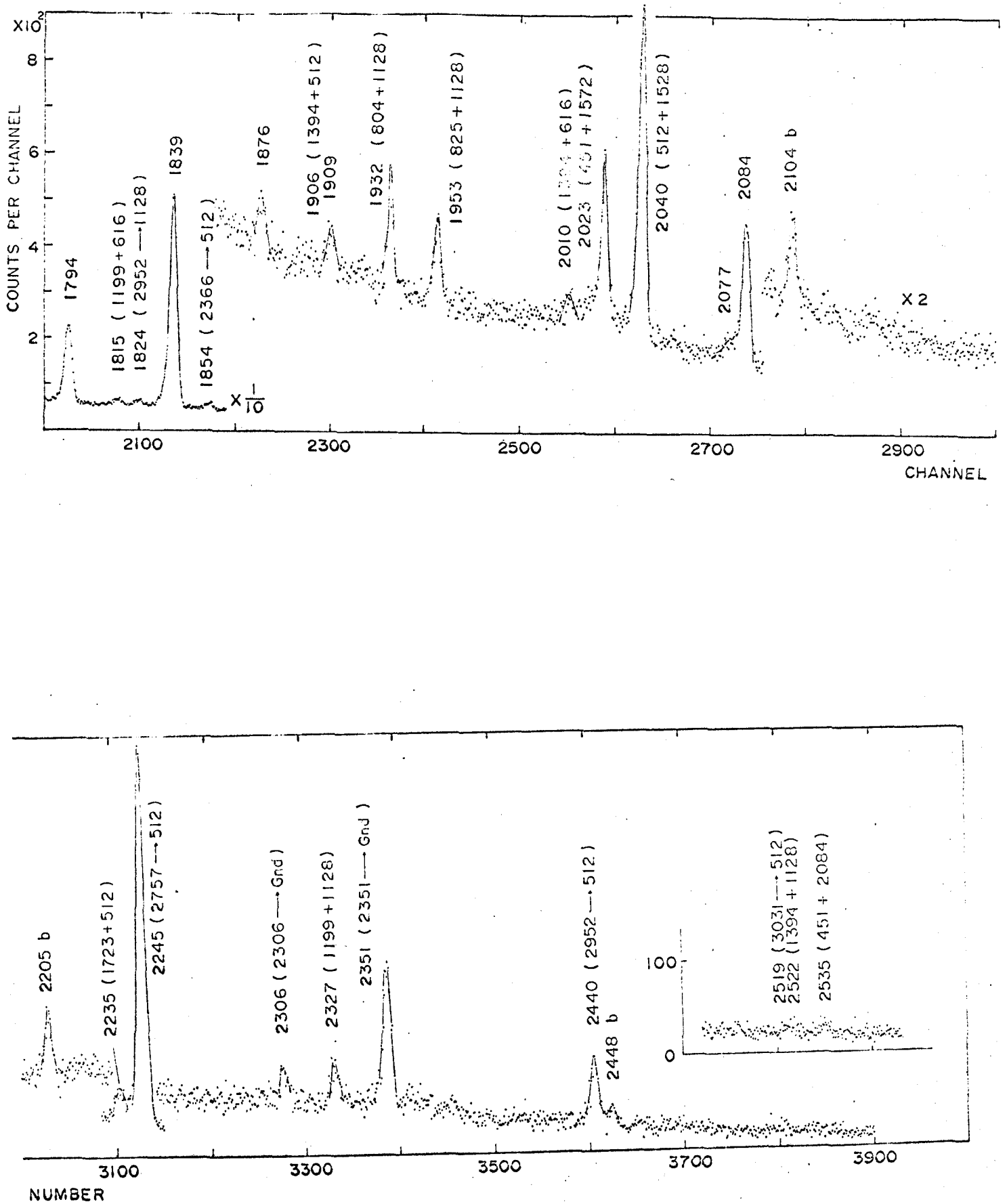
X10²
COUNTS PER CHANNEL
1794
1815 (1199+616)
1824 (2952 → 1128)
1839
1854 (2366 → 512)
X 1/10
1876
1906 (1394+512)
1909
1932 (804+1128)
1953 (825+1128)
2010 (1394+616)
2023 (451+1572)
2040 (512+1528)
2077
2084
2104 b
X 2
2100
2300
2500
2700
2900
CHANNEL
2205 b
2235 (1723+512)
2245 (2757 → 512)
2306 (2306 → Gnd)
2327 (1199+1128)
2351 (2351 → Gnd)
2440 (2952 → 512)
2448 b
2519 (3031 → 512)
2522 (1394+1128)
2535 (451+2084)
100
0
3100
3300
3500
3700
3900
NUMBER

Fig.12

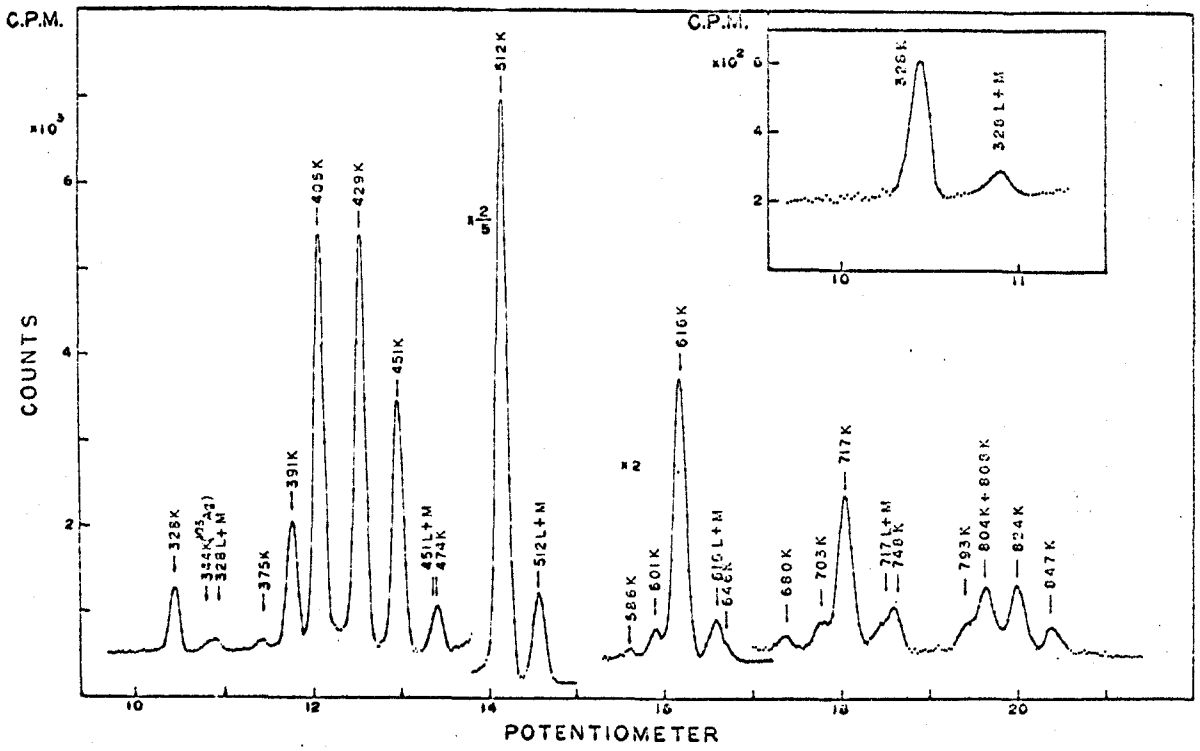
C.P.M.
COUNTS
POTENTIOMETER
328K
375K
391K
405K
429K
451K
512K
586K
601K
616K
680K
703K
717K
793K
824K
847K
C.P.M.
326K
326 L+M

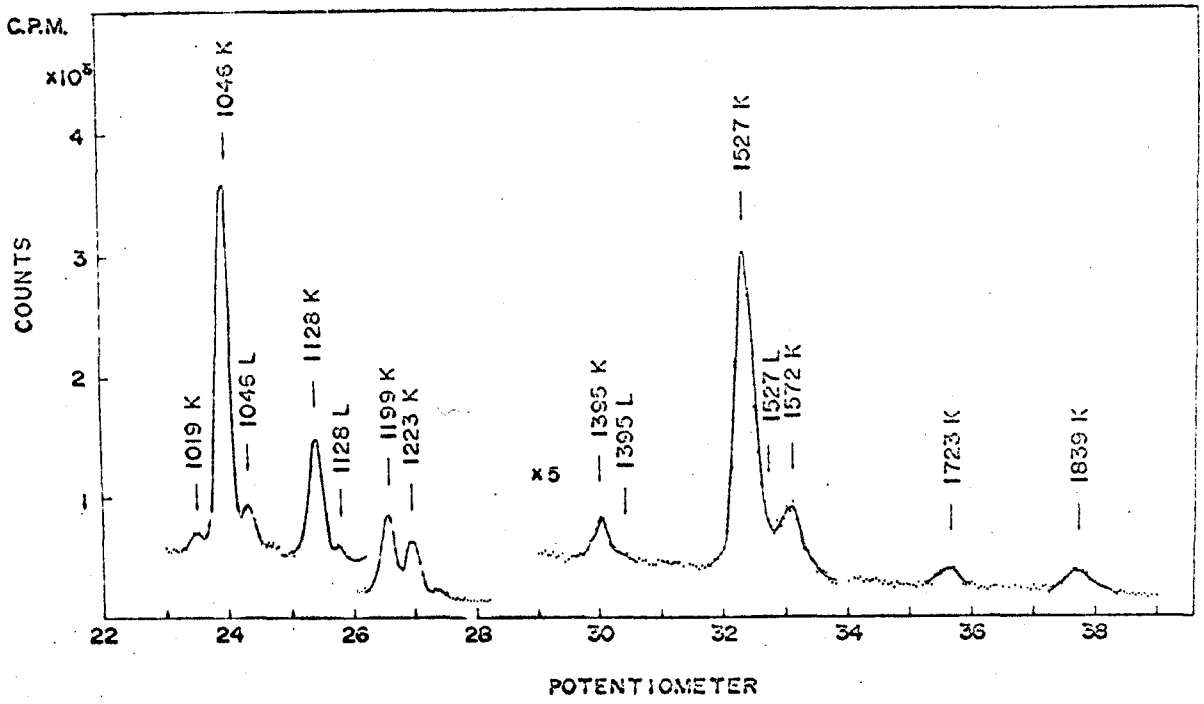
C.P.M.
COUNTS
POTENTIOMETER
1019 K
1046 K
1046 L
1128 K
1128 L
1199 K
1223 K
1395 K
1395 L
1527 K
1527 L
1572 K
1723 K
1839 K
x5

Fig.13

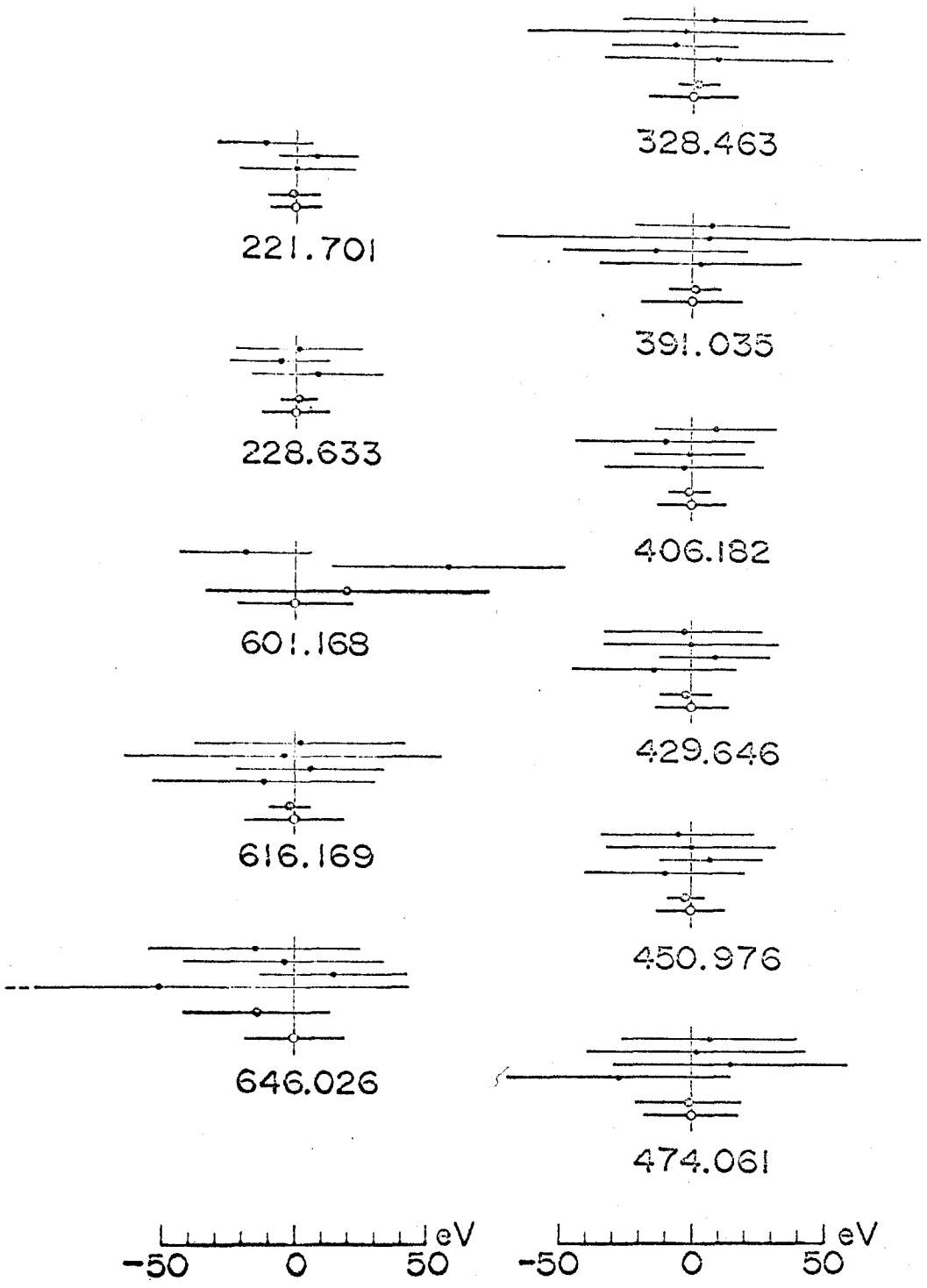
328.463
221.701
391.035
228.633
406.182
601.168
429.646
616.169
450.976
646.026
474.061
eV
-50
0
50
eV
-50
0
50

Fig.14

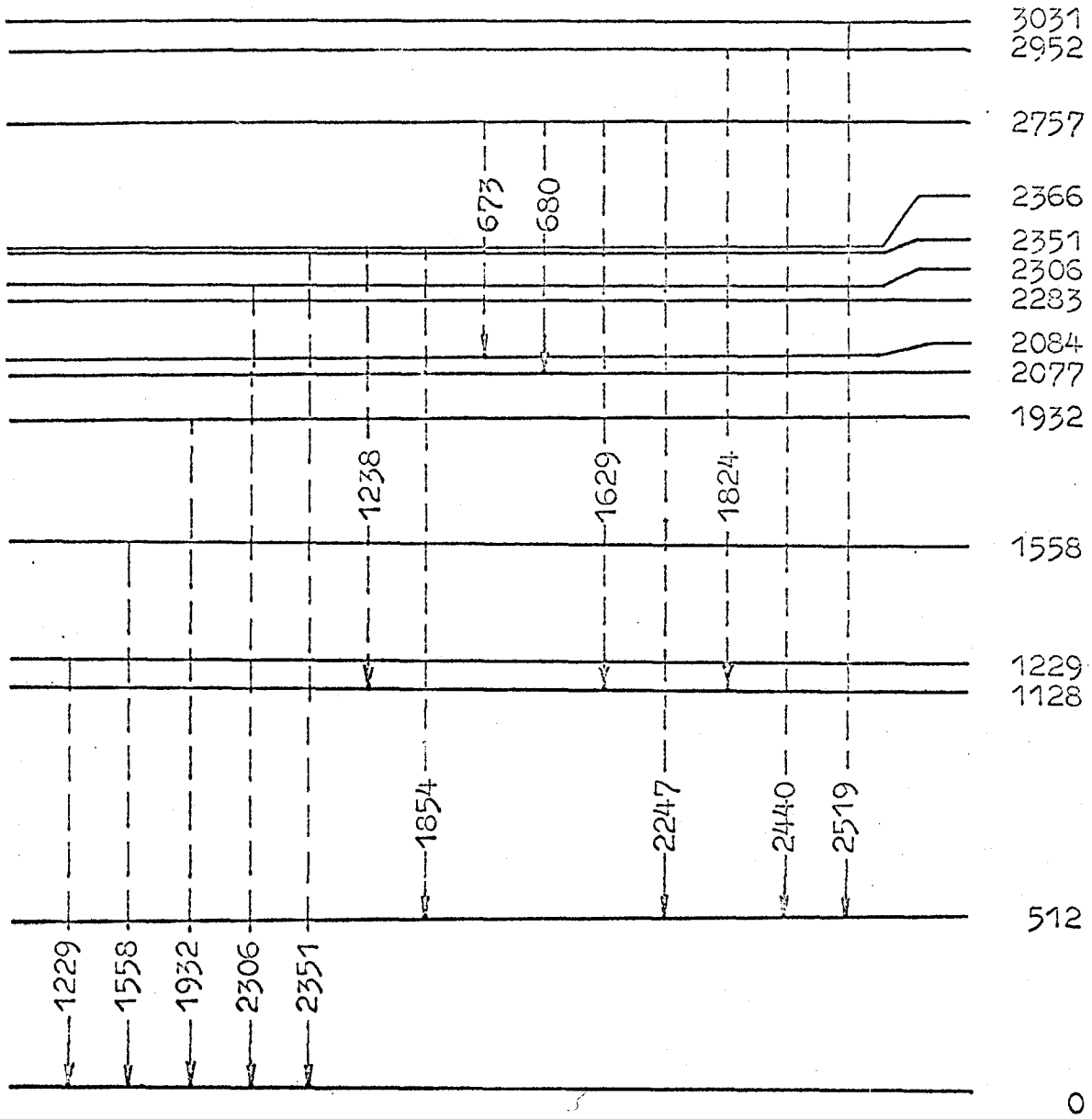
3031
2952
2757
2366
2351
2306
2283
2084
2077
1932
1558
1229
1128
512
0
673
680
1238
1629
1824
1854
2247
2440
2519
1229
1558
1932
2306
2351

106Pd

Fig.15

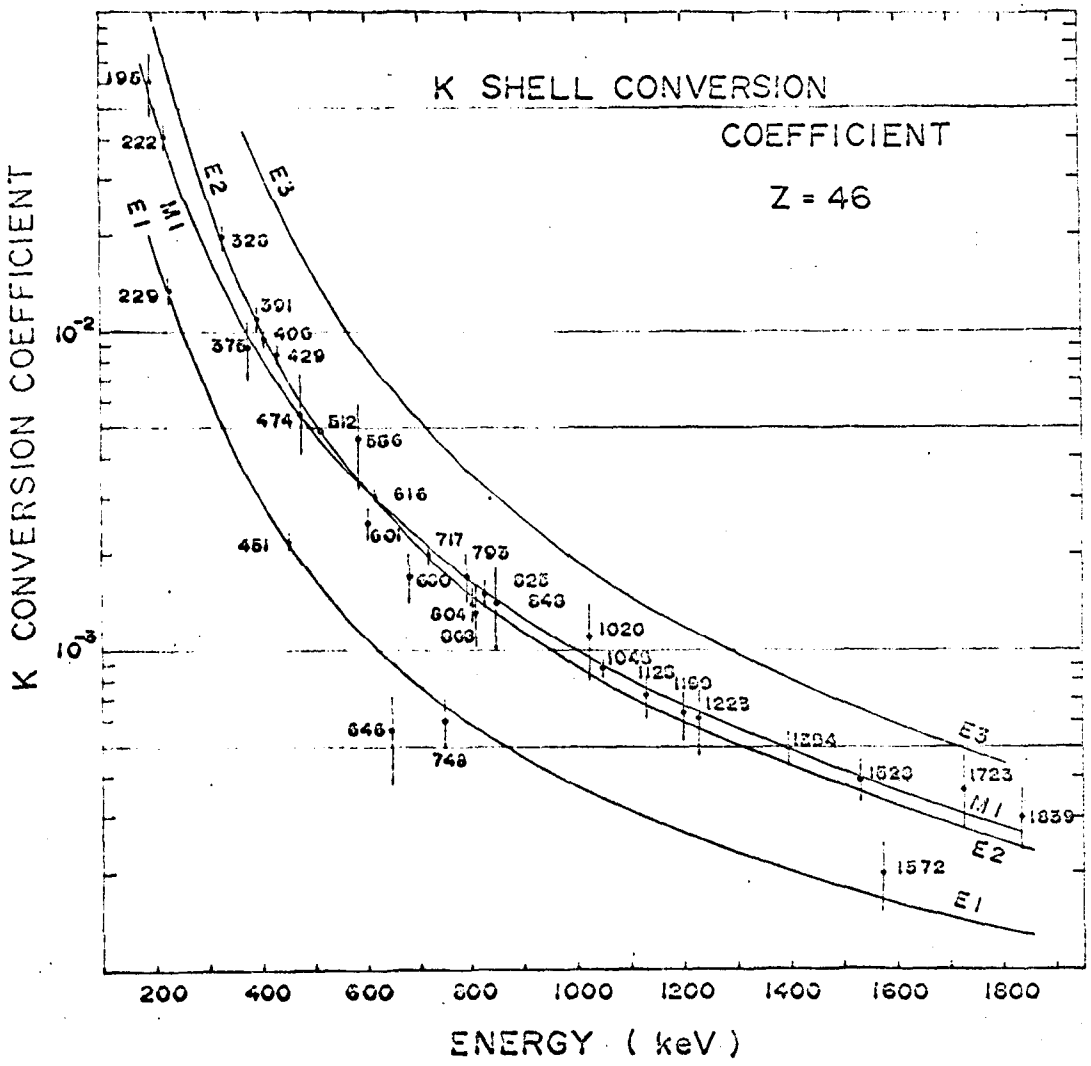
K SHELL CONVERSION
COEFFICIENT
Z = 46
K CONVERSION COEFFICIENT
ENERGY (keV)
E1
M1
E2
E3
196
222
229
320
376
391
406
429
451
474
512
556
616
691
717
793
820
843
1020
1045
1125
1190
1223
1294
1520
1572
1723
1839
646
748
200
400
600
800
1000
1200
1400
1600
1800

Fig.16

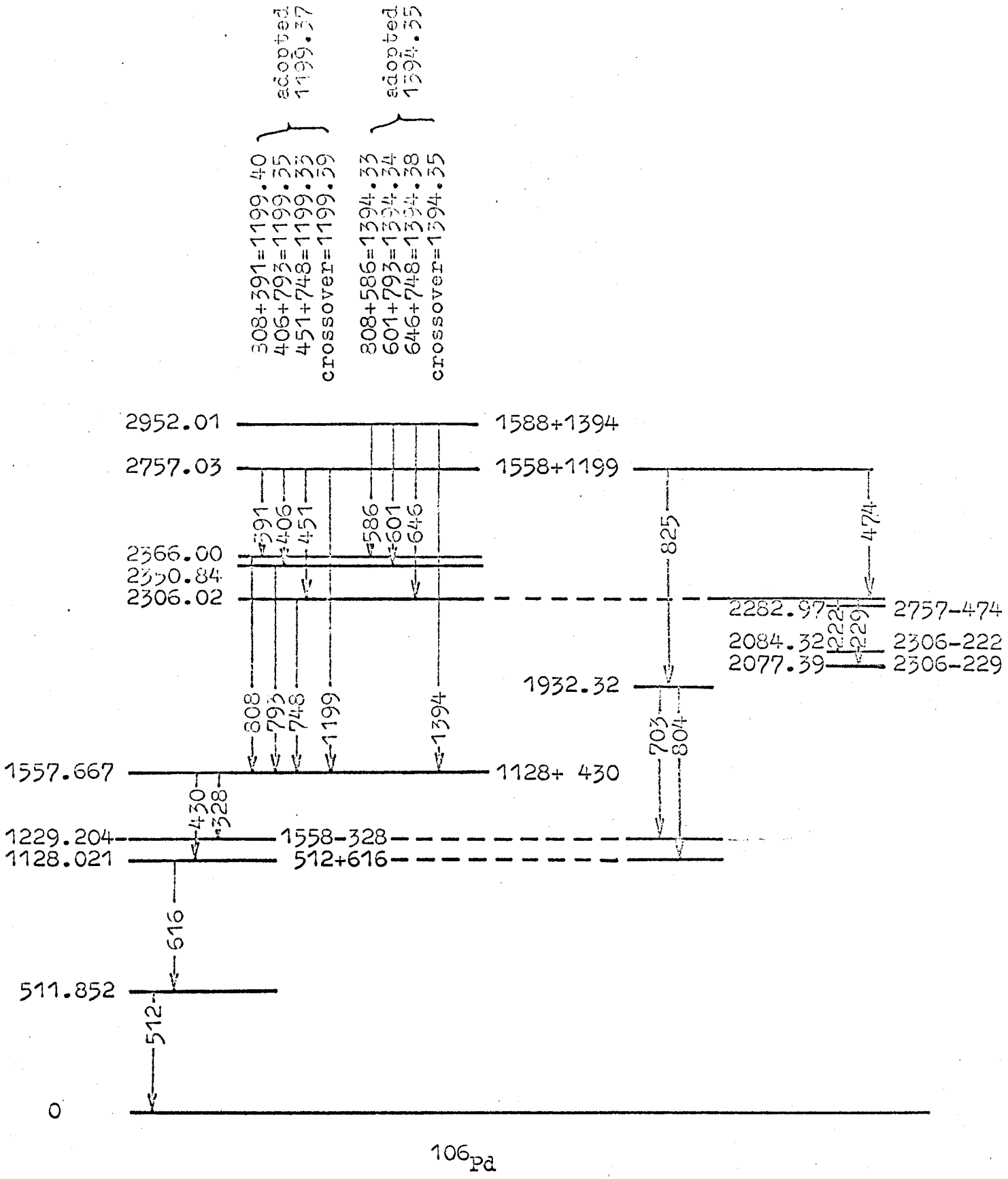
adopted 1199.37
adopted 1394.35
308+391=1199.40
406+793=1199.35
451+748=1199.33
crossover=1199.39
808+586=1394.33
601+793=1394.34
646+748=1394.38
crossover=1394.35
2952.01
1588+1394
2757.03
1558+1199
2366.00
2306.02
2282.97
2757-474
2084.32
2306-222
2077.39
2306-229
1932.32
1557.667
1128+ 430
1229.204
1558-328
1128.021
512+616
511.852
0
391
406
451
586
601
646
825
474
222
229
808
793
748
1199
1394
703
804
430
328
616
512
106Pd

Fig.17

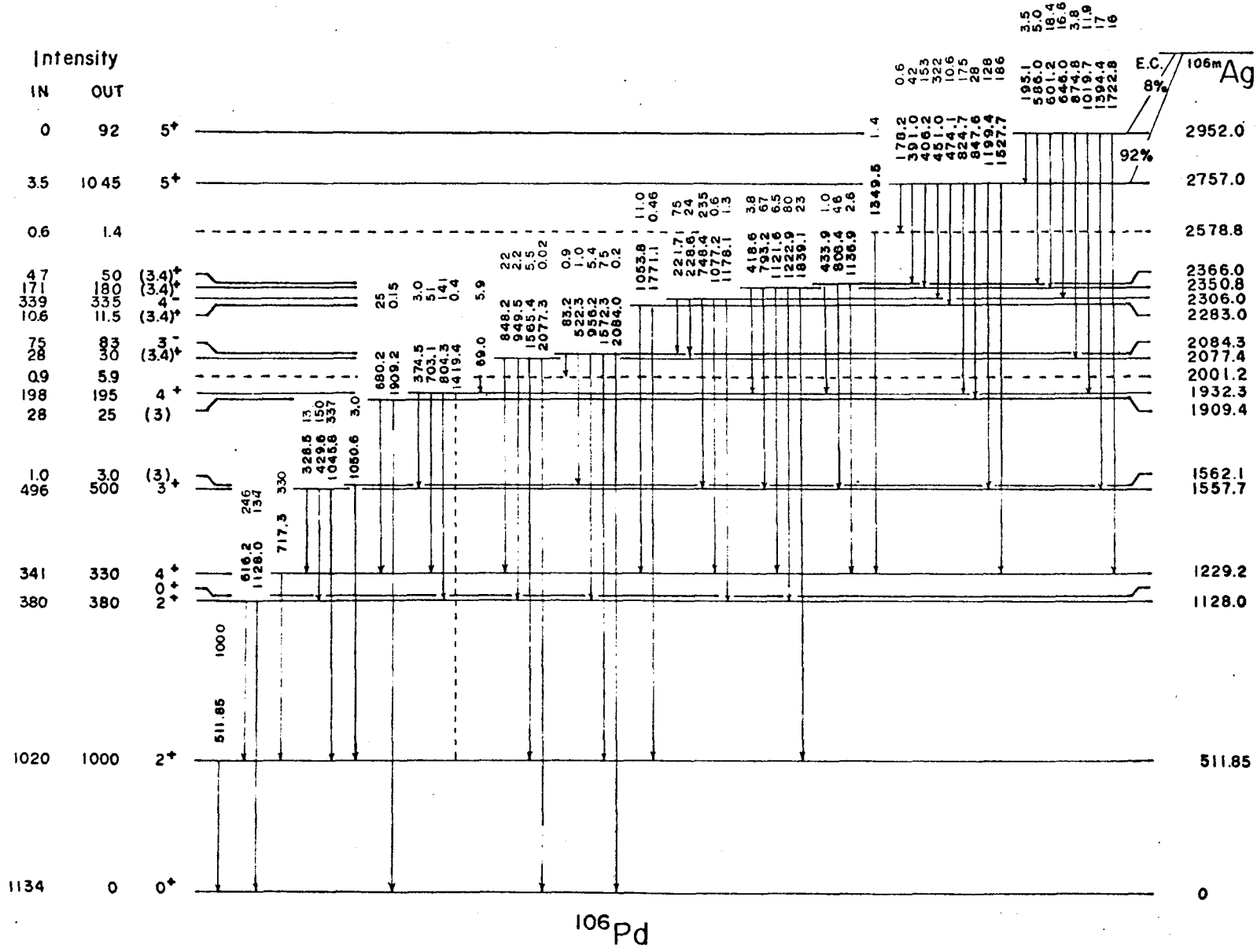

Fig.18

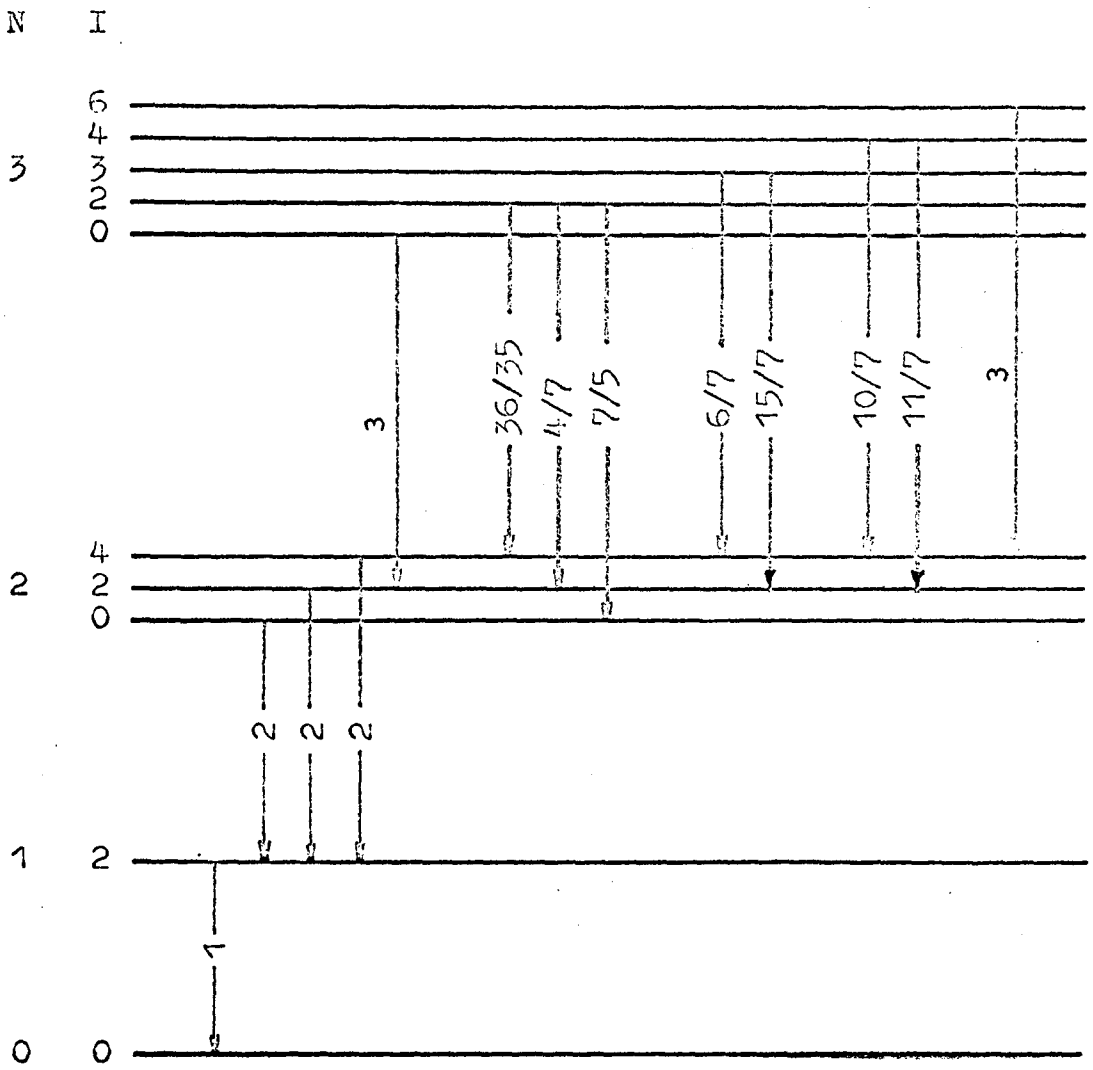

Fig.19

Appendix A

Absolute measurement of the 512 keV gamma ray energy

1. Introduction

The energy of 512 keV gamma ray from the first excited state in ^{106}Pd is very close to that of annihilation gamma ray. Therefore, an accurate comparison measurement of energy is possible for these gamma rays with a Ge(Li) spectrometer. Electron rest mass energy has been determined to be 511.006 ± 0.002 keV from the least square adiustment of fundamental constants in 1965[1)]. However, the energy difference between this value and the annihilation gamma-ray energy has not been established experimentally. In order to dertermine the energy of the 512 keV gamma ray, the energy was compared to those of annihilation gamma rays in several materials. The measurements were also aimed to obtain a reliable energy standard gamma ray in absolute scale. A long lived ^{106}Ru(1y) source was used for this purpose instead of ^{106m}Ag. The details of measurements and analyses are described in section 2 and 3 of this Appendix, respectively. In section 4, the results are discussed with the description of those of previous measurements which have aimed to determine accurate energies of nuclear gamma rays.

2. Measurements

The energy of 512 keV gamma ray was measured relative to the annihilation gamma ray energy. As is often experienced in laboratory works, the spectral peak of annihilation gamma ray show considerable line broadening due to Doppler shift arising from electron and/or positron or positronium velocity at annhilation. Moreover, the broadening width and peak center seems to fluctuate depending on annihilating materials. Because of these effects which might lead to indefinitness of peak center, the annihilation gamma ray has not been used as a precise energy standard. However, the recent progress of the Ge(Li) spectrometer make it possible to observe these effect in a rather quantitative way.

With the aim of making precise energy comparison measurement of 512 keV gamma ray and the annihilation one, a number of annihilation gamma ray sources of different annihilating material was prepared by using ^{22}Na as positron emitter. The ^{22}Na source was sandwiched in an annihilating material which has sufficient thickness to stop positrons in it. A 100 microcurie source covered with thin film, was also prepared to observe the annihilation in air.

The 20 cc and the 30 cc detector and the electronics system shown in Fig. 2 were used for this experiment. The comparison measurements were made in a following way; three gamma lines ^{192}Ir-468 keV, ^{106}Ru-512 keV and ^{207}Bi-570 keV were measured simultaneously, then ^{106}Ru source was removed and replaced by

annihilation gamma-ray source keeping all other condition in the same state. In this way, the 512 and 511 keV lines were measured alternativly. The 468 keV and the 570 keV lines lines were used for reference lines to check the gain and base-line drift over the measurement.

The observed line shapes of annihilation gamma ray in various materials are represented in Fig. A-1.

Fig. A-1

As seen in the Fig. A-1, the line width show considerable variation from one material to another. A 512 keV line which show the instrumental resolution is also shown for comparison. The annihilation line in air has the smallest broadening. It would be most adequate choice to use this line to determine the 512 keV line energy.

A series of comparison measurements was made by referring to this line only. The 512 keV line and the 511 keV line were measured alternatively in the same way described above. A total of nine spectrum was recorded, five of which are for 512 keV spectrum and four are for 511 keV line. These spectra are represented in Fig. A-2

Fig. A-2

The geometry of this measurement are shown in Fig. A-3

Fig. A-3

A merit for this annihilation gamma ray measurement is the $ suppression of Compton background due to ^{22}Na 1275 keV gamma ray. The detail of the results are described in following section.

3. Analyses and results

Results of preliminary measurements for peak widths and positions of the annihilation gamma rays in several materials are given in Table A-1

Table A-1

The materials in the table are classified conveniently in three categories: metal, insulater and gas. The observed energy differences between the 512 keV gamma ray and the annihilation gamma ray in the materials are given in column 4 of Table A-1. It should be noted that not only the peak width but also the peak position for annihilation gamma ray depend on the material used for annihilation. Moreover a temperature dependence was observed for the line width of teflon. Though the above classification is taken only as conventional one, the range of observed energy differences could also be classified according to this category. The energy of ^{106}Ru gamma ray was determined to be 511.84^{52}_{49} ± 0.010 keV from the observed energy difference 846 ± 8 eV for the annihilation gamma ray in air. The procedure to obtain this value is described below.

According to the kinematics of positron annihilation, the energies of two annihilation quanta are given by

$$E = mc^2 + \frac{1}{2}mv^2 \pm mc^2\beta\cos\vartheta$$

where ϑ is the angle between emitted quantum and linear momrntum of $e^+ - e^-$ system and β is v/c. The first and second terms

represent electron rest mass energy and kinetic energy, respectively. The third term represents the energy shift due to Doppler effect which gives a line broadening in the observed spectrum. The positive and negative shifts are observed with equal probability if the momentum of electron-positron pair is isotropic.

The observed line shapes are almost symmetric except an asymmetric tailing due to instrumental cause. Symmetric broadening are assumed throughout the analysis.

The analysis to determine the peak channels of the ^{106}Ru 512 keV gamma ray and the two reference gamma rays is a straightforward one. A computer program "SHAPE" was used to determine the peak channels of these gamma rays. The program performs a fit of peak shape including asymmetric tailing in low energy portion of peak. Details of the program is mentioned in Appendix B. An example of fit is given in Fig. A-4, together with

---

Fig. A-4

---

the deviations of each data point from fit curve. As seen in the figure, fit is satifactory one, though systematic deviation of up to 0.4 % of peak height remains.

The peak shape of annihilation gamma ray is expected to be the result of superposition of this asymmetric peak shape for monochromatic gamma ray. The weight of superposition is considered to be the energy distribution of annihilation

quantum and to be represented by a symmetric function. This symmetric energy distribution curve is the object of fit. A polynomial with even powers in an adequate order was used to express the symmetric energy distribution. The fitting calculations were executed by using a computer program "MULTI-PEEL" which was developed for this purpose. A result of this calculation is illustrated in Fig.A-5.

Fig.A-5

Deviations of each point is also represented in the figure. A parabola distribution was assumed for this case. As seen in the figure, the main component of the energy distribution is approximated well by a parabola. There can be seen two kind of systematic deviations in fit. The first is the deviation due to the incompleteness of the assumed parabola distribution. The second is the same type deviation as observed for monochromatic gamma ray, which is less significant. The center of the parabola distribution is taken as true peak center for annihilation peak. The true peak center by this definition locate at slightly higher energy than the appearant peak center which is given by usual analysis.

The complete results for nine run are represented in Fig.A-6 ~~and in~~ to Fig.A-8.

Fig. A-6

Fig. A-7

Fig. A-8

Fig. A-9

Fig. A-6 shows the peak channels for each run. The observed fluctuations are mainly caused by base line drift of amplifier. Fig. A-7 shows the relative channels normalized for ^{192}Ir 468 keV peak. Fluctuations due to amplifier gain drift or due to statistical cause or due to incompletness of analysis are observed for this case. Fig. A-8 shows the linearily interpolated energies for each run. The open circles under the designation 511 indicate the values by appearant peak centers, while the open circle with a center dot indicate those by true peak centers. The dots under designation 512 indicate those of ^{106}Ru gamma ray. Three vertical bars represent the position of mean value of each group. The energy differences are also indicated. The deviation from linearity is for this case about 60 eV and the energy differnce between these two group of peaks need not be corrected. Two other alternative values for energy difference are calculated by taking two successive runs in pair. These are represented in Fig. A-9. The quated uncertainties in the figures are standard deviations. The same results are tabulated in Table A-2

Table A-2

The electron rest mass energy is given to be 511.006±0.002 keV from the least square adjustment of universal constant in 1965.[1] Under an assumption that the annihilation gamma ray in air originate in considerable amount from positronium whose

binding energy is 6.8 eV[2] the energy of this annihilation gamma ray is lower than the electron rest mass energy if kinetic energy is considered separately.

The reported values for the fraction of positronium formation to total positrons in some gases are listed in Table A-3

Table A-3

These values are taken from the reference 2. According to the table the positronium formation fraction in air is about 1/4 if the contribution of oxygen and nitrongen are independent.

The mean kinetic energy of e^+ -e^- system is estimated to be less than 3 eV from the observed parabolic energy distribution. The base width of parabola distribution is about 3.4 keV. This value correspond to the maximum energy shift of 3 eV if the minor component of higher order is neglected.

These two kinds of corrections have opposite sign and equal order of magnitude. Therefore, a tentative value of 511.852 = 511.006 + 0.846 keV is adopted to discuss the levels in ^{106}Pd in ~~later section.~~ text It should be emphasized that this value is taken as conventional one and can not be free from the ambiguities within the limit described above. The well defined value in this measurement is the observed energy difference 846 ± 8 eV.

4. Discussion

The energy of 512 keV gamma ray in ^{106}Pd was measured by referring to that of annihilation one in air. As a result the energy difference of 846 ± 8 eV was obtained for these two gamma rays. There still remain ambiguities of about 3 eV to define the absolute value of 512 keV gamma ray energy from this observed energy difference. Similar comparison measurements were made for a few materials. Some remarkable results were obtained from measurements, though they are still preliminary ones at present. The purpose of this section is to give a brief discussion on the problem of absolute measurement of nuclear gamma ray energies.

The well defined value of electron rest mass energy 511.006 ± 0.002 keV which is given as an out put of the least square adjustment of universal constants in 1965 would provide a reliable energy marker for nuclear gamma rays if the difference between this value and that of annihilation gamma ray energy were known with good accuracy. The first nuclear gamma ray whose energy was determined accurately by referring to annihilation gamma ray energy is the ^{198}Au 412 keV gamma ray.[3] Using an iron free beta ray spectrometer of 1 meter radius and applying an external conversion technique with uranium foils Murray et al. measured the momentum ratio of K external conversion electron of annihilation gamma ray and L external conversion electron of 412 keV gamma ray. On the basis of 1965 constants and the uranium K-X ray energy the gamma ray energy was determined to be 411.795 ± 0.007 keV. In their experiment alternative sets of water and

ice were used as sources of annihilation gamma ray to peel out the narrow width component which originate from the thermalized positron in ice. An energy value of 511.003 keV was assumed for this annihilation gamma ray to give the final result. The value is corrected for binding energy of positronium in ice and no estimation was made for possible binding state of positron in ice which might results a slight decrease of annihilation gamma ray energy from it. The energy value 411.795 ± 0.007 keV gives a precise calibration point to the Chalk River beta-ray spectrometer and a number of standard gamma-ray energies were determined on this base.[3] These are designated by C in Table 1.

One more energy base for precise measurement of nuclear gamma ray energies is the wave length of W-Kα_1. For this case relative values of wave length are measured with crystal spectrometers. The wave length of W-Kα_1 X ray is defined as 208.5770[4] X-ray unit. Two conversion factors are used to convert the measured wave length into absolute scale. These are

$$\Lambda = 1.002076 \pm 0.000007 \text{ mA/x.u.}^{4)}$$

and $$E\lambda = 12398.10 \pm 0.13 \text{ eV.A}^{1)}$$

By using these conversion factors the energy of W-Kα_1 X ray is determined to be 59.31824 ± 0.00075 keV. A number of nuclear gamma ray energies were also measured on this basis by using crystal spectrometers.

These two energy scales could be compared in some way. There are a few nuclear gamma rays which are measured in both scales. But it is difficult to obtain useful evidence from

these data because of their insufficient accuracies. A few direct measurements to examine the consistency of these two energy bases have been made and ~~thses~~ these data are somewhat in conflict. Knowles measured in his first[5] and second[6] experiments the ratio of wave lengths of the annihilation radiation and the W-Kα_1 X ray using a flat crystal spectrometer. Reigy and Wiedenbeck[7] calibrated his bent crystal spectrometer with the ^{198}Au 412 keV gamma ray and measured the energy of W-Kα_1 X ray. Greenwood et al.[8] measured the energy difference between the ^{192}Au 412 keV gamma ray and the ^{183}Ta 406 keV gamma ray whose energy was given precisely by reffering to the W-Kα_1 X ray energy. These results are summarized in Table A-4.

Table A-4

Column 1 to 3 of the table are taken from reference 8. The column 4 is added for convenience. As indicated in the table, the mc^2 base is slightly higher for all cases. The result of Knowles's second experiment which is the most precise one show that there is a significant discrepancy between the two energy scales.

The results in present experiment show that there can be considerable fluctuation in the annihilation gamma ray energy depending on the material in which positrons annihilate. The energy differences between the annihilation gamma rays in metals and the ^{106}Ru 512 keV gamma ray are higher by about 20 to 30 eV than for air, as shown in Table A-1, while the differences for

insulaters by about 10 eV. These observed fluctuations in Table A-1 have a possibility to explain the fluctuation in Table A-4. In knowles's first experiment water was used to annihilate positrons. No description was found about the source material for annihilation gamma rays in his second experiment. The observed energy difference of about 10 eV between the annihilation gamma ray in air and in the insulaters used in present experiment and the result of Greenwood et al. in Table A-4 are in equal order of magnitude. Under an assumption that the annihilation gamma ray in ice would have an energy decrease of this order of magnitude due to the possible binding state of positron in ice, the result of Greenwood et al indicate a more satisfactory agreement of the two energy bases. The basic problem to be solved at first to perform such a comparison measurement is the one associated with the possible binding state energy of positron in materials. The technique adopted in present experiment would provide an useful method for this purpose.

References of Appendix A

1) E.R.Cohen and J.W.M.DuMond, Rev.Mod.Phys. 37 (1965) 537

2) J.Green and J.Lee, Positronium Chemistry, Academic Press

3) G.Murray,R.L.Graham and J,S.Geiger, Nucl.Phys. 45 (1963) 177, Nucle.Phys. 63 (1965) 353

4) J.A.bearden, Rev.Mod.Phys. 39 (1967) 78, Phys.Rev. 137 (1965) B181

5) J.W.Knowles, Can.J.Phys. 40(1962) 257

6) J.W.Knowles, Proceeding of the second international conference on nuclidic masses,Vienna,1963 P. 113

7) J.J.Reidy and M.L.Wiedenbeck, Nucl.Phys. 79(1966) 193

8) R.C.Greenwood,R.G.Helmer and R.J.Gehrke, Nucl. Inst. Meth. 77 (1970) 141

Figure captions of Appendix A

Fig.A-1 Observed peak widths of annihilation gamma rays in some materials. Peak width of monochromatic gamma ray is that of the 512 keV gamma ray.

Fig.A-2 An example of a spectrum pair for comparison measurements. The 511 keV peak is that of annihilation gamma ray in air.

Fig.A-3 Geometry for the measurement of the annihilation gamma ray in air.

Fig.A-4 An example of peak shape fit. The fit includes the asymmteric tailing in lower energy side of peak. Deviations of data points from the fitted curve are shown in the lower part of the figure.

Fig.A-5 An example of peak shape fit for the annihilation gamma ray in air. The peak shape is represented by superposing that of monochromatic gamma ray. Dots connected with a solid line represent the weight of this superposition. It was obtained through a fitting calculation by using a computer program MULTI-PEEL. A parabola is assumed for this case. Deviations in fit are also indicated. The deviation is a symmetric one which verifys the assumed symmetric energy distribution of the annihilation gamma ray.

Fig.A-6 Plots of peak center channels obtained from nine runs in a series of comparison measurements. Dots and open circles designated as 468,511,512 and 570 represent peak center channels of the ^{192}Ir, annihilation, ^{106}Ru and ^{207}Bi gamma rays of corresponding energy, respectively. The observed fluctuation was mainly caused by the base line drift of biased amplifier.

Fig.A-7 Plots of peak center channels in relative scale. All the dots and open circles correspond to those in Fig.A-6. These were obtained in the usual analysis. The open circles and the open circles with a center dot under the designation 511 represent the apearant and true peak centers of the annihilation gamma ray. The latter were obtained by using the computer program MULTI-PEEL.

Fig.A-8 Plots of linearily interpolated energy in each run. Open circles with and without a center dot correspond to those in Fig.A-7 Three vertical lines indicate the mean values of each group.

Fig.A-9 Plots of observed energy differences between the succesive runs. Even and odd number pairs are classified by dots and open circles. These provide two independent sets of data. Mean values are calculated separately.

Table A-1

Observed Line Broadening for Annihilation Gamma Rays in some Materials and the Energy Differences between ^{106}Ru 512 kev Gamma Ray and Annihilation Gamma Rays

Material	Annihilation Gamma Ray		Energy Difference (eV)
	FWHM(keV)	Broadening(keV)[a]	
Al	2.9	2.4	865
Bi	2.8	2.2	874
Cu	3.4	2.9	874
Al_2O_3	3.7	3.3	856
Teflon(18°C)	3.2	2.7	858[b]
Teflon(275°C)	3.0	2.5	859
Air	2.4	1.6	346[c] + 8

a) These values are obtained by subtracting the instrumental resolution 1.6 keV, in quadrature, from the FWHM values.

b) Mean of two measurements

c) Result of series measurements

Table A-2

Results of Energy Comparison Measurements

Run No.	Linearly interporated Energy[a]		Pair Run No.	Energy Difference in successive Run Pair(eV)	
	^{106}Ru 512 keV Gamma Ray (keV)	Annihilation Gamma Ray (keV)			
1	511.781				
			1-2	833	
2		510.948			
			3-2		848
3	511.796				
			3-4	852	
4		510.944			
			5-4		841
5	511.785				
			5-6	844	
6		510.941			
			7-6		850
7	511.791				
			7-8	849	
8		510.942			
			9-8		854
9	511.796				
Average	511.790 ± 0.007	510.944 ± 0.003		845 ± 8	848 ± 5

Energy Difference

511.790 - 510.944 = 0.846 ± 0.008

a) Correction for deviation from linearity(~ 60 eV) was not made.

Table A-3

Positronium Formation in Gases

Gas	Formation fraction (f,%)	Pressure (P, atom)
Argon	27 ± 3 (a)	1
	30 (b)	27
	31 ± 3 (c)	1
	36 ± 6 (d)	1.2
Neon	55 ± 6 (d)	1.2
Helium	32 ± 3 (c)	1
Krypton	25 (e)	
Nitrogen	21 ± 1 (c)	1
	34 (f)	15.5
Hydrogen	38.4 (f)	15,5
	35 ± 3 (c)	1
Oxygen	50(g, b cf. f)	
	40 ± 4 (h)	
Carbon dioxide	25 (i)	
	30 (a)	<1

References of this Table

a) Gittelman, B., and Deutsch, M.(1956). Ann. Progr. Report, Lab. Nucl. Sci. Massachusetts Institute of Technology.

b) Heinberg, M,and Page, L.A.(1957). Phys. Rev. 107, 1589.

c) Pond, T. A. (1952). Phys. Rev. 85, 489.

d) Marder, S., Hughes, V. W., Wu, C. S., and Bennett, W. (1956). Phys. Rev. 103, 1258.

e) Gittelman, B., and Deutsh, M.(1958). Ann. Progr. Report, Lab. Nucl. Sci., Massachusetts, Institute of Technology, p. 139.

f) Benedetti, S. DE, and Siegel, R.(1954) Phys. Rev. 94,955.

g) Obenshain, F. E., and Page, L. A.(1962). Phys. Rev. 125, 573.

h) Celitans, G. J., and Green, J. H.(1964a). Proc. Phys. Soc.(London). In press.

i) Deutsch, M.(1953). Progr. Nucl. Phys. 3,131.

Table A-4

COmparison of the two energy scales

Reference	Comparison method	Result of comparison	
		Increase in W-K_{α_1} energy[e] (ppm)	Decrease in mc^2 energy[f] (eV)
Knowles[a]	$\lambda(mc^2)/\lambda(WK\alpha_1)$	12 ± 31	6 ± 15
Knowles[b]	$\lambda(mc^2)/\lambda(WK\alpha_1)$	76 ± 14	39 ± 7
Reidy and Wiedenbeck[c]	$\lambda(412)/\lambda(WK\alpha_1)$	2 ± 42	1 ± 21
Greenwood et al	$E_{412} - E_{406}$	17 ± 28	9 ± 14

a) J.W.Knowles, Can.J.Phys. 40 (1962) 257

b) J.W.Knowles, Proceedings of the second international conference on nuclidic masses,Vienna,1963 P.113

c) J.J.Reidy and M.L.Wiedenbeck, Nucl.Phys. 79 (1966) 193

d) R.C.Greenwood,R.G.Helmer and R.J.Gehrke, Nucl.Instrum.Meth. 77 (1970) 141

e) Increase necessary to the W-K_{α_1} energy to bring the two energy scales into agreement.

f) Decrease necessary to the mc^2 energy to bring the two energy scales into agreement

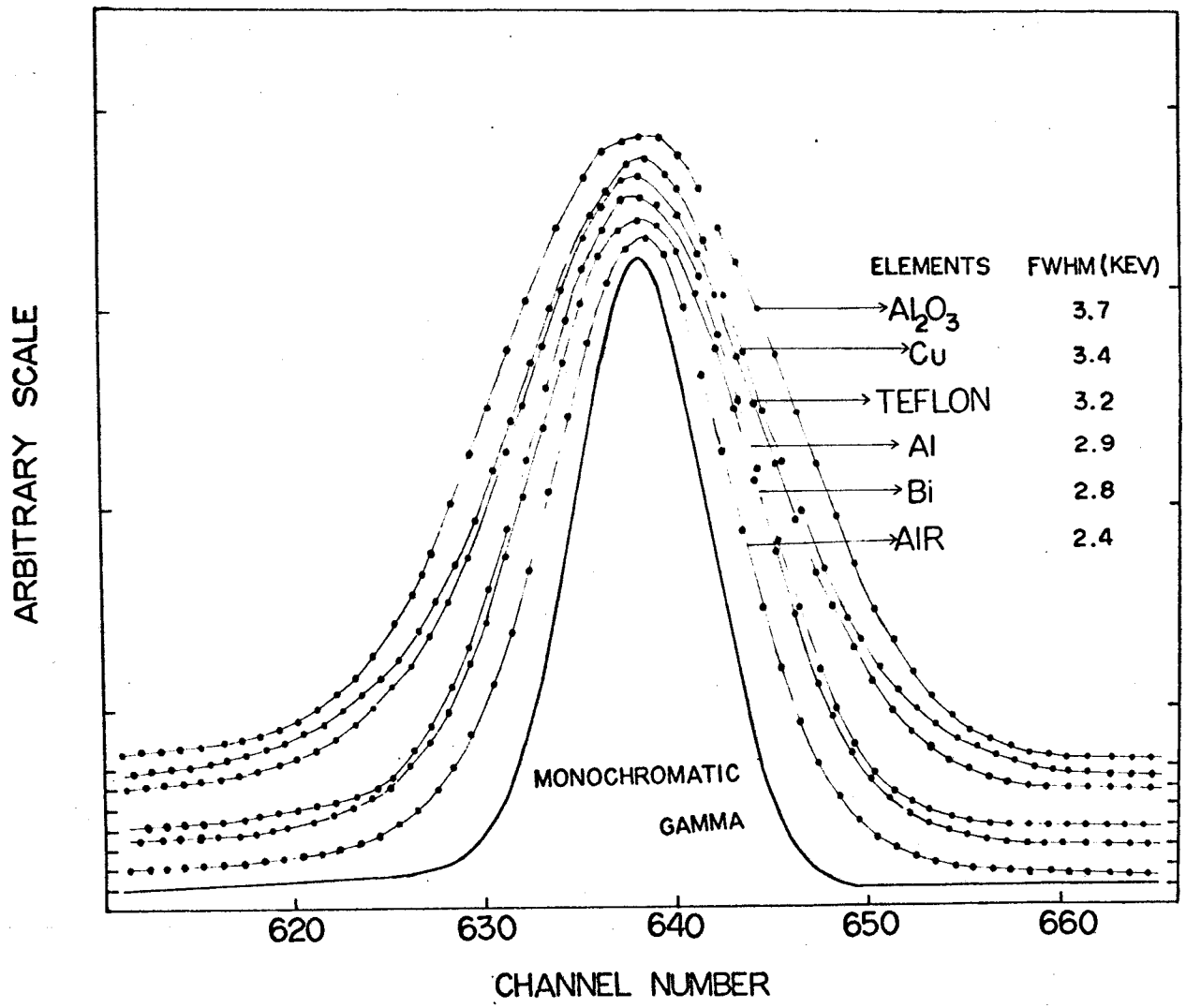
ARBITRARY SCALE
ELEMENTS
FWHM (KEV)
Al_2O_3 3.7
Cu 3.4
TEFLON 3.2
Al 2.9
Bi 2.8
AIR 2.4
MONOCHROMATIC
GAMMA
620
630
640
650
660
CHANNEL NUMBER

Fig.A-1

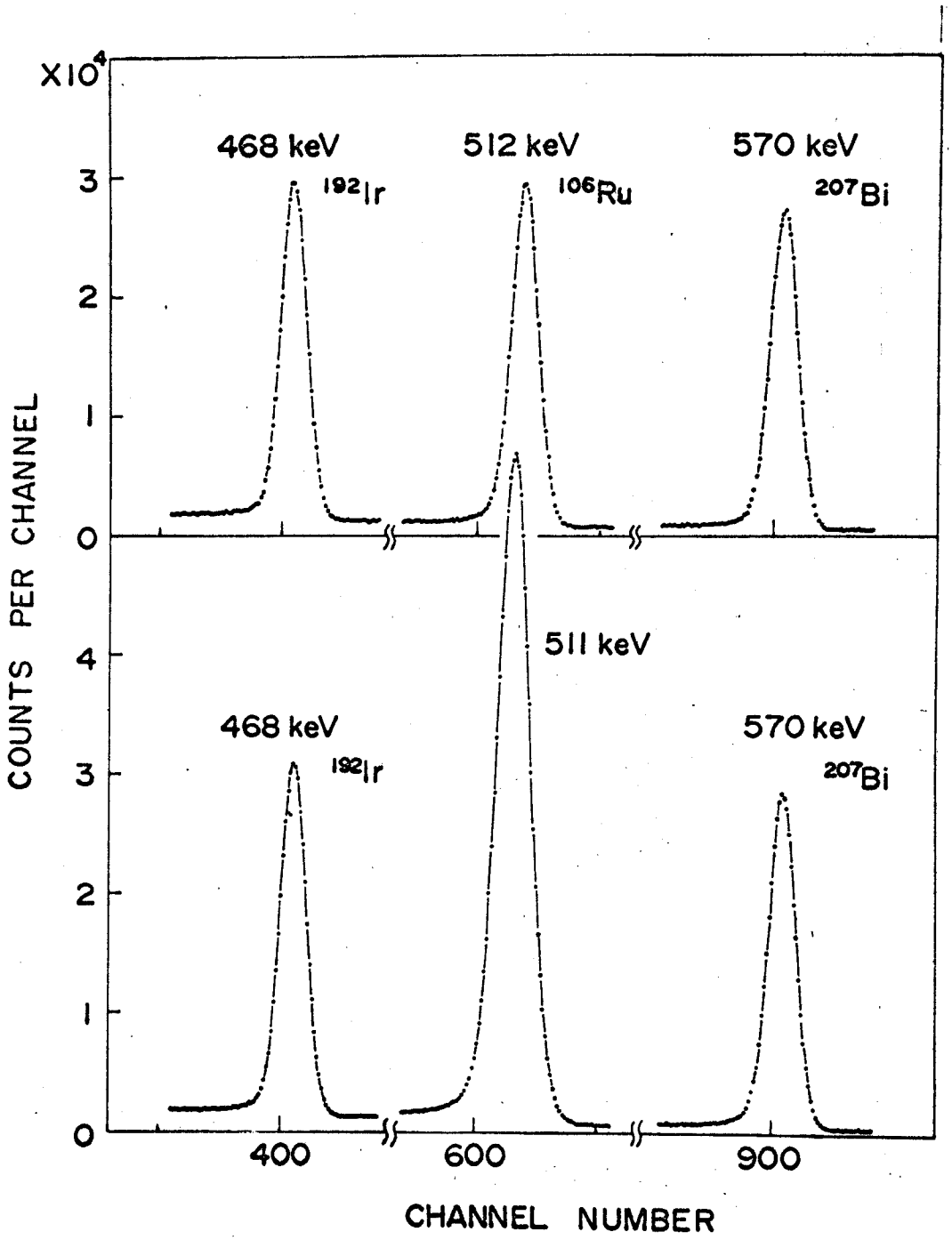
X10⁴
468 keV
192Ir
512 keV
106Ru
570 keV
207Bi
511 keV
468 keV
192Ir
570 keV
207Bi
COUNTS PER CHANNEL
CHANNEL NUMBER
0
1
2
3
4
400
600
900

Fig.A-2

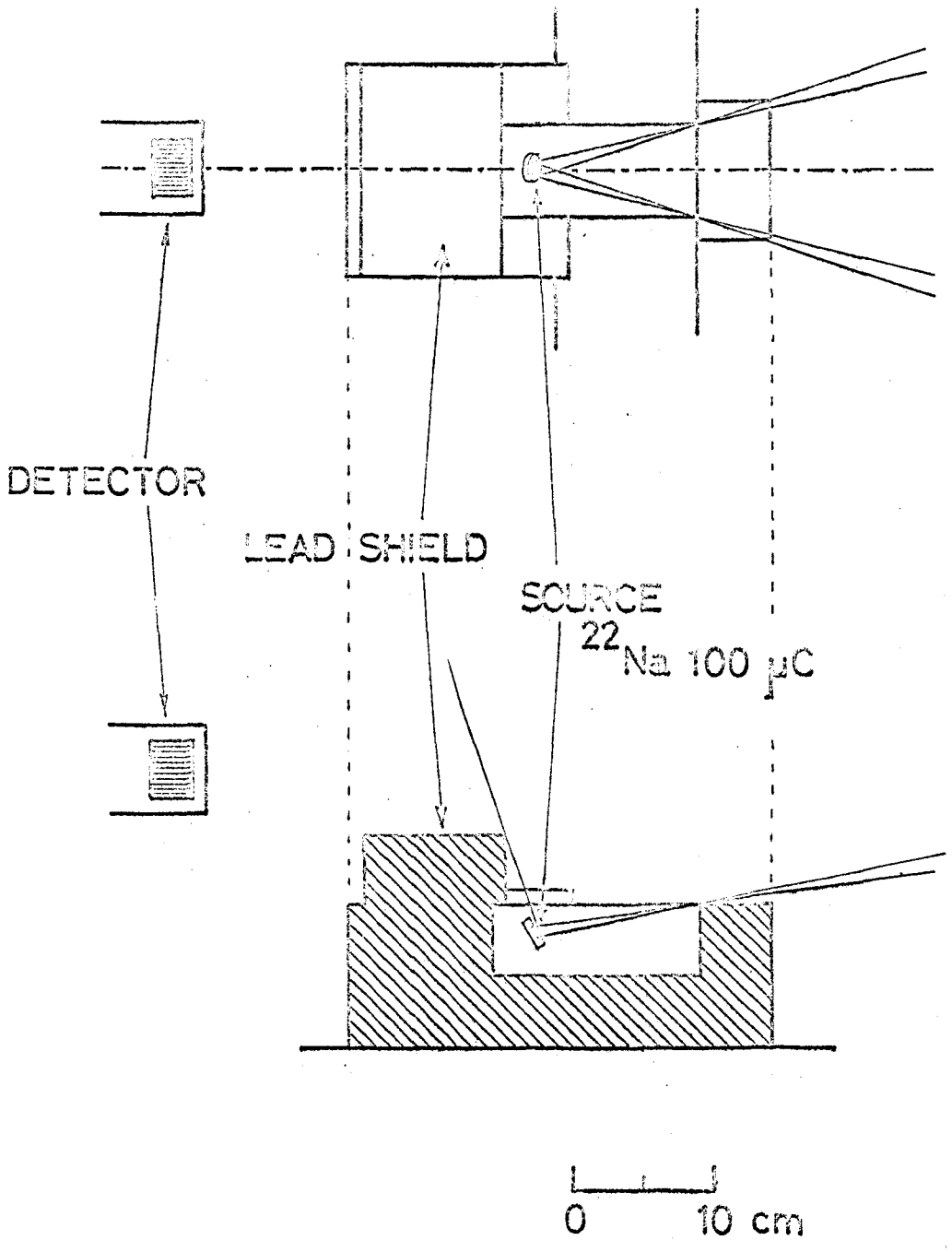

Fig.A-3

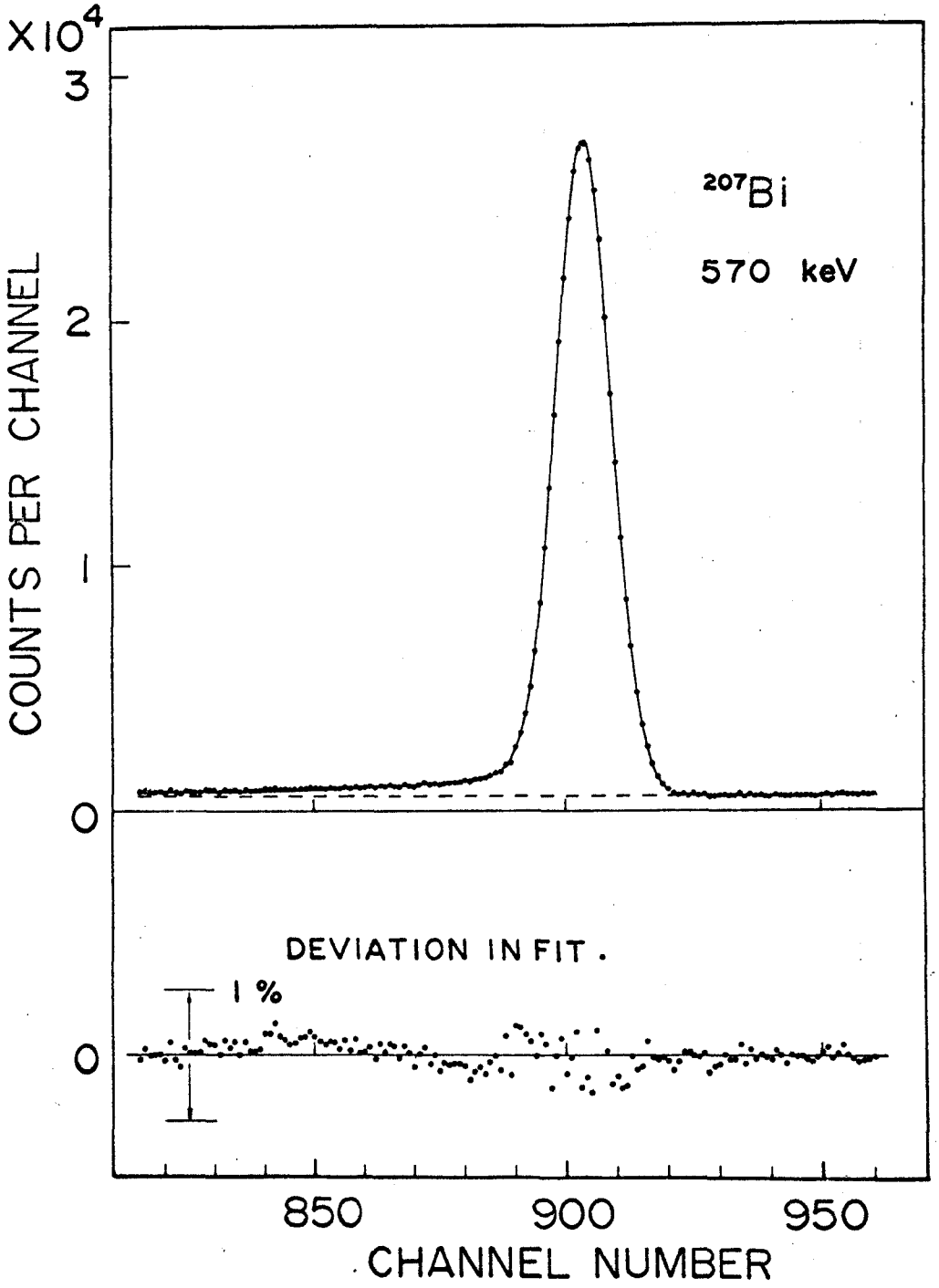
X10^4
3
2
1
0
COUNTS PER CHANNEL
207Bi
570 keV
DEVIATION IN FIT.
1 %
0
850
900
950
CHANNEL NUMBER

Fig.A-4

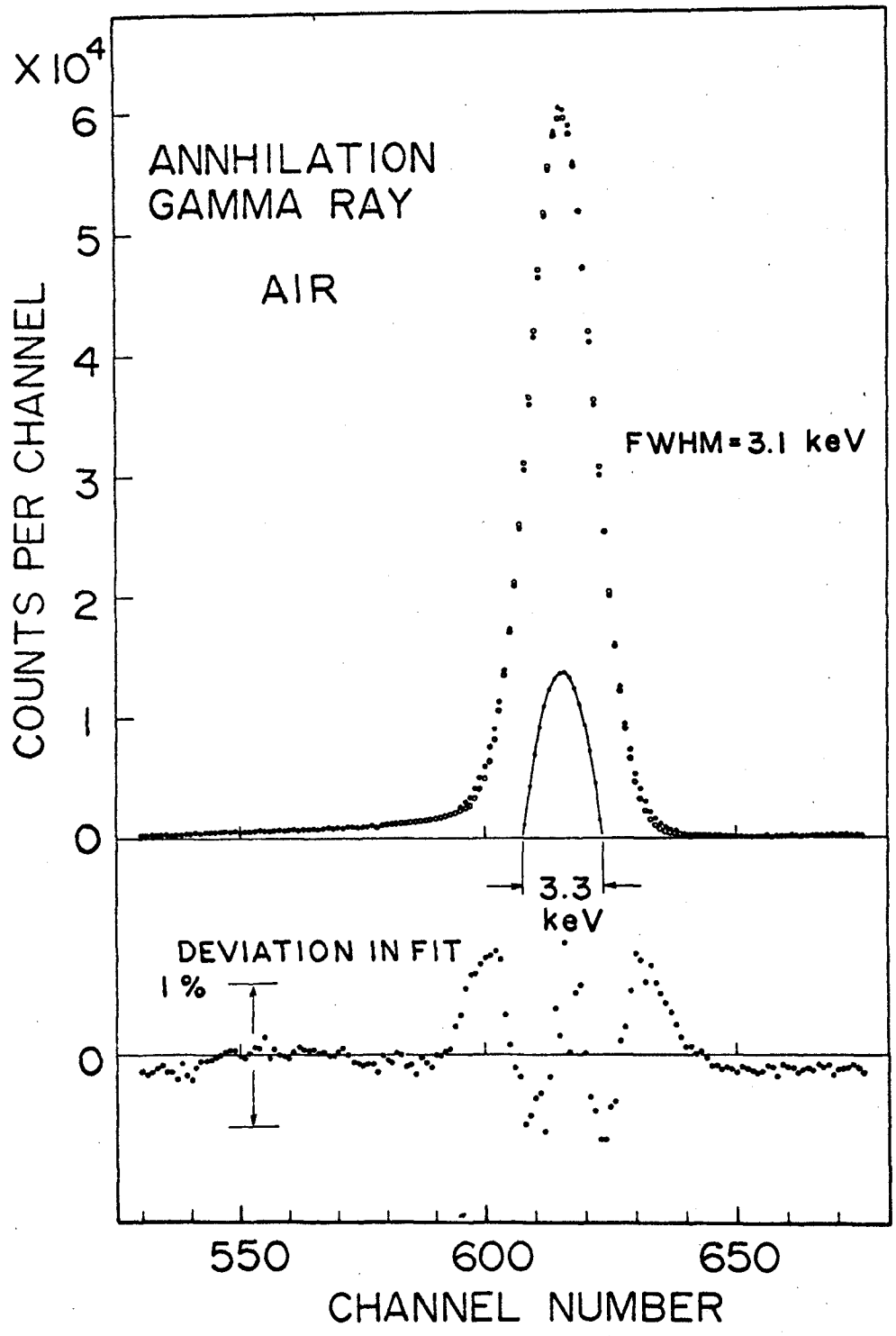
X 10^4
6
5
4
3
2
1
0
ANNHILATION
GAMMA RAY
AIR
FWHM=3.1 keV
COUNTS PER CHANNEL
3.3
keV
DEVIATION IN FIT
1 %
0
550
600
650
CHANNEL NUMBER

Fig.A-5

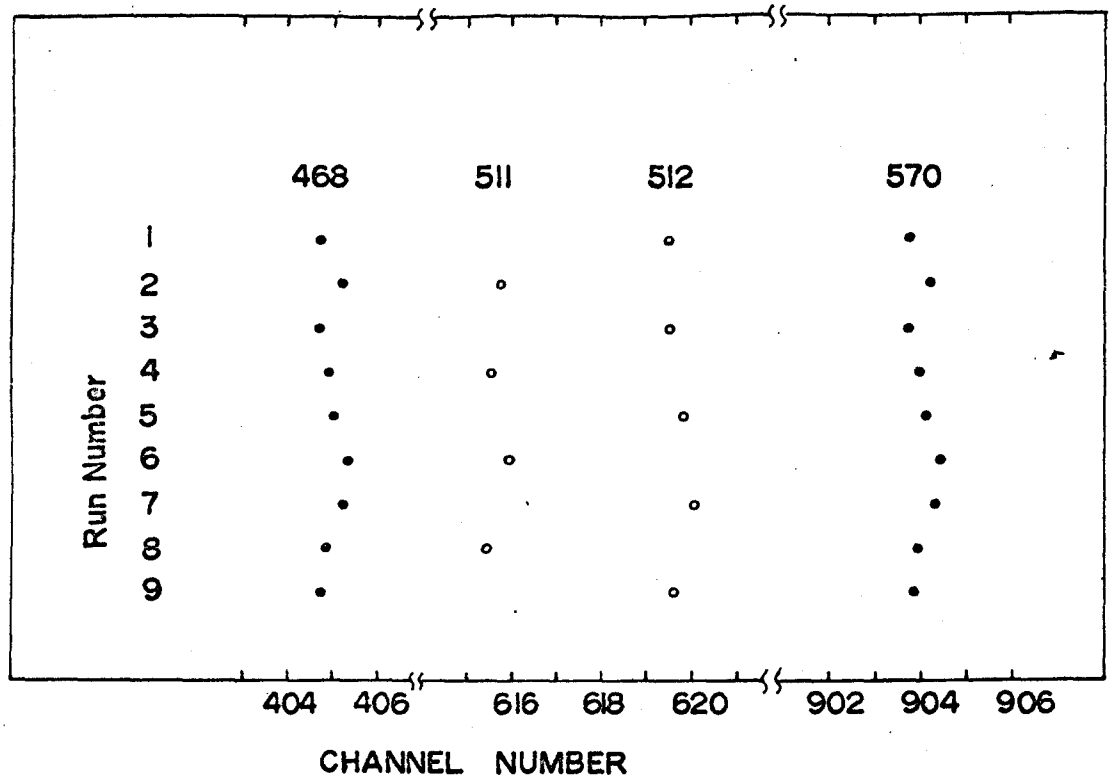
468
511
512
570
Run Number
1
2
3
4
5
6
7
8
9
404
406
616
618
620
902
904
906
CHANNEL NUMBER

Fig.A-6

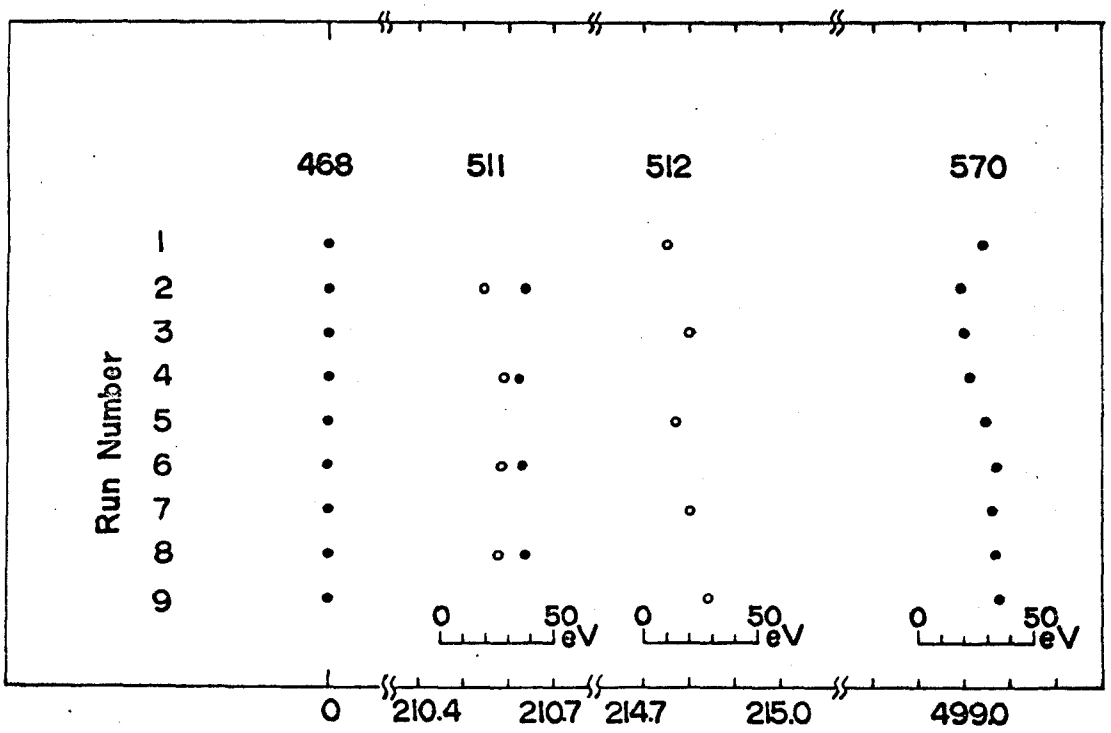
468
511
512
570
Run Number
1
2
3
4
5
6
7
8
9
0
50
eV
0
50
eV
0
50
eV
0
210.4
210.7
214.7
215.0
499.0
CHANNEL NUMBER (RELATIVE SCALE)

Fig.A-7

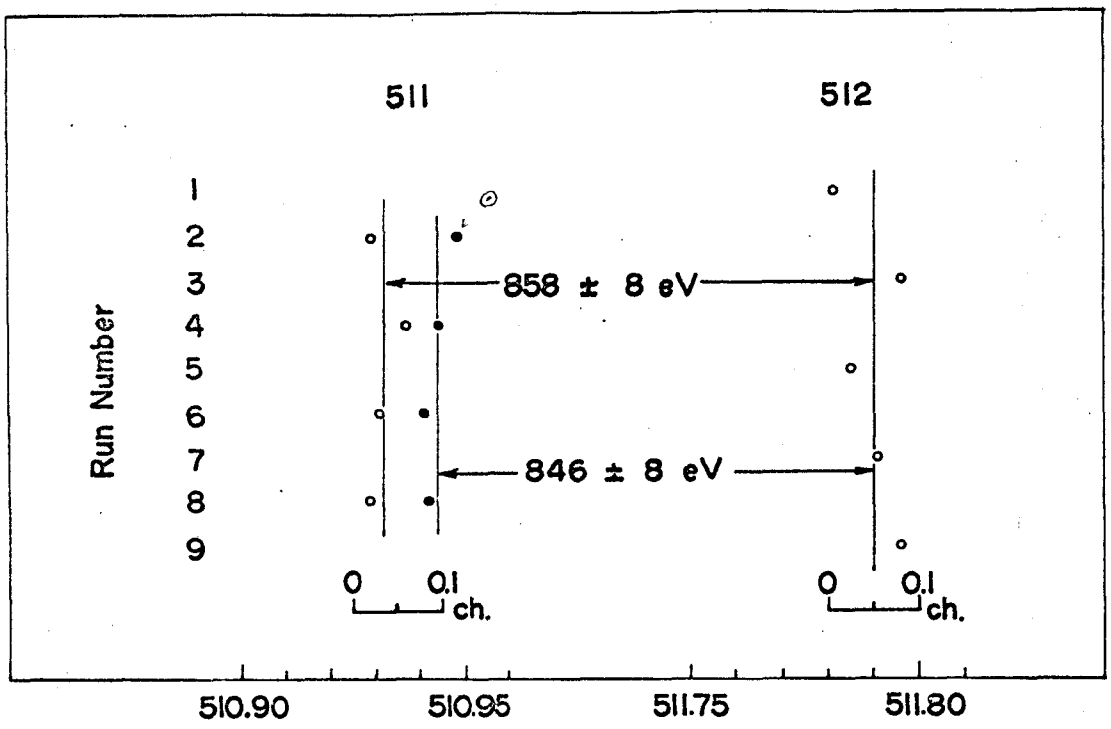
511
512
Run Number
1
2
3
4
5
6
7
8
9
858 ± 8 eV
846 ± 8 eV
0
0.1
ch.
0
0.1
ch.
510.90
510.95
511.75
511.80
LINEAR INTERPOLATION ENERGY (keV)

Fig.A-8

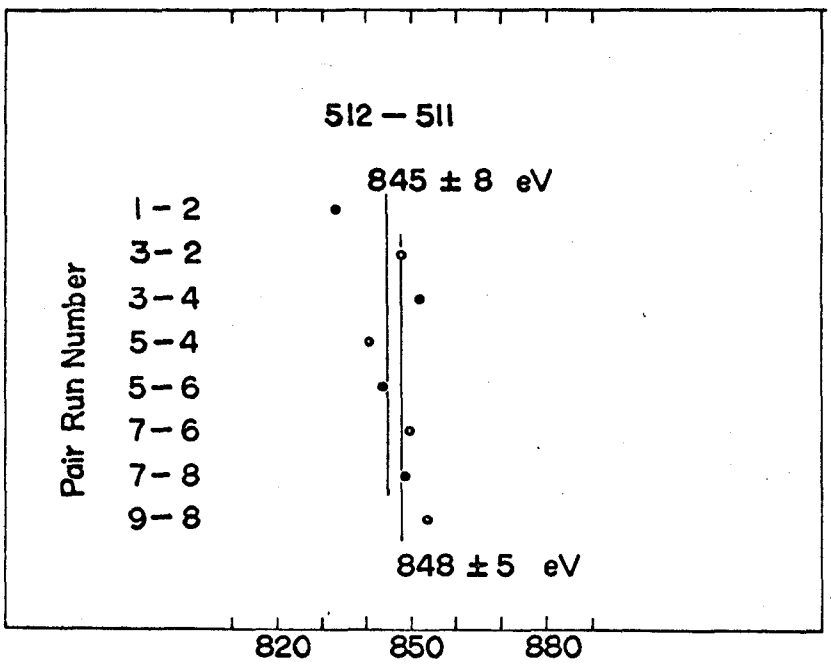
512 — 511
845 ± 8 eV
Pair Run Number
1 - 2
3 - 2
3 - 4
5 - 4
5 - 6
7 - 6
7 - 8
9 - 8
848 ± 5 eV
820
850
880
ENERGY DIFFERENCE (eV)

Fig.A-9

Appendix B

Computer programs for gamma ray spectrum analysis.

In order to utilize the capability of Ge(Li) spectrometers, some computer programs were developed to analyse gamma ray full energy peaks in spectra. The program which was used most frequently in present work is "STANDARD ANALYSIS". It was used for energy determinations of most of the prominent peaks. One more program which was used successfully is "SHAPE". It was used to represent the shape of an well isolated peak with considerable precision and can be used for further developement of analysis programs. The details of these two programs are described in this Appendix.

1. Computer program "STANDARD ANALYSIS"

This program was developed with the aim of attaining a good precision in determination of peak channel as well as obtaining a reliable estimate of uncertainty. A Gaussian function is used to represent data points of a peak. As is well known, the main component of a gamma ray peak shape can be well approximated by the function. The function include three parameters to be fitted. The background under a peak is represented with a straight line and fixed for fitting calculation. A method of nonlinear least square fit is applied for calculation. An example of the fit is shown in Fig.B-1. Fit deviations are also represented for three different fit regions which are indicated by the designations a,b and c.

As seen in the figure, the peak center is rather insensitive for the choice of the fit region in this case. The FWTM region which is designated as a in the figure was adopted to give the final results in most cases of analyses.

There are three kinds of possible sources of uncertainty in determination of peak channels; the statistical fluctuation, the ambiguity in back ground and the fluctuation in the adopted fit region. The first is calculated on the basis of the convenient statistical theory[1]. The second is estimated by changing the adopted background line within its possible maximum range. The third is also checked by adopting the different choice of the fit region. The uncertainties estimated above are added in quadrature to give the final one.

The uncertainty in the linear interpolation of peak energy is also calculated in this program by using the formula

$$(\Delta E)^2=\left(\frac{E_2-E_1}{n_2-n_1}\right)^2\left\{\Delta n^2+\lambda^2(\Delta n_2)^2+(1-\lambda)^2(\Delta n_1)^2\right\}$$

$$\lambda=\left(\frac{n-n_1}{n_2-n_1}\right)$$

where n_1, n_2 and n are the peak channels of the energy standard gamma rays and that of the unknown energy and E_1, E_2 and E are the corresponding energies of them. The uncertainty due to the deviation from linearity is estimated separately by an graphical method as described in text.

2. Computer program "SHAPE"

This program has an aim to represent the shape of a gamma ray peak in more satisfactory way than the program STANDARD ANALYSIS. As seen in Fig.B-1, the higher energy portion of the peak shape can be well approximated by a Gaussian. Relatively large deviations from the fit are seen for the low energy portion due to the asymmetric tailing of the peak.

In order to include this asymmetric tailing in the fit, the following functions are adopted to represent the shape of a gamma ray peak.

$$y_i = f_1(x_i; a_1, b_1, n_1) + f_2(x_i; a_2, b_2, n_2) + f_3(x_i: a_3, b_3, n_3)$$

$$f_1(x_i: a_1, b_1, n_1) = a_1 \exp\left[-4\ln 2\left(\frac{x_i - n_1}{b_1}\right)^2\right]$$

$$f_2(x_i: a_2, b_2, n_2) = a_2\left(\frac{n_2 - x_i}{b_2}\right)\exp\left[\frac{x_i - n_2}{b_2} + 1\right] \quad \text{for } x_i \leq n_2$$

$$= 0 \quad \text{for } x_i > n_2.$$

$$f_3(x_i: a_3, b_3, n_3) = a_3 \quad \text{for } x_i \leq n_3$$

$$= a_3 / \left\{1 + \left(\frac{x_i - n_3}{b_3}\right)^2\right\} \quad \text{for } x_i > n_3$$

The parameter sizes in these functions are shown in Fig.B-2. An example of fit is shown in Fig.A-4 in Appendix A. The parameters a_3, b_3 and n_3 are fixed relative to the other parameters. The background line under the peak is taken conveniently as $y_i = c_1 x_i + c_0$. Parameters a_1, b_1, n_1, a_2, b_2 and n_2 are taken as free ones. It is also possible to include c_0 and c_1 of background parameters in fit as free ones. Among these freely fitted parameters, systematic energy dependence are observed for the parameters b_1 and b_2 and for their relative values a_2/a_1 and $n_1 - n_2$. An example of these energy dependence is shown in Fig.B-3. The energy dependence of these parameters can be utilized to reduce the number of the free parameters in fitting caluculation. It will be important for the analysis of weak peaks as well as doublet peaks.

Reference of Appendix B

1) P.R.Bevington, Data reduction and Error Analysis for the physical Sciences, McGraw- Hill Book Company, 1969

Figure Captions of Appendix B

1) An example of fit with a Gaussian. Three different fit regions are chosen. Fit deviations are also represented.
2) A schematic illustration of the parameter sizes.
3) Energy dependence of the peak shape parameters. The spectrum in Fig.10 in text are analysed in this example.

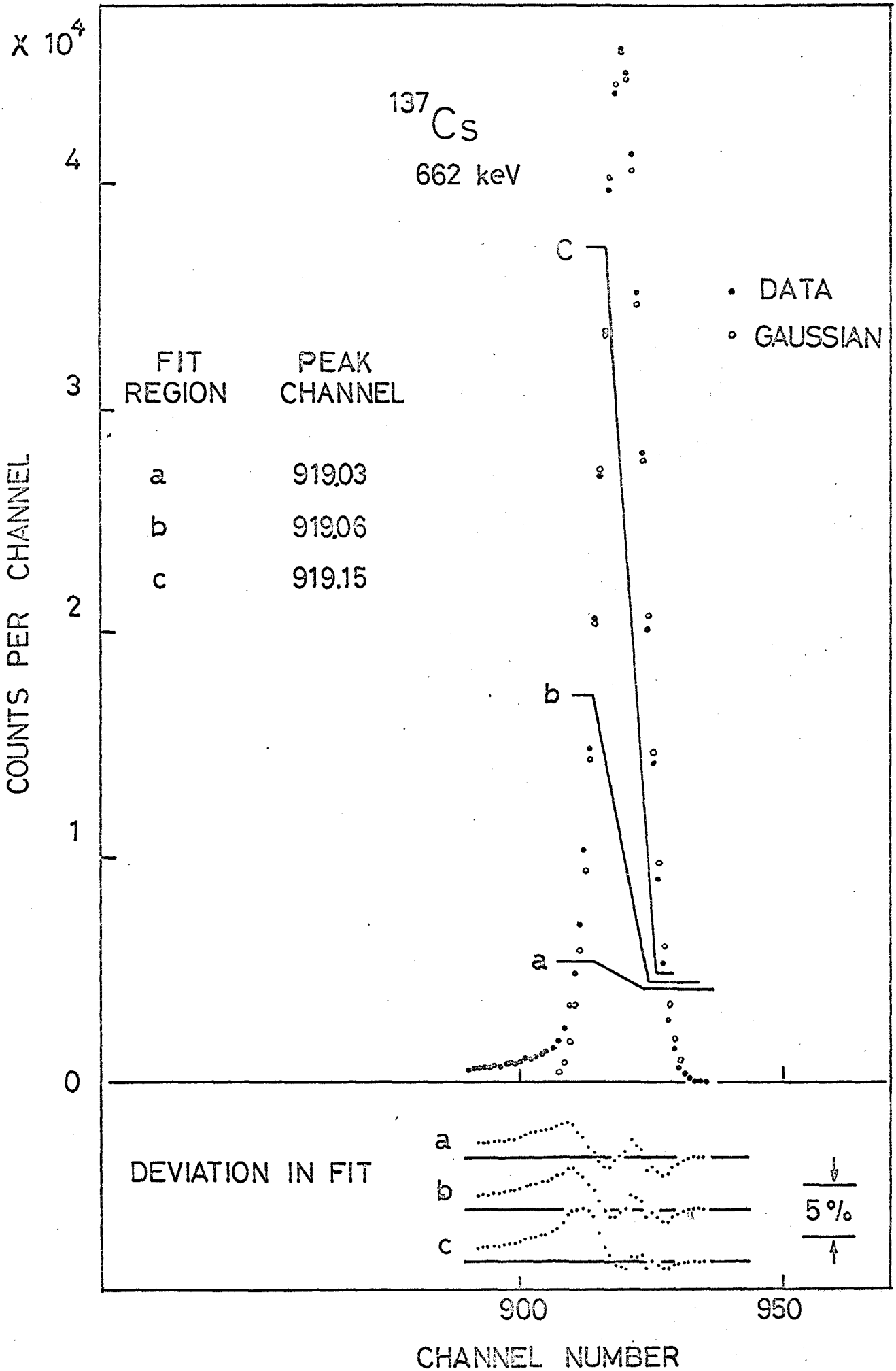
X 10^4
4
3
2
1
0
COUNTS PER CHANNEL
137Cs
662 keV
c
b
a
• DATA
○ GAUSSIAN
FIT REGION
PEAK CHANNEL
a 919.03
b 919.06
c 919.15
DEVIATION IN FIT
a
b
c
5%
900
950
CHANNEL NUMBER

Fig. B-1

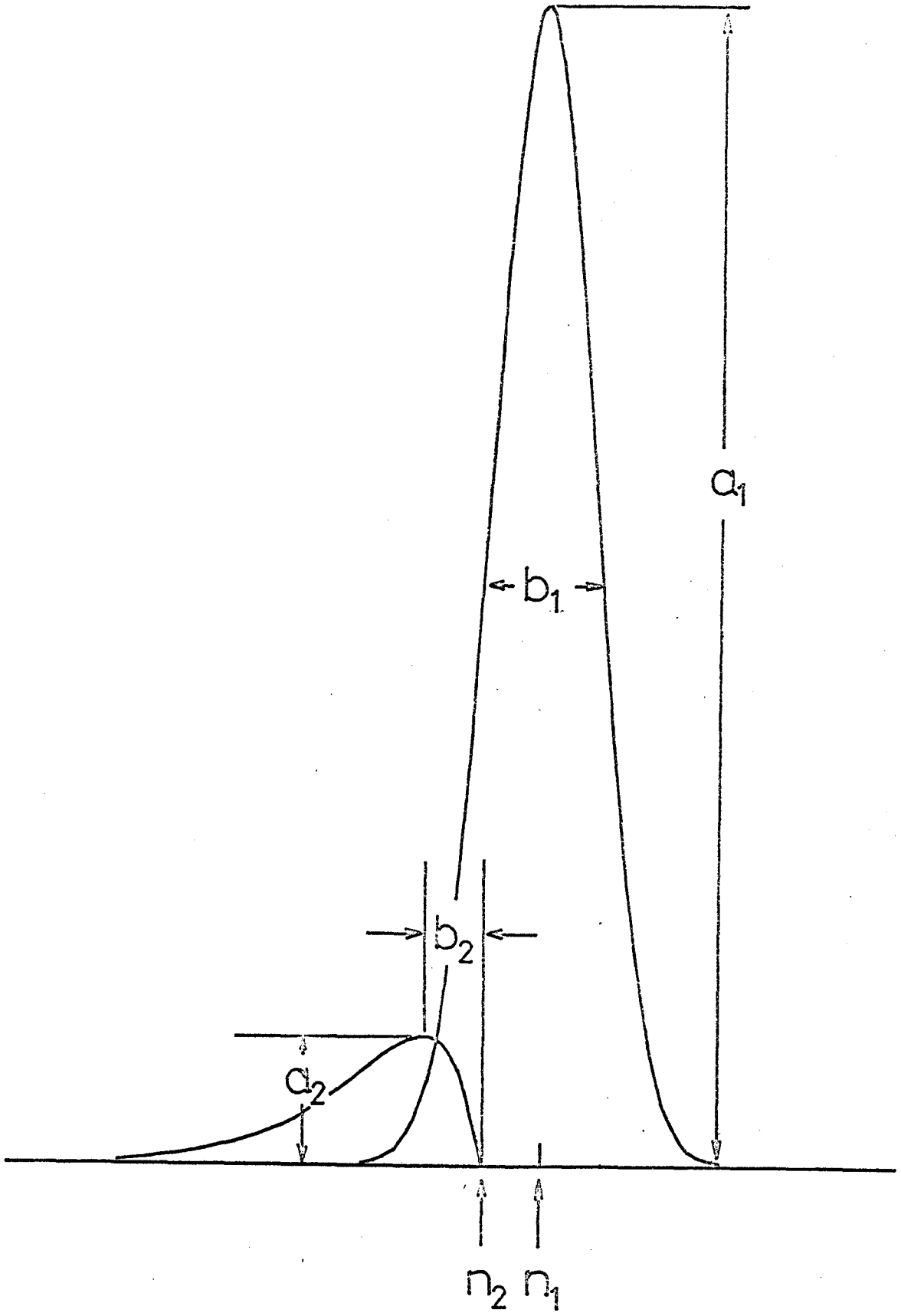

Fig.B-2

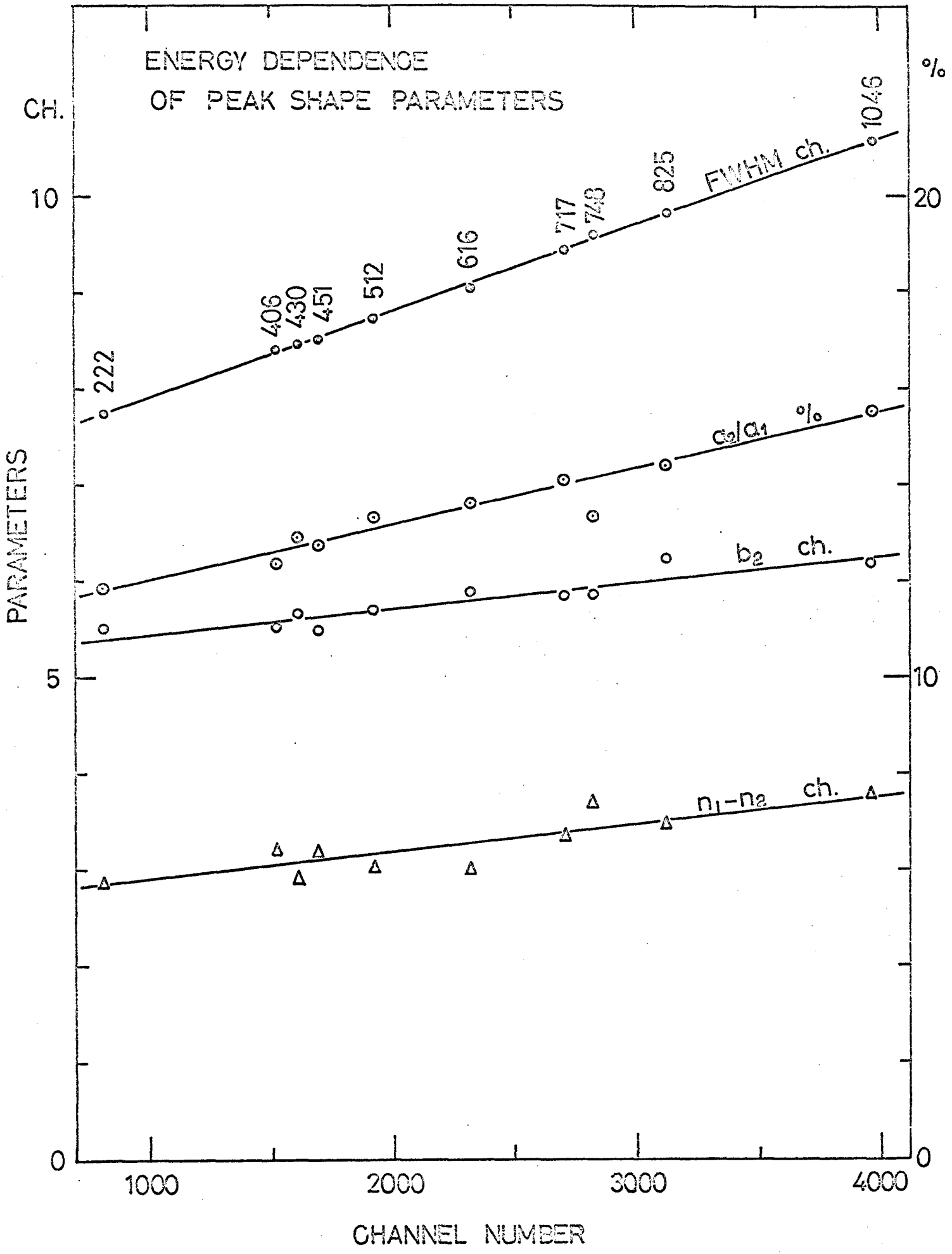
ENERGY DEPENDENCE
OF PEAK SHAPE PARAMETERS
CH.
%
PARAMETERS
FWHM ch.
a_2/a_1 %
b_2 ch.
n_1-n_2 ch.
222
406
430
451
512
616
717
743
825
1046
10
20
5
10
0
0
1000
2000
3000
4000
CHANNEL NUMBER

Fig.B-3

Appendix C

Orange type beta-ray spectrometer

An eight gap orange type beta ray spectrometer was used to measure internal conversion electrons in present experiment. In this Appendix the design and performance of the spectrometer are described in some length to supplement the description of the corresponding section in text.

1. Constructional design.

The horizontal section of the spectrometer is shown in Fig.8 in text. In Fig.C-1 the schematic view of the vertical section of the spectrometer is also represented. The construction is in principle almost identical with that used in the original model.[1] Eight magnets are sustained with two stainless frames to which a vacuum chamber is also installed. The entrance buffles consist of two coaxial cylinders and can be driven by screws. Each gap has a shutter to stop the electrons independently from others. Fig.C-2 show the electron counter assembly. An cylindrical antheracene crystal is used to detect electrons. The diameter of this crystal is chosen to be 25 mm from the relative transmission curves which are also shown in Fig.C-2. Two brass rings are used as detector slit.

2. Gap characteristcs

Each gap has a slightly differnt focussing characteristics. The coil current necessary to focus the electrons of the same energy varies from gap to gap, though the fluctuation is limited

within 1 %. The fluctuation can be compensated by shunting the coil current of each gap by a small fraction. The coil currents to focus the ^{137}Cs 662-K line before and after this adjustment are represented in Fig.C-3. Eight dots connected with a dashed line show the current of each gap before adjustment. Eight dots connected with a solid line indicate the corresponding one after adjustment. Eight peaks in the left side of the figure are those measured with a single gap of corresponding number after adjustment, while a large one in the right is the same peak measured with all gap. The resultant fluctuation can be limited within 0.3 %.

3. Resolution and transmission

The optimum positions of source and detector slit are chosen to attain a highest transmission. The focussing characteristics of each gap is represented in Fig.C-4. Eight peaks in the left side of the figure are those measured by using all gaps. Eight dots connected with a solid line show the corresponding coil currents. The definition of the angle in ordinate is also shown in the figure. Better resolution can be obtained with the entrance buffle angle between 80° and 105°.

The resultant overall resolution and transmission are shown in Fig.C-5. Solid lines connect the points with same entrance buffle openings, while dashed lines connect those with same detector slit width. From these curves the desired condition of measurement can be chosen for a particular experiment.

Reference of Appendix C

1) O.Kofoed-Hansen, J.Lindhard and O.B.Nielsen, Mat.Fys.Medd., Dan.Vid.Selsk. 29,No.16 (1950)

Figure Captions of Appendix C

Fig.C-1 Horizontal section of the spectrometer.

Fig.C-2 Electron counter and its mounting. Relative transmission for differnt scintillator diameter is also shown.

Fig.C-3 Fluctuation in coil currents necessary to focus the ^{137}Cs 662-K conversion electron.

Fig.C-4 Focussing characteristics of each gap.

Fig.C-5 Resolution and transmission for all gaps.

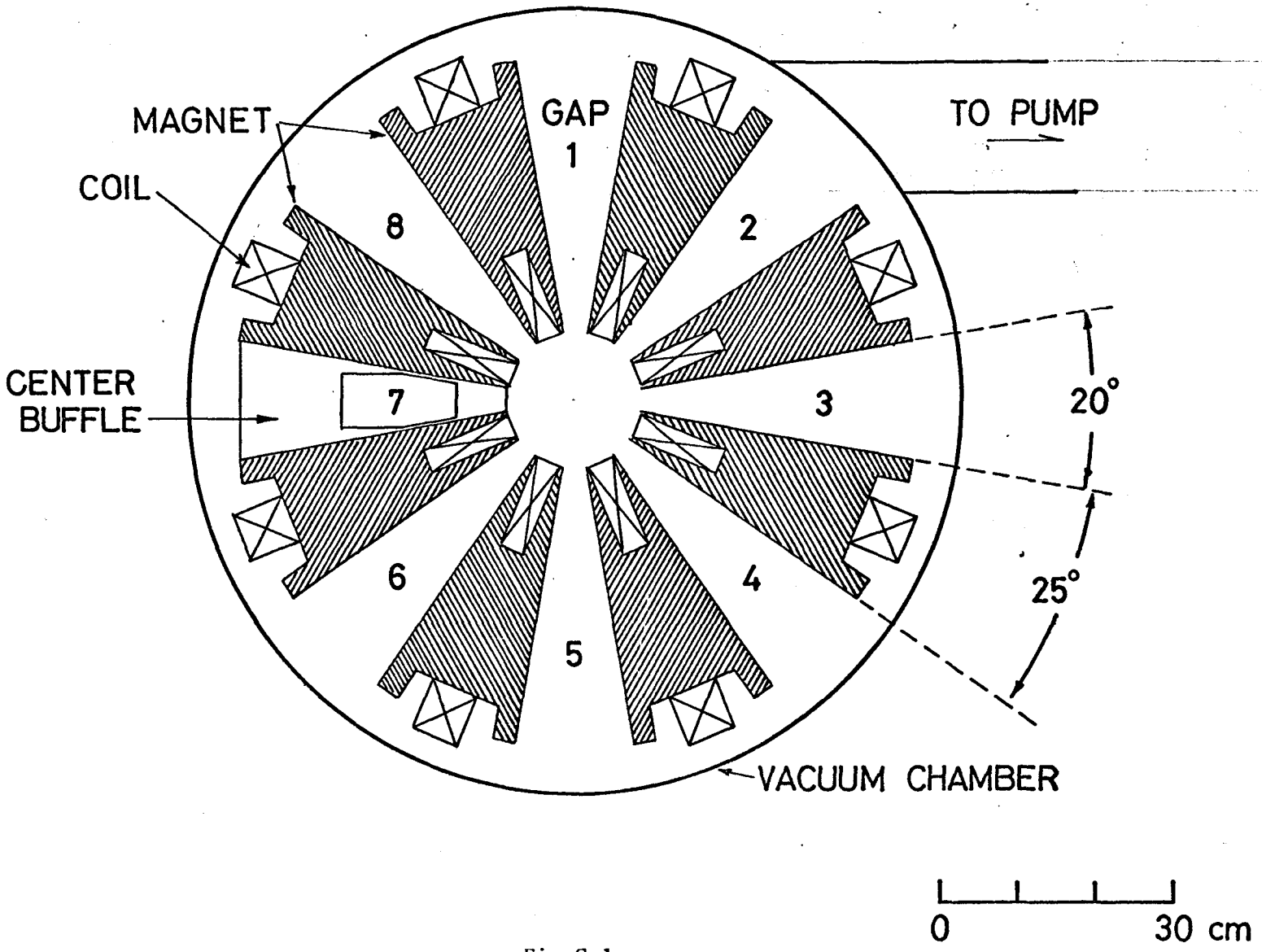
MAGNET
COIL
CENTER
BUFFLE
GAP
1
2
3
4
5
6
7
8
TO PUMP
20°
25°
VACUUM CHAMBER
0
30 cm

Fig.C-1

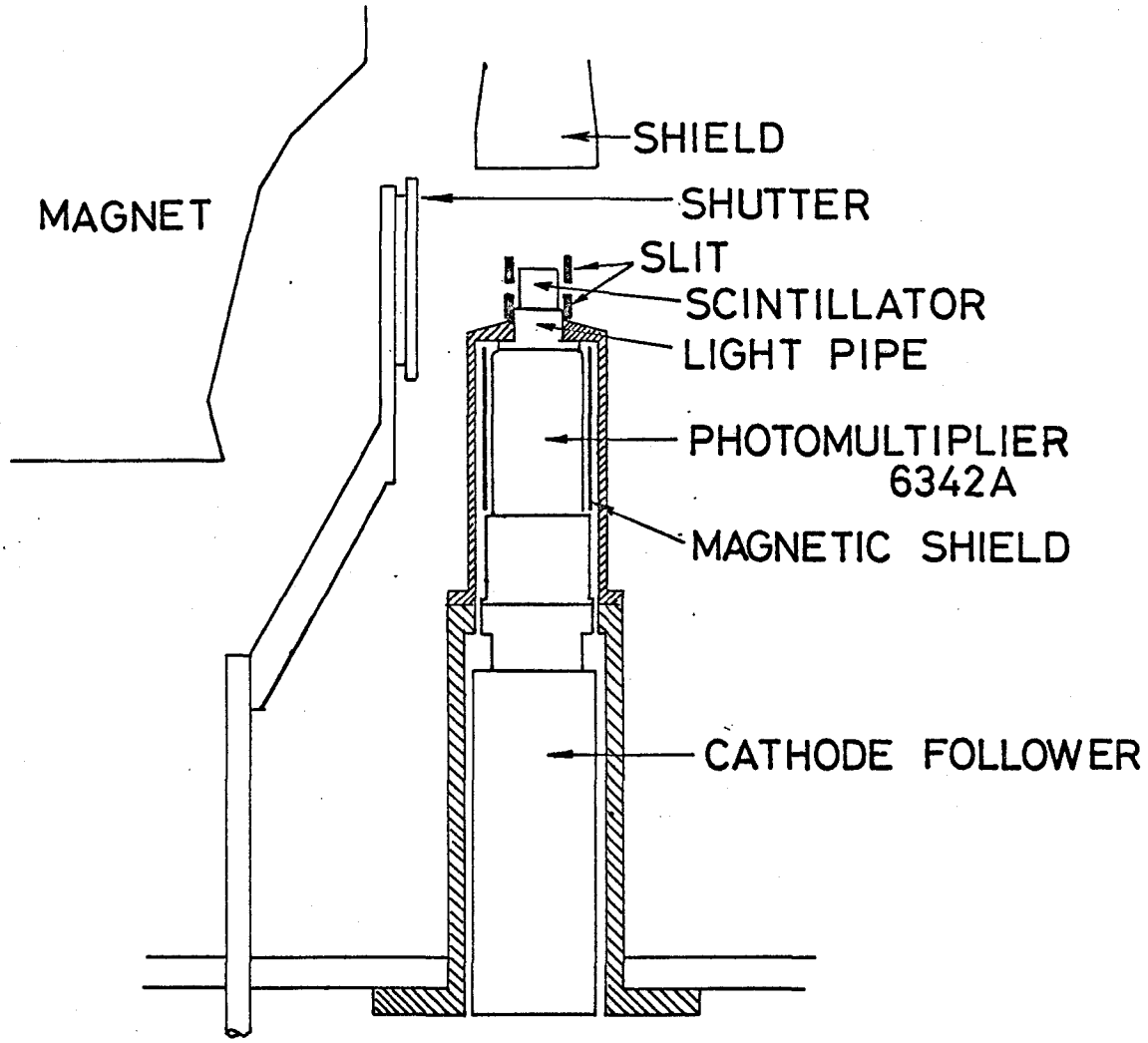
MAGNET
SHIELD
SHUTTER
SLIT
SCINTILLATOR
LIGHT PIPE
PHOTOMULTIPLIER
6342A
MAGNETIC SHIELD
CATHODE FOLLOWER

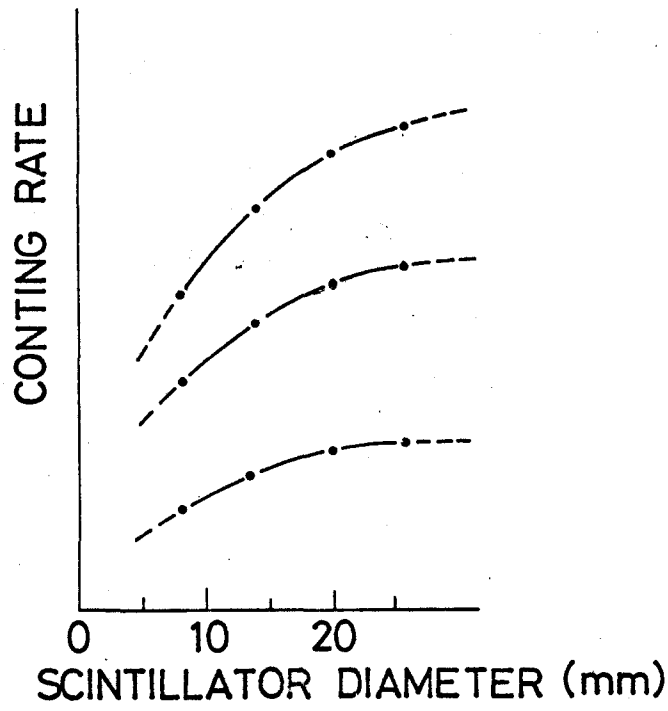
CONTING RATE
0
10
20
SCINTILLATOR DIAMETER (mm)

Fig.C-2

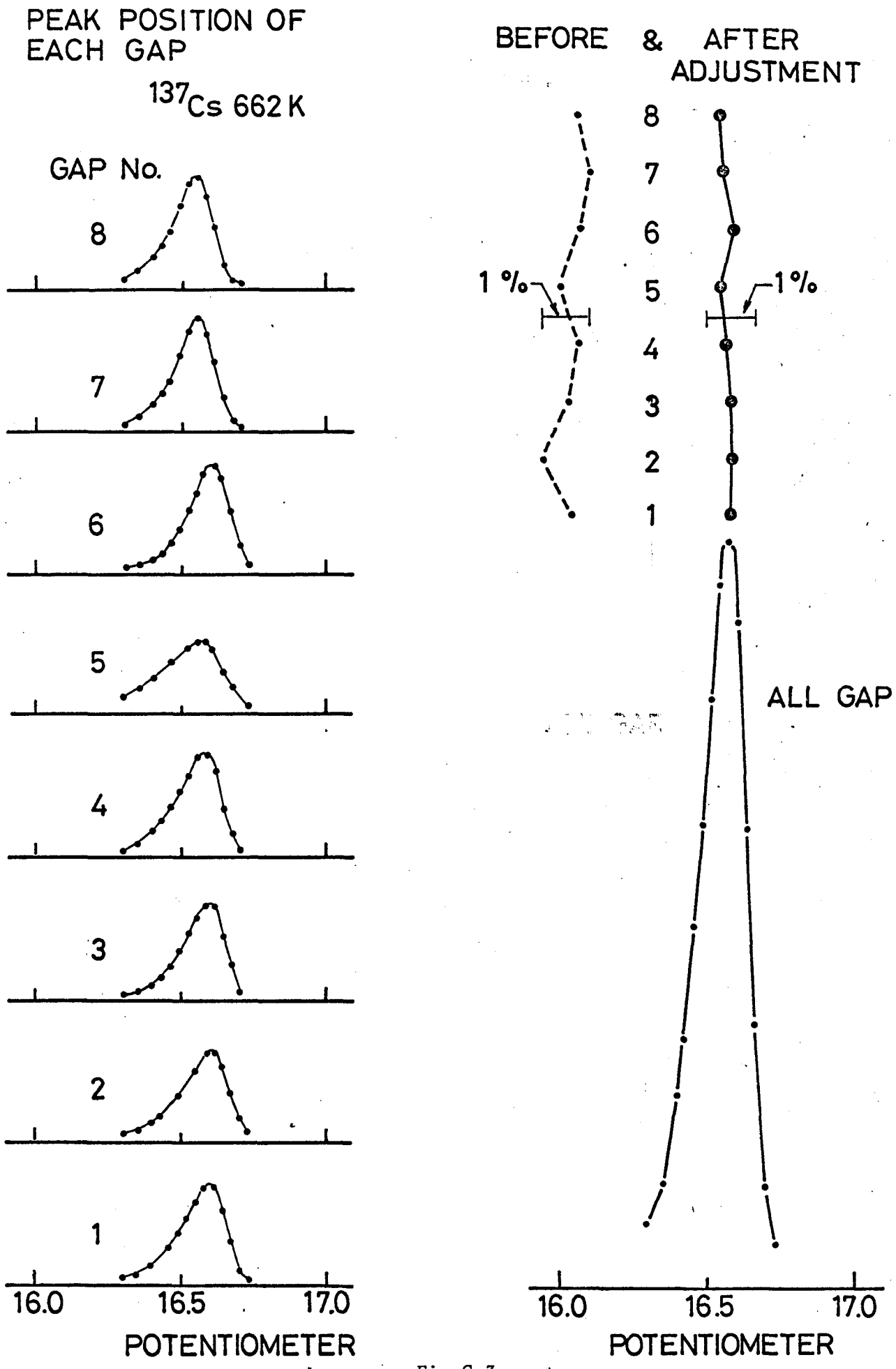
PEAK POSITION OF EACH GAP
^{137}Cs 662 K
GAP No.
8
7
6
5
4
3
2
1
16.0
16.5
17.0
POTENTIOMETER
BEFORE & AFTER ADJUSTMENT
1 %
1 %
8
7
6
5
4
3
2
1
ALL GAP
16.0
16.5
17.0
POTENTIOMETER

Fig.C-3

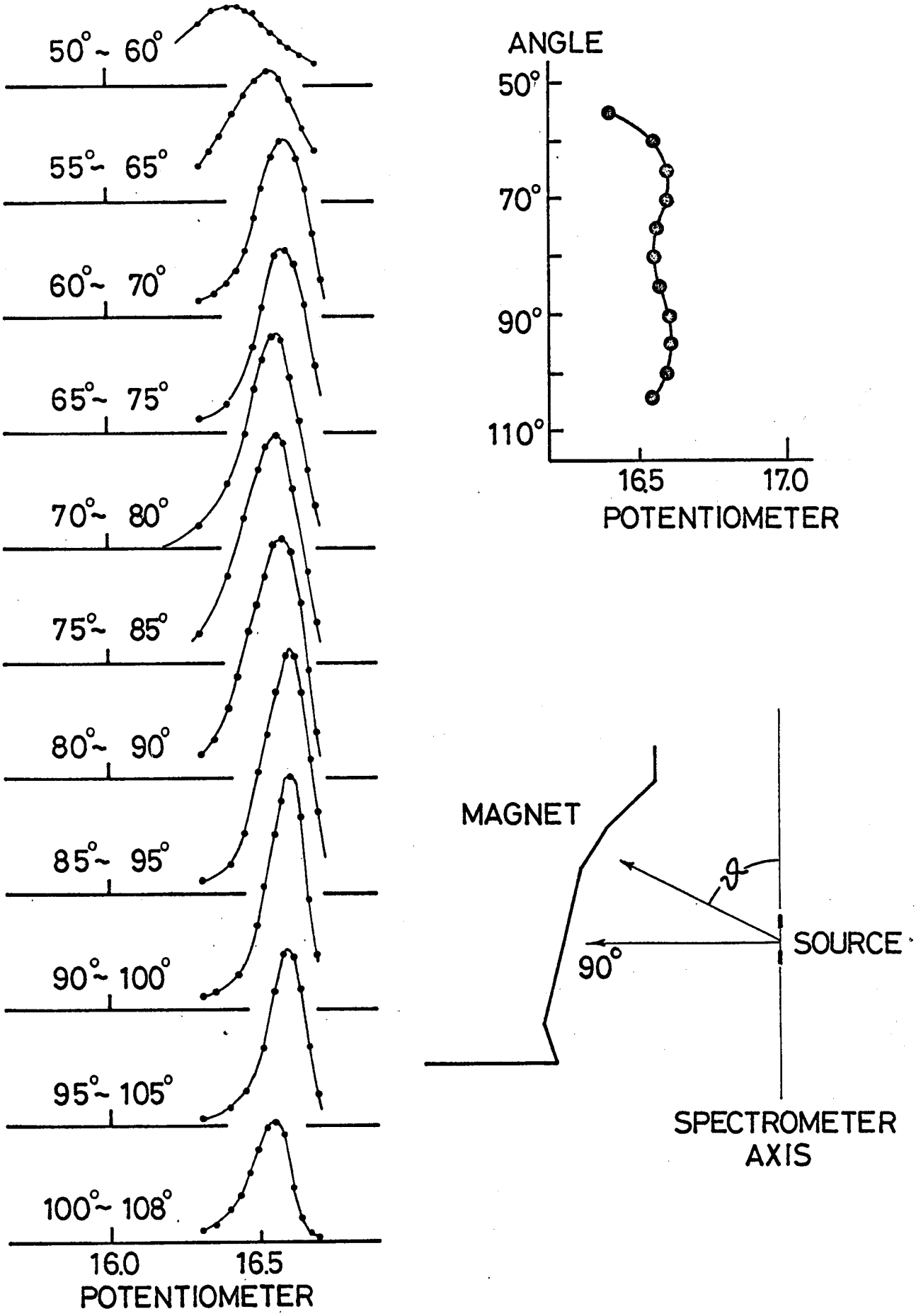
FOCUSSING CHARACTERISTICS
50°~ 60°
55°~ 65°
60°~ 70°
65°~ 75°
70°~ 80°
75°~ 85°
80°~ 90°
85°~ 95°
90°~ 100°
95°~ 105°
100°~ 108°
16.0
16.5
POTENTIOMETER
ANGLE
50°
70°
90°
110°
16.5
17.0
POTENTIOMETER
MAGNET
ϑ
SOURCE
90°
SPECTROMETER
AXIS

Fig.C-4

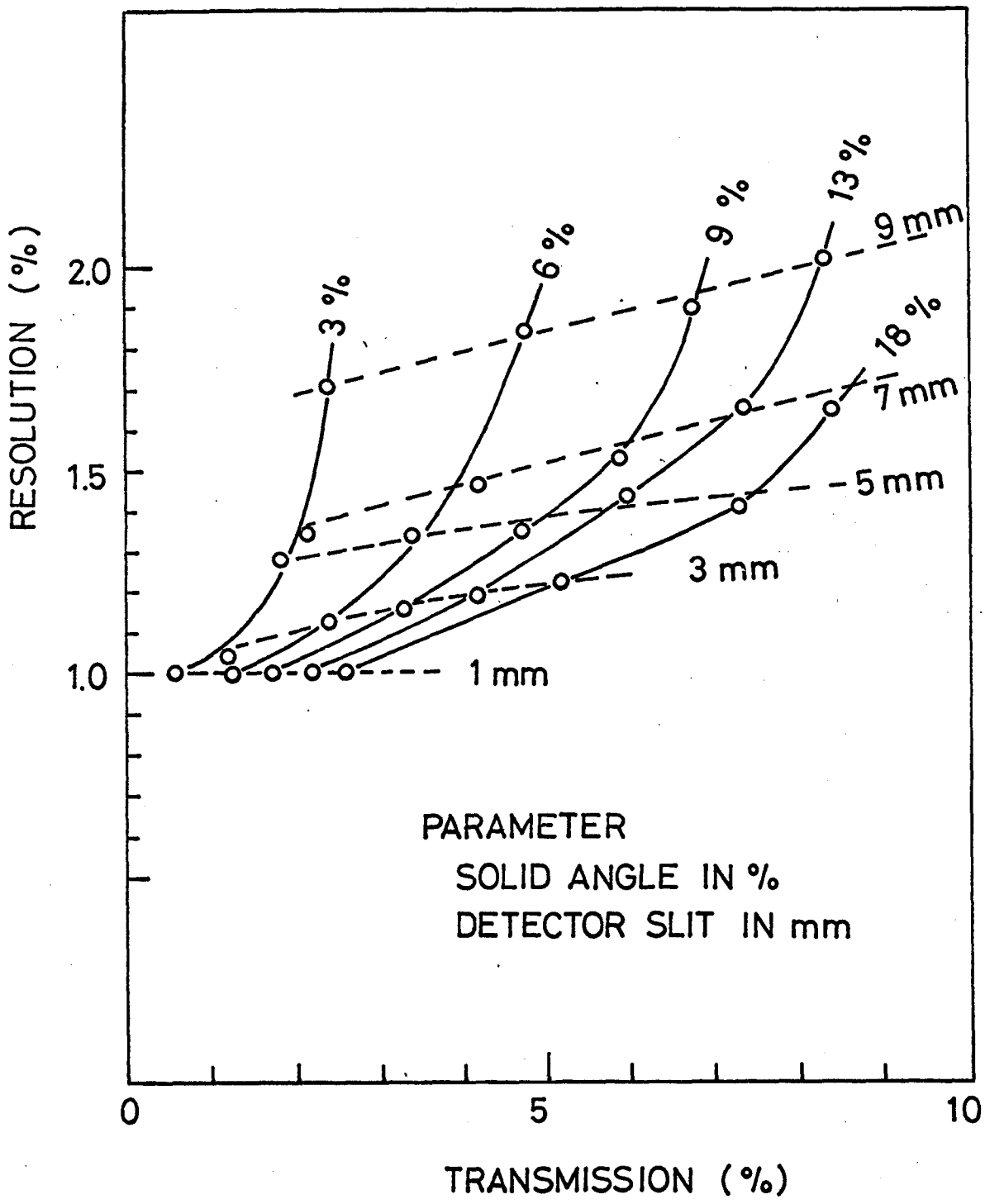
RESOLUTION (%)
2.0
1.5
1.0
0
5
10
TRANSMISSION (%)
3 %
6 %
9 %
13 %
18 %
9 mm
7 mm
5 mm
3 mm
1 mm
PARAMETER
SOLID ANGLE IN %
DETECTOR SLIT IN mm

Fig.C-5